Kinetics of Simultaneous Diffusion and Reaction for the Nitrification Process in Suspended Growth Systems

Wen Kang Shieh
Enrique J. La Motta

KINETICS OF SIMULTANEOUS DIFFUSION AND REACTION FOR THE NITRIFICATION PROCESS IN SUSPENDED GROWTH SYSTEMS

By

Wen Kang Shieh
Research Assistant

Enrique J. La Motta
Assistant Professor of Civil Engineering

Environmental Engineering Program
Department of Civil Engineering
University of Massachusetts
Amherst, Massachusetts   01003

June 1978

Massachusetts Division of Water Pollution Control
Research and Demonstration Project No. 76-10(1)

ii

ACKNOWLEDGEMENTS

ENGINEERING RELEVANCE

The goal of zero discharge of pollutants, to be attained by 1983, requires advanced wastewater treatment to remove pollutants from the effluents of existing wastewater treatment facilities. One of the pollutants of concern is nitrogen, whose removal is efficiently carried out using biological treatment.

The study described in this report is aimed at developing rational design criteria for the biological nitrification process using separate-stage activated sludge units. Rational design of a biological reactor is possible only when the kinetics of the process is understood. A suspension of microorganisms, such as the activated sludge, has two phases, namely, the liquid and the microbial flocs. In addition the substrate consumption reaction requires these two phases to proceed at the rate it does. Therefore, the activated sludge system is kinetically heterogeneous, which means that interphase and intraphase mass transport must be considered as factors affecting the overall rate of substrate utilization.

Although there is abundant literature concerning the behavior of biological nitrification units, most of these studies have neglected to consider the effect of diffusional resistances on the substrate uptake rate. The results of the present investigation demonstrate that neglecting such an effect can lead to errors in the evaluation of kinetic constants. Thus, it is not surprising to find a wide variation in the values of the constants reported in the literature.

The research reported herein identifies and evaluates the magnitude of diffusional resistances on the rate of nitrification. The true, or intrinsic rate was observed by eliminating mass transfer effects, and, therefore, the intrinsic kinetic constants could be measured. It was found that parameters such as substrate concentration and detention time affect the value of these constants, a fact that has been generally ignored in the past.

It is hoped that this research will help sanitary engineers to understand better the factors which affect the nitrification rate. With this understanding, improvements in the design criteria for nitrification units may be achieved.

Enrique J. La Motta, PhD
Assistant Professor of
Civil Engineering

ABSTRACT

Nitrification kinetics in the activated sludge process were studied extensively in this investigation. A modified kinetic model, which incorporated the consideration of internal diffusional resistances of ammonium with simultaneous Michaelis-Menten reaction is presented; the concept of effectiveness factor is used to evaluate the significance of mass transfer resistances on the overall nitrification rate in the system. Both batch and continuous flow experiments were performed to verify the applicability of this model.

Based on experimental results of the batch experiments, a pH of 8.0 and a temperature of $30^{\circ}C$ were the optimum operating conditions for nitrification. It was also found that floc size has a profound effect on the observed nitrification rate; a floc radius of 18 μm was determined as the appropriate size for the observation of intrinsic nitrification rate.

The batch experiments also confirmed that the Michaelis-Menten kinetics is an appropriate expression for describing the observed intrinsic nitrification rate. However, both kinetic parameters, k and K_s, are strongly affected by the initial substrate concentrations in the low concentration ranges and become constant in the higher concentration range. This demonstrated that both parameters cannot be considered constants unless a sufficiently high initial substrate concentration is introduced.

The experimental results obtained from the continuous flow experiments also confirmed the applicability of Michaelis-Menten kinetics to the activated sludge nitrification process. Two important

conclusions were drawn. First, the intrinsic values of k and K_s obtained in the continuous flow experiments are different from those obtained in the batch experiments. This clearly demonstrates that information obtained from batch cultures cannot be applied directly to the design of study of the continuous flow experiments. Second, the constant k was found to vary with detention time, that is, larger values of k were observed under shorter detention times. The value of k approached asymptotically the respective value in the batch experiments.

Study of the effect of mass transfer resistances on the overall nitrification rate revealed that, under the influence of significant internal-diffusion effects, the kinetic expression apparently maintains the same form; however, a smaller value of k and a larger value of K_s were observed. The overall effect is a decrease of the observed nitrification rate. The proposed model was able to predict the degree of influence of internal diffusion on the observed rate; both predicted and experimental results were in good agreement.

TABLE OF CONTENTS

LIST OF TABLES

LIST OF FIGURES

LIST OF SYMBOLS

a:	empirical constant in Eq. (3-7)
a_i:	undetermined coefficient in Eq. (2-24)
A:	constant in Eq. (A2-4)
A_p:	surface of the floc particle, mm^2
A'_p:	projected area of the floc particle, mm^2
A'_{p_i}:	projected area of the floc particle i, mm^2
b:	empirical constant in Eq. (3-7)
B:	constant in Eq. (A2-4)
$\bar{B}$:	coefficient matrix in Eq. (2-30)
B_{ij}:	element in matrix $\bar{B}$
d:	particle diameter, μm
d_i:	impeller diameter, cm
d_r:	rotor diameter, cm
d_v:	vessel diameter, cm
D:	diffusivity, cm^2/sec
D_A:	molecular diffusivity of component A in the liquid, cm^2/sec
D_e:	effective diffusivity, cm^2/sec
$\bar{D}$:	coefficient matrix in Eq. (2-30)
f:	dimensionless substrate concentration

$\bar{f}$:   matrix form of solution $f(\xi)$ at collocation points ξ_j

F: dimensionless substrate concentration as defined by Eq. (A2-2)

k: saturation utilization rate of substrate per unit mass of floc particle, mol/mg-day

k':   observed saturation utilization rate, mol/mg-day

k_b: maximum uptake rate as defined in Eq. (5-5), mol/mg-day

k_1:   first-order kinetic constant, ℓ/mg-day

k_o: zero-order kinetic constant, mol/mg-day

k_o':   initial substrate uptake rate in the batch experiments, mol/mg-day

k_{CA}:   mass transfer coefficient, cm/sec

K_m: constant as defined in Eq. (5-5)

K_s: Michaelis constant, mol/ℓ

K_s':   observed Michaelis constant, mol/ℓ

L: characteristic length, cm

N: mass flux of substrate, mol/cm^2-day

N':   mass flux of substrate, mol/mg-day

N_{Nu}:   Nusselt Number

N_{Pe}:   Peclet Number

N_{Re}:   Reynolds Number

N_{Sc}:   Schmidt Number

$P_i(\xi^2)$:   Jacobi Polynomials of degree 2i

Q: flowrate, mℓ/min

Q':   seed stream flowrate, mℓ/min

$\bar{Q}$:   coefficient matrix in Eq. (2-30)

$\bar{Q}^{-1}$:   inverse of $\bar{Q}$

$\bar{Q}^{T}$:   transpose of $\bar{Q}$

$Adj\bar{Q}$:   adjoint of $\bar{Q}$

r: distance in the radial direction from the center of the floc, μm

$\bar{r}$:   rpm, rev/sec

Δr: shell thickness as defined in Eq. (2-12), μm

r_{in}:   biochemical reaction rate of substrate per unit volume of floc particle, mol/cm^3-day

r_{A}:   chemical reaction rate of component A, mol/ℓ-day

R: radius of floc particle, μm

$\bar{R}$:   average radius of floc particle, μm

S: substrate concentration, mol/ℓ

ΔS: concentration drop through the boundary layer surrounding the floc particle, mol/ℓ

S_{e}:   effluent substrate concentration, mol/ℓ

S_{i}:   influent substrate concentration, mol/ℓ

S_{o}:   initial substrate concentration, mol/ℓ

S_{A}:   concentration of component A, mol/ℓ

t: time, min

v: reaction rate, mol/ℓ-day

$\vec{v}$:   velocity vector

v':   characteristic velocity, cm/sec

v_f: relative velocity between particle and liquid, cm/sec

v_i: intrinsic substrate uptake rate, mol/mg-day

v_{mi}:   net growth rate of biomass, mg/ℓ-day

v_o: observed substrate uptake rate, mol/mg-day

v_x: velocity component in x direction, cm/sec

v_y: velocity component in y direction, cm/sec

v_z: velocity component in z direction, cm/sec

V_p: volume of the floc particle, mm^3

X: biomass concentration, mg/ℓ

X':   biomass concentration in seed stream, mg/ℓ

X_e: biomass concentration in effluent, mg/ℓ

$\bar{X}$:   average biomass concentration, mg/ℓ

Greek Symbols

$\vec{\nabla}$:   divergency

∇^2:   Laplacian

ν: kinematic viscosity, stokes

ρ: density of biomass, mg/cm^3

ρ_ℓ: density of fluid, mg/cm^3

ξ: dimensionless radius $= r/R$

ξ_j: collocation point

α_i: constant in Eq. (2-27)

$\bar{\alpha}$:   coefficient matrix in Eq. (2-30)

β: S_e/K_s, dimensionless

ϕ: Thiele's type modulus, dimensionless

η: effectiveness factor, dimensionless

η_e: experimental effectiveness factor, dimensionless

μ_ℓ: viscosity of fluid, poises

C H A P.T E R   I

INTRODUCTION

The activated sludge process has long been recognized as one of

the most versatile processes for the treatment of both domestic and

industrial wastes. Although many modifications of the process have

been made since its first introduction in 1913 in England, the basic

characteristics of these modifications are still similar. In the

aeration tank, the waste is mixed with a large mass of microorganisms

(activated sludge) for a period of time. The oxygen required is

supplied by either diffused air or mechanical systems. The

biodegradable portion of the waste (substrate) is used by the

microorganisms during this period. Then the mixed liquor flows into

a sedimentation tank, where the flocculated sludge settles out, thus

producing a clear effluent. A portion of the settled sludge is

returned to the aeration tank while the remaining sludge undergoes

separate treatment and disposal[81].

Generally speaking, the activated sludge process, as well as

other biological waste treatment processes, consists of different types

of biochemical reactions which depend on such factors as characteristics

of both wastewater and microorganisms, and environmental and operating

1

conditions. They differ from pure chemical reactions in many aspects, such as the complexity of the reaction mixtures, the increase of mass of microorganisms with simultaneous decrease of mass of substrate, the ability of microorganisms to synthesize their own catalysts (enzymes) - to name but a few among these differences[10].

In general, biochemical reactions are either homogeneous or heterogeneous, depending on the number of phases involved in the transformations. All biochemical reactions that occur in the activated sludge process can be classified as heterogeneous, that is, they require more than one phase to proceed, namely, an aqueous phase (substrate or nutrient medium), a solid phase (microorganisms), and a gaseous phase (air). This feature, along with other inherent properties of heterogeneous systems might exert a profound effect on the overall performance of the process.

Two types of information are essential in understanding the activated sludge process[65]. The first one is related to the transport mechanisms of substrate through the different phases. Because of the heterogeneous nature of the system, transport of substrate occurs not only in the nutrient medium but also within the sludge floc. The second type of information concerns the kinetics of the process, that is, the utilization rate of substrate by the

microorganisms. The overall efficiency of the process is controlled

by the slowest step in the overall sequence. The determination of the

slowest or rate-limiting step is possible only by quantitative analysis

of each one of the steps involved in the process.

A large amount of research has been conducted in modeling the

activated sludge process. The work of various investigators has

provided a substantial amount of information about the kinetics of the

process$^{(4, 68, 82, 98, 107, 127)}$. However, most of this work has been

based on the implicit assumption that the system is homogeneous; in

other words, interphase transport of substrate has been neglected.

Although these models seem to be able to predict successfully the

performance of the process, its intrinsic or true kinetics may not have

been revealed by them. The effect of mass transfer resistances has

been well documented in both catalytic and enzymatic processes. A

reduction of the overall efficiency, and the alteration of the true

reaction order have been reported. Considering that the activated

sludge process is an autocatalytic system, i.e., it creates its own

enzymes, it is evident that neglecting the effect of mass transfer

resistances may lead to erroneous conclusions when analyzing kinetic

information.

The investigation reported herein represents an overall effort to

determine, both analytically and experimentally, the important steps

occurring in the utilization of ammonium by a suspended growth of

nitrifying bacteria (nitrifiers). The broad objective of this

investigation is to present a fundamental study of both transport and

reaction phenomena during nitrification in the activated sludge process.

A physico-biochemical model, which incorporates important process

parameters under different operating conditions is presented. It is

hoped that such an effort will provide useful information for a sound

design of the biological nitrification process.

Need for Nitrogen Removal

The removal of nitrogen compounds from wastewater has recieved

much attention recently for several reasons. The discharge of nutrients

(mainly N and P) into surface water systems has stimulated the growth

of aquatic plants thus accelerating the eutrophication rate[80]. The

growth of algae in lakes and streams has affected as much as 56% of

surface water supplies in the United States and has caused such problems

as the production of taste and odor, increased color and turbidity,

diurnal variation of pH, increased chlorine demand[32, 115, 116],

increased cost of water treatment, and destruction of the recreational

value of the water facility[109]. The decomposition of dead algae has

caused oxygen depletion in water, with the resulting formation of

anaerobic zones. The reduced forms of iron and manganese existing in

this zone have caused problems to water supplies[32].

The oxygen demand of nitrogen compounds has been observed in the

BOD test. It has been verified that such demand is exerted by a group

of bacteria named nitrifiers while using ammonium as substrate. The

discharge of reduced forms of nitrogen compounds, therefore, will exert

extra oxygen demand on receiving waters. The Potomac Estuary in the

United States and the Thames Estuary in Great Britain[90, 93] are

typical examples of estuaries which are greatly affected by such oxygen

demand.

When chlorine is added to wastewaters containing ammonia,

chloramines are formed. Compared to free chlorine forms, chloramines

are less effective as disinfectants[93, 133]. In such cases, free

chlorine residuals are obtained only after the addition of large

quantities of chlorine; therefore, the existence of ammonia in wastewater

will increase chlorine dosage requirement for the same level of

disinfection.

Nitrates were identified as a public health hazard, being a cause

of methemoglobinemia in infants[93]. Nitrate is reduced to nitrite in

the baby's stomach after ingestion; then it reacts with the hemoglobin

in the blood to form methemoglobin, which is incapable of carrying oxygen to body tissue; the result is suffocation. Since 1945, about 2000 cases have been reported in the United States and Europe with a mortality rate of 7 to 8%[93].

At low concentrations, ammonia has been found to be toxic to fish, especially at higher pH when the ammonium ion is transformed to ammonia[93, 119].

While reclaimed wastewater is adequate for industrial reuse, ammonia may need to be removed because it is corrosive to copper fittings[93, 119]. Furthermore, ammonia may stimulate bacterial growth in cooling towers and distribution networks, causing adverse effects in the operation of the systems.

In summary, the increasing concern for maintaining the quality of surface waters has focused attention on nitrogen as a major water pollutant. The effluent standards in the future will require, directly or indirectly, nitrogen removal.

C H A P T E R   I I

THEORETICAL CONSIDERATIONS

Since microorganisms in the activated sludge process tend to
agglomerate forming large particles, it is reasonable to use the floc
particle rather than the individual microorganism as the basic unit in
model development.

As depicted in Figure 2-1[10] there are several transport and
reaction steps that must occur before substrate can be used by
microorganisms. Substrate in the nutrient medium is transferred through
the liquid to the outer surface of the floc particle by means of either
molecular diffusion or convection (step 1). Upon reaching the outer
surface, substrate must be transferred through a boundary layer
surrounding the floc particle. This is termed "external diffusion" or
"film diffusion" of substrate (step 2). The rate of transfer will be
of the form $k_{CA}\Delta S$, where k_{CA} is a mass transfer coefficient and ΔS is
the concentration drop of substrate across the boundary layer. The
porous structure of the floc particle adds another resistance to the
transport of substrate within the matrix. This is the "internal
diffusion" or "intraparticle diffusion" (step 3). This type of diffusion
can be described by Fick's law, which states that the mass flux of

7
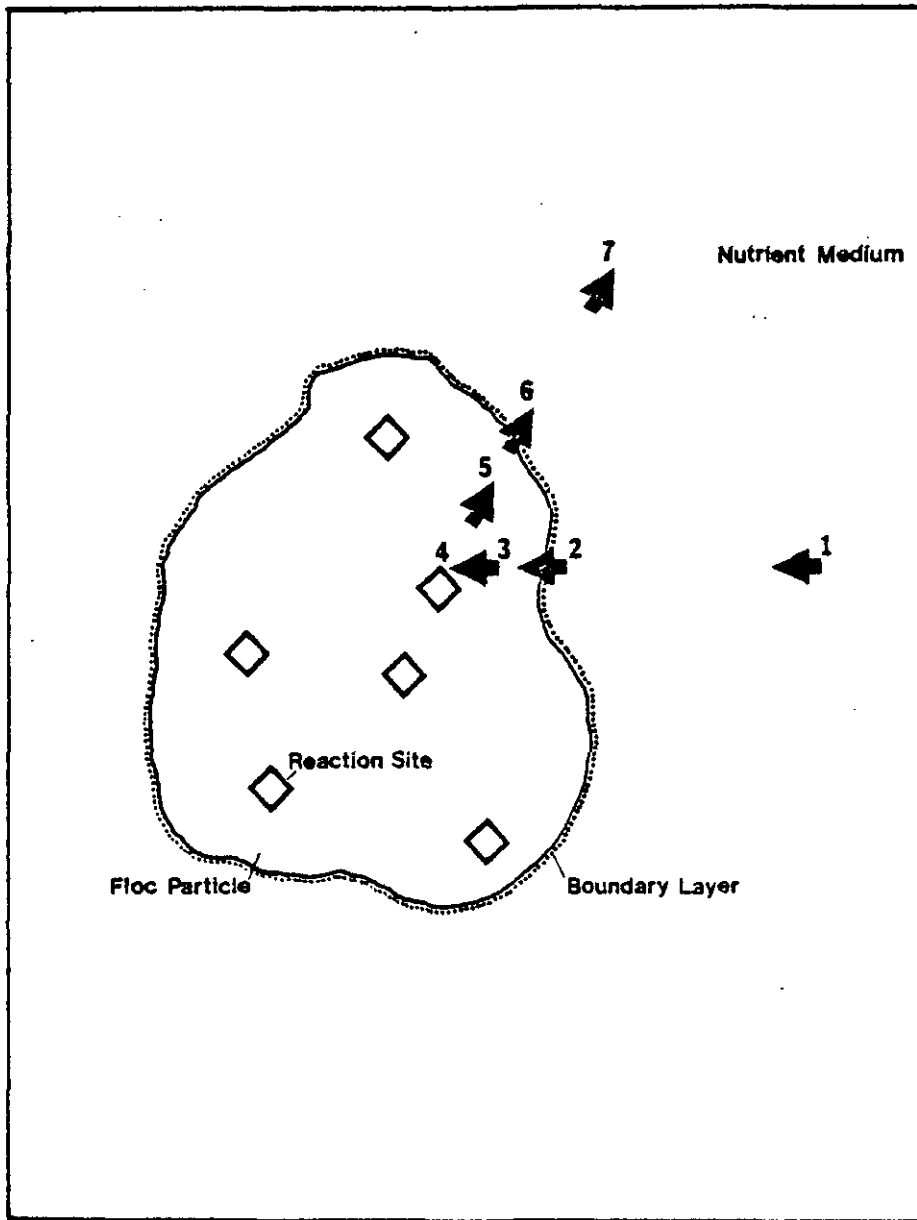
Figure 2-1 Transport and Reaction Steps of Substrate in
the Activated Sludge Process

substrate is proportional to the local concentration gradient; the proportionality constant is termed effective diffusivity D_e. Biochemical reaction will occur once substrate reaches the reaction sites, and reaction products will be formed (step 4).

The remaining steps take place in the reverse order, and they are: diffusion of products within the floc matrix to the outer surface (step 5); transport of products through the boundary layer and back to the bulk of liquid (step 6); and the transport of products in the nutrient medium (step 7).

Steps 3 and 4 occur simultaneously, thus they will have a single rate. Steps 1 and 2, and the overall diffusion-and-reaction phenomenon (steps 3 and 4) occur in series; therefore the slowest step will become the rate-limiting one in these sequential steps. Since substrate consumption reactions are irreversible, the formation of products and their subsequent diffusion within the floc matrix will not become rate-limiting. Therefore, steps 5, 6, and 7 can be neglected in the determination of the rate-limiting step as long as there is no product accumulation in the environment.

The significance of transport in the bulk of liquid, external diffusion, internal diffusion, and reaction on the overall rate of substrate consumption can be analyzed by the traditional chemical

engineering approach and will be discussed in detail in the following sections.

Transport of Substrate in the Nutrient Medium in Laminar Flow

The material contained in a fluid is transported by two different mechanisms: convection and molecular diffusion[46]. Convective mass transfer implies the movement of material by virtue of fluid flow. Diffusion in the liquid state is generally attributed to hydrodynamic or activated-state mechanisms[22, 46]. For a liquid of constant density, ρ_ℓ, containing a component A, the concentration of this component in the liquid, S_A, can be described by the continuity equation

$$\frac{\partial S_A}{\partial t} + \vec{v} \cdot \vec{\nabla} S_A = D_A \nabla^2 S_A + r_A \tag{2-1}$$

where

$\vec{v}$ = fluid velocity vector

$\vec{v} \cdot \vec{\nabla} S_A$ = convective mass transfer contribution

$D_A \nabla^2 S_A$ = molecular diffusion contribution

r_A = chemical reaction contribution

D_A = molecular diffusivity of A in the liquid (constant)

The derivation of Eq. (2-1) is described in detail elsewhere[22, 46, 110, 123].

In Cartesian coordinates, Eq. (2-1) can be represented by

$$\frac{\partial S_A}{\partial t} + v_x \frac{\partial S_A}{\partial x} + v_y \frac{\partial S_A}{\partial y} + v_z \frac{\partial S_A}{\partial z} = D_A(\frac{\partial^2 S_A}{\partial x^2} + \frac{\partial^2 S_A}{\partial y^2} + \frac{\partial^2 S_A}{\partial z^2}) + r_A \quad (2\text{-}2)$$

where v_x, v_y, v_z are the velocity components in the x, y, and z

directions respectively.

If steady state is assumed to exist in the liquid and the reaction

rate of component A in the liquid is negligible (this is the case in

the activated sludge process, where reactions occur in the solid phase),

then Eq. (2-2) is reduced to

$$v_x \frac{\partial S_A}{\partial x} + v_y \frac{\partial S_A}{\partial y} + v_z \frac{\partial S_A}{\partial z} = D_A(\frac{\partial^2 S_A}{\partial x^2} + \frac{\partial^2 S_A}{\partial y^2} + \frac{\partial^2 S_A}{\partial z^2}) \quad (2\text{-}3)$$

The predominance of each side of Eq. (2-3) on the overall mass

transfer process can be judged by the value of a parameter called

Peclet Number, N_{Pe}, defined by

$$N_{Pe} = \frac{v'L}{D} \quad (2\text{-}4)$$

where

  v' = characteristic velocity

  D = diffusivity

  L = characteristic length

If $N_{Pe} \gg 1$, then convection is the main mechanism of the overall

mass transfer process. On the other hand, if $N_{Pe} \ll 1$, diffusion is predominant.

The Peclet Number can be expressed as a product of two terms:

$$N_{Pe} = \frac{v'L}{D} = (\frac{v}{D})(\frac{v'L}{v})$$

$$= N_{Sc} \cdot N_{Re} \qquad (2\text{-}5)$$

where

v = kinematic viscosity

N_{Sc} = Schmidt Number

N_{Re} = Reynolds Number

If the component A is ammonium ion (NH_4^+) and the liquid is water with a temperature of $30^{\circ}C$, then

$v = 0.8039 \times 10^{-2}\ cm^2/sec$

$D = 1.736 \times 10^{-5}\ cm^2/sec$

Thus

$$N_{Sc} = 463.08 \text{ and } N_{Pe} = 463.08 N_{Re} \qquad (2\text{-}6)$$

It is clear that even at low Reynolds numbers, N_{Pe} will always be large, indicating that the convection term predominantes over the diffusion terms. Therefore, the right side of Eq. (2-3) can be neglected yielding

$$v_x \frac{\partial S_A}{\partial x} + v_y \frac{\partial S_A}{\partial y} + v_z \frac{\partial S_A}{\partial z} = 0 \qquad (2\text{-}7)$$

Obviously S_A = constant is a solution of Eq. (2-7).

Thus it is reasonable to assume a constant substrate concentration in the bulk of liquid far from the floc surface. However, the conditions prevailing at the immediate neighborhood of the floc surface are different, as discussed in the subsequent section.

External Diffusion of Substrate Through the Boundary Layer Surrounding the Floc

It has been shown in the previous section that the substrate concentration in the bulk of liquid is constant. However, this solution does not satisfy the conditions existing at the outer surface of the floc particle, where the substrate concentration is always less than that in the bulk of liquid. The region in which the concentration of substrate drops from the value at the liquid bulk to that at the floc surface is termed concentration boundary layer. Its dimensions depend on factors such as fluid velocity, type of substrate, substrate concentration in the bulk of liquid, etc. The evaluation of mass transfer in this layer can be carried out by using a well-known mass transfer correlation for flow past spheres[13, 14, 22, 79, 85, 87, 110]

$$N_{Nu} = \frac{k_{CA}d}{D} = 2.0 + 0.6\left(\frac{v_f d}{v}\right)^{0.5} \left(\frac{v}{D}\right)^{0.33} \tag{2-8}$$

where

k_{CA} = mass transfer coefficient

d = particle diameter

N_{Nu} = Nusselt Number

v_f = relative velocity between particle and liquid

For the ammonium ion in water, with a temperature of $30°C$, k_{CA} can be evaluated for different v_f at a certain particle size. The detailed calculation is in Appendix 1. Table 2-1 shows the k_{CA} values with v_f varied from 0 to 1.0 cm/sec. Two particle sizes were used in this calculation.

It is interesting to note that k_{CA} increases as v_f increases which means the larger the difference of relative velocity between particle and fluid the faster the mass transfer rate. It is also important to point out that particle size has a strong effect on the value of k_{CA}; decreasing d by one half increases k_{CA} by roughly 60%, which indicates that the mass transfer rate is higher for small particles.

The mass flux of substrate, N, across the outer surface of the floc is related to the concentration drop through the boundary layer, as shown by Eq. (2-9)

$$N = k_{CA}\Delta S \qquad\qquad (2-9)$$

If the mass flux is expressed in terms of mass of substrate per unit mass of floc particle per unit time, then

TABLE 2-1

VALUES OF MASS TRANSFER COEFFICIENT AS A FUNCTION
OF RELATIVE VELOCITY BETWEEN PARTICLE AND FLUID
AT TWO PARTICLE SIZES

v_f(cm/sec)	d(μm)	$k_{CA} \times 10^3$(cm/sec)
0.0	120	2.893
	60	5.786
0.1	120	5.488
	60	9.455
0.2	120	6.563
	60	10.974
0.3	120	7.387
	60	12.140
0.4	120	8.083
	60	13.123
0.5	120	8.695
	60	13.989
0.6	120	9.249
	60	14.772
0.7	120	9.758
	60	15.492
0.8	120	10.232
	60	16.162
0.9	120	10.677
	60	16.792
1.0	120	11.098
	60	17.387

$$N' = \frac{NA_p}{\rho V_p} = \frac{A_p}{\rho V_p} \cdot k_{CA} \Delta S \qquad (2\text{-}10)$$

where

N' = mass flux of substrate in terms of mass of substrate per unit

mass of floc per unit time

A_p = external surface area of the floc particle

V_p = volume of the floc particle

ρ = density of the floc particle

The resulting concentration drop through the boundary layer, as

a function of v_f, for two different particle sizes, at different N'

values is shown in Figures 2-2 and 2-3; ρ was assumed to be 57 mg/cm^3.

It is clear that the concentration drop through the boundary layer

is relatively insignificant as long as v_f is above 0.1 cm/sec. The v_f

value in the activated sludge process will certainly be above this

value because of the vigorous agitation[13, 14, 85]. It is, therefore,

reasonable to conclude that external diffusion resistances will cause an

insignificant concentration drop through the boundary layer surrounding

an activated sludge floc particle. Thus

$\Delta S = 0$, or

$$S_{outer\ surface} = S_{bulk\ fluid} \qquad (2\text{-}11)$$

Mueller[85], Baillod[13, 14], Toda[124], and other investigators
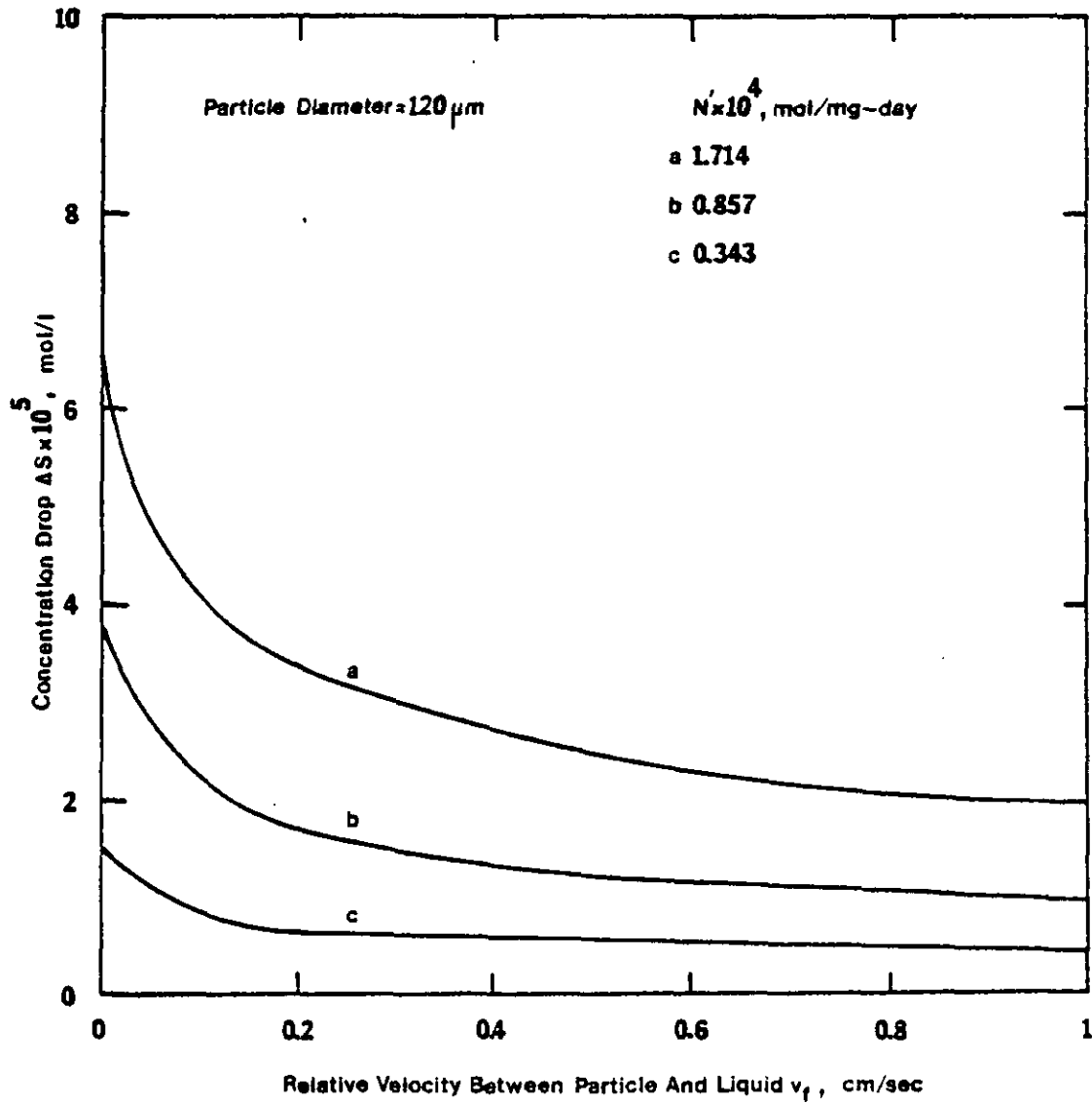
Figure 2-2 Concentration Drop Through the Boundary Layer at a Particle Diameter of 120 μm
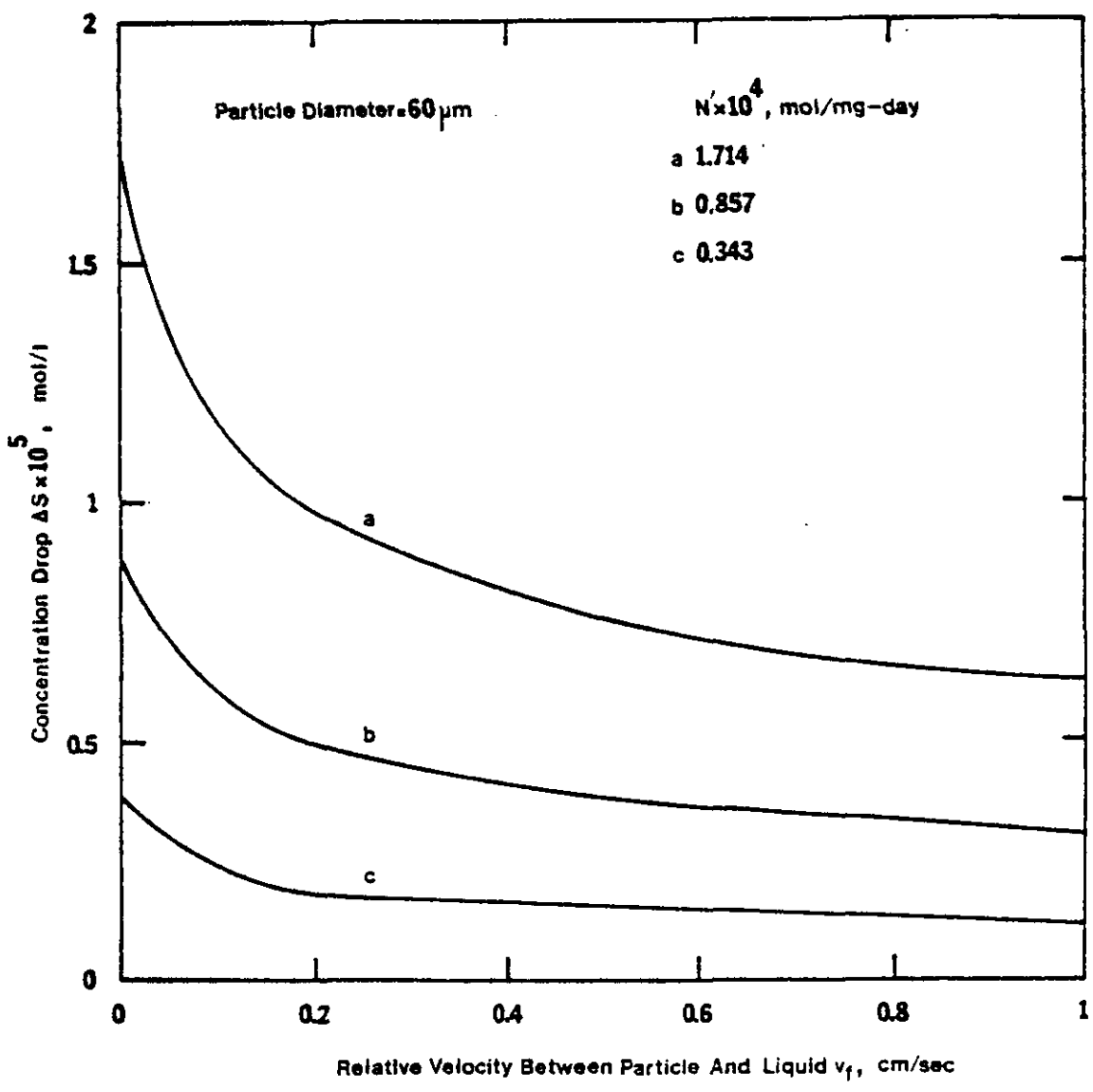
Figure 2-3 Concentration Drop Through the Boundary Layer at a
Particle Diameter of 60 μm

have reached the same conclusion, either experimentally or analytically.

Development of the Kinetic Model

Based on the analysis in the previous sections, only internal diffusion of substrate and its biochemical reaction rate need to be considered. The following assumptions are made in the development of the kinetic model being proposed:

(a) Single soluble substrate, i.e., ammonium.

(b) Steady state operation.

(c) Spherical floc particle.

(d) Excess oxygen available, so dissolved oxygen will not become a limiting factor.

(e) Michaelis-Menten kinetics for substrate conversion, i.e., $r_{in} = \rho k S/(K_s + S)$, where r_{in} is the true reaction rate (mol/ℓ-day); k is the saturation utilization rate of substrate per unit mass of floc particle (mol/mg-day); K_s is Michaelis constant (mol/ℓ); and ρ is the density of the floc particle (mg/cm^3).

(f) The effective diffusivity D_e, the Michaelis constant K_s, and the saturation utilization rate of substrate k are constant for a specific operating condition.

Consider Figure 2-4, which shows a cross section of a spherical particle with a radius of R in which diffusion and reaction of substrate are taking place. A shell mass balance on substrate yields:

$$NA|_r - NA|_{r + \Delta r} = 4\pi r^2 \Delta r . r_{in} \qquad (2-12)$$

where N is the mass flux of substrate passing in the r-direction through an imaginary spherical surface with thickness Δr at a distance r from the center of the sphere, and A the surface area of the shell. The sink term r_{in} represents the biochemical reaction rate of substrate per unit volume of the floc and therefore the term $4\pi r^2 \Delta r . r_{in}$ gives the mass of substrate being consumed in the shell per unit time. There is no accumulation term since a steady state situation was assumed.

By recognizing that $A = 4\pi r^2$, then Eq. (2-12) becomes

$$N|_r . 4\pi r^2 - N|_{r + \Delta r} . 4\pi (r + \Delta r)^2 = 4\pi r^2 \Delta r . r_{in} \qquad (2-13)$$

Division by $4\pi \Delta r$ and letting $\Delta r \rightarrow 0$ gives

$$\lim_{\Delta r \rightarrow 0} \frac{N|_{r + \Delta r} . (r + \Delta r)^2 - N|_r . r^2}{\Delta r} = -r^2 . r_{in} \qquad (2-14)$$

or

$$\frac{d}{dr}(Nr^2) = -r^2 . r_{in} \qquad (2-15)$$

The mass flux of substrate N is related to the local concentration gradient in the r-direction (dS/dr) by

$$N = -D_e \frac{dS}{dr} \tag{2-16}$$

where D_e is the effective diffusivity which must be measured experimentally[22].

Assuming that D_e is a constant, substitution of Eq. (2-16) into Eq. (2-15) yields

$$\frac{D_e}{r^2} \frac{d}{dr} (r^2 \frac{dS}{dr}) = r_{in} \tag{2-17}$$

If the reaction kinetics follows the Michaelis-Menten expression, then

$$\frac{D_e}{r^2} \frac{d}{dr} (r^2 \frac{dS}{dr}) = \frac{\rho k S}{K_s + S} \tag{2-18}$$

The boundary conditions of Eq. (2-18) are

$$\begin{aligned} &\text{B.C. 1} \quad S = S_e \quad \text{at } r = R \\ &\text{B.C. 2} \quad \frac{dS}{dr} = 0 \quad \text{at } r = 0 \end{aligned} \tag{2-19}$$

where S_e is the steady state substrate concentration in the bulk of liquid. Figure 2-5 shows schematically the boundary conditions stated in Eq. (2-19).

The first boundary condition states that external diffusion resistances are negligible, so that the substrate concentration at the outer surface of the floc particle is the same as that in the
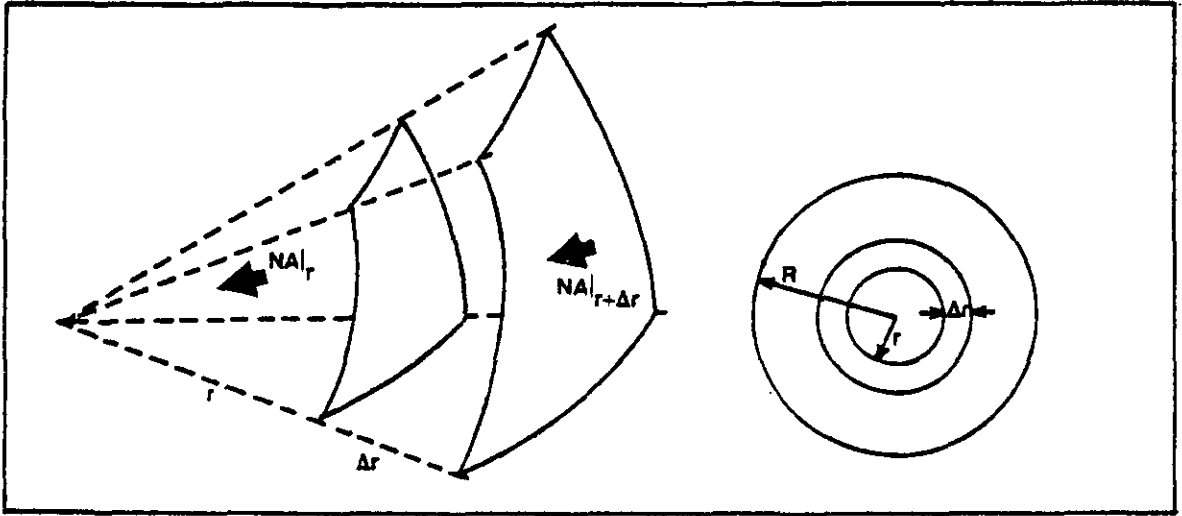
Figure 2-4 Mass Balance of Substrate for the Spherical Shell of
Thickness Δr
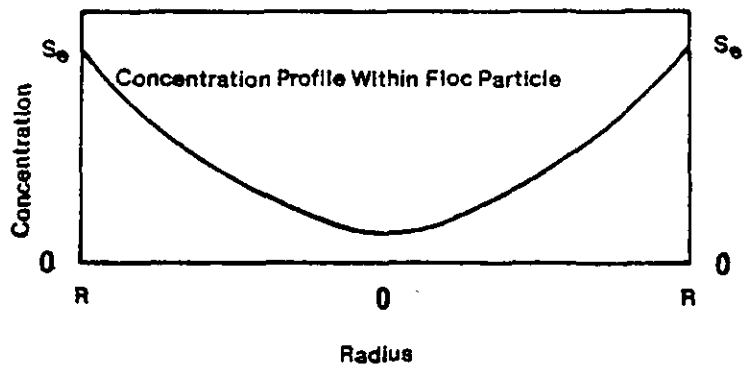
Figure 2-5 Boundary Conditions of
Eq. (2-18)

bulk of liquid.

Since substrate diffusion takes place in the radial direction, mass transfer must cease when the substrate reaches the center of the floc. Thus, by Eq. (2-16), $N|_{r=0} = -D_e(dS/dr) = 0$, or, $dS/dr = 0$, as stated by the second boundary condition.

It is convenient to express Eq. (2-18) in dimensionless form. For this purpose, the following variables are introduced: $f = S/S_e$; and $\xi = r/R$.

Then Eq. (2-18) can be rewritten as follows:

$$\frac{1}{\xi^2}\frac{d}{d\xi}(\xi^2\frac{df}{d\xi}) = \frac{(\frac{\rho k R^2}{D_e K_s}) \cdot f}{1 + \frac{S_e}{K_s} f} = \frac{\phi^2 f}{1 + \beta f} \qquad (2-20)$$

where

$\phi = R(\rho k/D_e K_s)^{0.5}$, a Thiele-type modulus

$\beta = S_e/K_s$

The dimensionless boundary conditions are

B.C. 1 $f = 1$ at $\xi = 1$

B.C. 2 $\frac{df}{d\xi} = 0$ at $\xi = 0$
$\qquad (2-21)$

It is interesting to note that ϕ, the Thiele-type modulus, is a measure of the reaction rate relative to the diffusion rate[6], for its

square could be written as

$$\phi^2 = \frac{\dfrac{\rho k R^2}{K_s}}{D_e} = \frac{3\dfrac{\rho k}{K_s}\dfrac{4}{3}\pi R^3 S_e}{4\pi R^2 D_e (S_e/R)} \tag{2-22}$$

The numerator is then the disappearance rate of substrate when the whole floc particle is exposed to an ambient substrate concentration, S_e, while the denominator is the transport rate of substrate into the the floc particle when the gradient at the outer surface is S_e/R. Small values of ϕ are obtained when the particles are small, the diffusivity is large, or the reaction rate is intrinsically low[111]. Internal diffusion has no effect on the rate per particle under such circumstances. On the other hand, for large values of ϕ, internal diffusion has a large effect on the rate, that is, under these conditions, diffusion into the particle is relatively slow, so that the reaction occurs before the substrate has diffused far into the particle[111].

At sufficiently high values of S_e and low values of R, substrate will substantially penetrate to the center of the floc. In this case, both substrate concentration and reaction rate decrease continuously from the outer surface to the center. This rate has been variously called macroscopic, apparent, or observed rate. The maximum rate would

occur if the whole floc particle were exposed to the substrate

concentration in the liquid bulk. This would be possible if there was

no internal diffusion of substrate. In this case the true, or intrinsic

rate would be observed.

A parameter which has found a great deal of applications in

heterogeneous catalysis can also be applied to estimate the effect of

internal diffusion resistances in biological wastewater treatment

systems. Such a parameter is called effectiveness factor η, which is

defined as follows[10, 22, 111]:

$$\eta = \frac{\text{Observed or apparent rate}}{\substack{\text{Rate which would be obtained} \\ \text{with no concentration gradient} \\ \text{within the biomass}}} \qquad (2\text{-}23)$$

In the case being analyzed, the observed reaction rate is

$$\int_0^R r_{in}(S,r)4\pi r^2 dr$$

$$= \int_0^1 r_{in}(f,\xi)4\pi R^3 \xi^2 d\xi$$

$$= 4\pi R^3 \int_0^1 r_{in}(f,\xi)\xi^2 d\xi$$

The maximum possible reaction rate is

$$\int_0^R r_{in}(S_e,R)4\pi r^2 dr$$

$$= \int_0^1 r_{in}(1,1)4\pi R^3 \xi^2 d\xi$$

$$= 4\pi R^3 r_{in}(1,1)\int_0^1 \xi^2 d\xi$$

$$= \frac{4}{3} \pi R^3 r_{in}(1,1)$$

Therefore,

$$\eta = \frac{3 \int_0^1 r_{in}(f,\xi)\xi^2 d\xi}{r_{in}(1,1)} \qquad (2-24)$$

It is clear that internal diffusion is significant as $\eta \to 0$ and insignificant as $\eta \to 1$.

The concentration profile of substrate within the floc particle, which is the solution of Eq. (2-20), has to be determined before η can be calculated. Differential equations of the same form as Eq. (2-20) are not always analytically solvable and therefore numerical methods must be used. Among these methods, the orthogonal collocation method was chosen for this investigation because it is simple and powerful. Details of this method can be found elsewhere[30, 31, 47, 95, 128]. Only a brief discussion will be presented here.

Orthogonal Collocation Method

For the type of differential equation such as Eq. (2-20), with boundary conditions described by Eq. (2-21), the solution $f(\xi)$ can be chosen as follows[128]:

$$f(\xi) = f(1) + (1 - \xi^2) \sum_{i=0}^{n} \alpha_i P_i(\xi^2) \qquad (2-25)$$

where α_i are undetermined coefficients and $P_i(\xi^2)$ are Jacobi Polynomials of degree $2i$.

$$P_i(\xi^2) = 1 + \frac{(-i)(i+\frac{a}{2}+1)}{1!(\frac{a}{2})}\xi^2 + \dots + \frac{(i)(-i+1)..(-1)..(i+\frac{a}{2}+i)}{(i)!(\frac{a}{2})(\frac{a}{2}+1)....(\frac{a}{2}+i-1)}\xi^{2i}$$

$$(2-26)$$

where $a = 1, 2, 3$ are for rectangular, cylindrical and spherical coordinate systems respectively.

The collocation points ξ_j, $j = 1, 2, \dots, n$ are defined as the roots of the polynomials $P_i(\xi^2) = 0$.

Since $P_i(\xi^2)$ are polynomials of degree $2i$, the trial function as shown in Eq. (2-25) can be rewritten as[31]

$$f(\xi) = \sum_{i=1}^{n+1} \alpha_i \xi^{2i-2} \tag{2-27}$$

where α_i are constants.

If Eq. (2-27) is substituted into Eq. (2-20) and then evaluated at collocation points ξ_j, n equations will be generated which can be used to solve for n coefficients α_i. Thus the values of $f(\xi)$ and its Laplacian at collocation points are

$$f(\xi)\Big|_{\xi_j} = f(\xi_j) = \sum_{i=1}^{n+1} \alpha_i \xi_j^{2i-2} \tag{2-28}$$

and

$$\nabla^2 f(\xi)\big|_{\xi_j} = \frac{1}{\xi^2}\frac{d}{d\xi}(\xi^2\frac{df}{d\xi})\big|_{\xi_j} = \{\xi^{-2}\frac{d}{d\xi}(\xi^2\frac{d}{d\xi}\sum_{i=1}^{n+1}\alpha_i\xi^{2i-2})\}\big|_{\xi_j}$$

$$= \{\xi^{-2}\frac{d}{d\xi}(\xi^2\sum_{i=1}^{n+1}(2i-2)\alpha_i\xi^{2i-3})\}\big|_{\xi_j}$$

$$= \{\xi^{-2}\sum_{i=1}^{n+1}(2i-2)(2i-1)\alpha_i\xi^{2i-2}\}\big|_{\xi_j}$$

$$= \{\sum_{i=1}^{n+1}(2i-2)(2i-1)\alpha_i\xi^{2i-4}\}\big|_{\xi_j} \tag{2-29}$$

Both Eqs. (2-28) and (2-29) can be expressed in matrix notation as follows[31]:

$$\bar{f} = \bar{Q}\bar{\alpha} \tag{2-30}$$

$$\overline{\nabla^2 f} = \bar{D}\bar{\alpha}$$

where

$$\bar{Q} = \begin{vmatrix} \xi_1^0 & \xi_1^2 & \cdots & \xi_1^{2n} \\ \xi_2^0 & \xi_2^2 & \cdots & \xi_2^{2n} \\ \vdots & \vdots & \cdots & \vdots \\ \xi_{n+1}^0 & \xi_{n+1}^2 & & \xi_{n+1}^{2n} \end{vmatrix}$$

$$\bar{D} = \begin{vmatrix} 0 & 6 & 20\xi_1^2 & \cdots & (2n)(2n+1)\xi_1^{2n-2} \\ 0 & 6 & 20\xi_2^2 & \cdots & (2n)(2n+1)\xi_2^{2n-2} \\ \vdots & \vdots & \vdots & \vdots & \vdots \\ 0 & 6 & 20\xi_{2n+1}^2 & \cdots & (2n)(2n+1)\xi_{n+1}^{2n-2} \end{vmatrix}$$

$$\bar{\alpha} = \begin{vmatrix} \alpha_1 \\ \alpha_2 \\ \vdots \\ \alpha_{n+1} \end{vmatrix}$$

Solving for $\bar{\alpha}$, then

$$\bar{\alpha} = \bar{Q}^{-1}\bar{f}$$

(2-31)

$$\overline{\nabla^2 f} = \bar{D}\bar{\alpha} = \bar{D}\bar{Q}^{-1}\bar{f} = \bar{B}\bar{f}$$

Therefore, Eq. (2-29) becomes

$$\nabla^2 f(\xi)\Big|_{\xi_j} = \sum_{i=1}^{n+1} B_{ij} f(\xi)\Big|_{\xi_j} = \sum_{i=1}^{n+1} B_{ij} f(\xi_j)$$

(2-32)

where B_{ij} are elements of matrix B.

Then, Eq. (2-20) is converted to

$$\sum_{i=1}^{n+1} B_{ij} f(\xi_j) = \frac{\phi^2 f(\xi_j)}{1 + \beta f(\xi_j)}$$

(2-33)

The effectiveness factor can be evaluated by the following equation.

$$\eta = \frac{3\int_0^1 r_{in}(f,\xi)\xi^2 d\xi}{r_{in}(1,1)} = \frac{3 \sum_{i=1}^{n+1} w_i r_{in}\{f(\xi_j),\xi_j\}}{r_{in}(1,1)} \qquad (2\text{-}34)$$

where w_i are weights which can be calculated by the following equation.

$$\bar{w} = \{ \int_0^1 \xi^2 d\xi \quad \int_0^1 \xi^4 d\xi \quad \ldots \quad \int_0^1 \xi^{2(n+1)} d\xi \} \bar{Q}^{-1} \qquad (2\text{-}35)$$

It would be useful to know what degree of approximation is needed (i.e., the required number of collocation points, j) for the calculation of the effectiveness factor. When $1 \gg \beta f$, Eq. (2-20) is reduced to a first order equation, for which the analytical solution is available. The details of calculation of the effectiveness factor for a first order reaction is shown in Appendix 2, where it is shown that

$$\eta = \frac{3}{\phi^2}(\phi\coth\phi - 1) \qquad (A2\text{-}9)$$

The approximate values of η can be calculated through Eq. (2-36).

$$\sum_{i=1}^{n+1} B_{ij} f(\xi_j) = \phi^2 f(\xi_j) \qquad (2\text{-}36)$$

B_{ij} values were taken from Ref. (128). Table 2-2 shows both exact and approximate values of the effectiveness factor as a function of the Thiele-type modulus ϕ, and Figure 2-6 shows schematically the comparison of the exact and approximate values of η.

It is seen that for lower values of ϕ (say, $\phi \leq 4$), a single-point

TABLE 2-2

COMPARISON OF EXACT AND APPROXIMATE VALUES OF η
AS A FUNCTION OF ϕ, FOR DIFFERENT NUMBER OF
COLLOCATION POINTS. FIRST ORDER REACTION

ϕ	Exact	$i = 1$	$i = 2$	$i = 3$
1	0.9391	0.9391	0.9391	0.9391
2	0.8060	0.8069	0.8060	0.8060
3	0.6716	0.6769	0.6717	0.6716
4	0.5630	0.5774	0.5632	0.5630
5	0.4801	0.5070	0.4806	0.4801
6	0.4167	0.4581	0.4182	0.4167
7	0.3673	0.4235	0.3703	0.3674
8	0.3281	0.3987	0.3331	0.3286
9	0.2963	0.3803	0.3073	0.2996
10	0.2700	0.3665	0.2803	0.2706
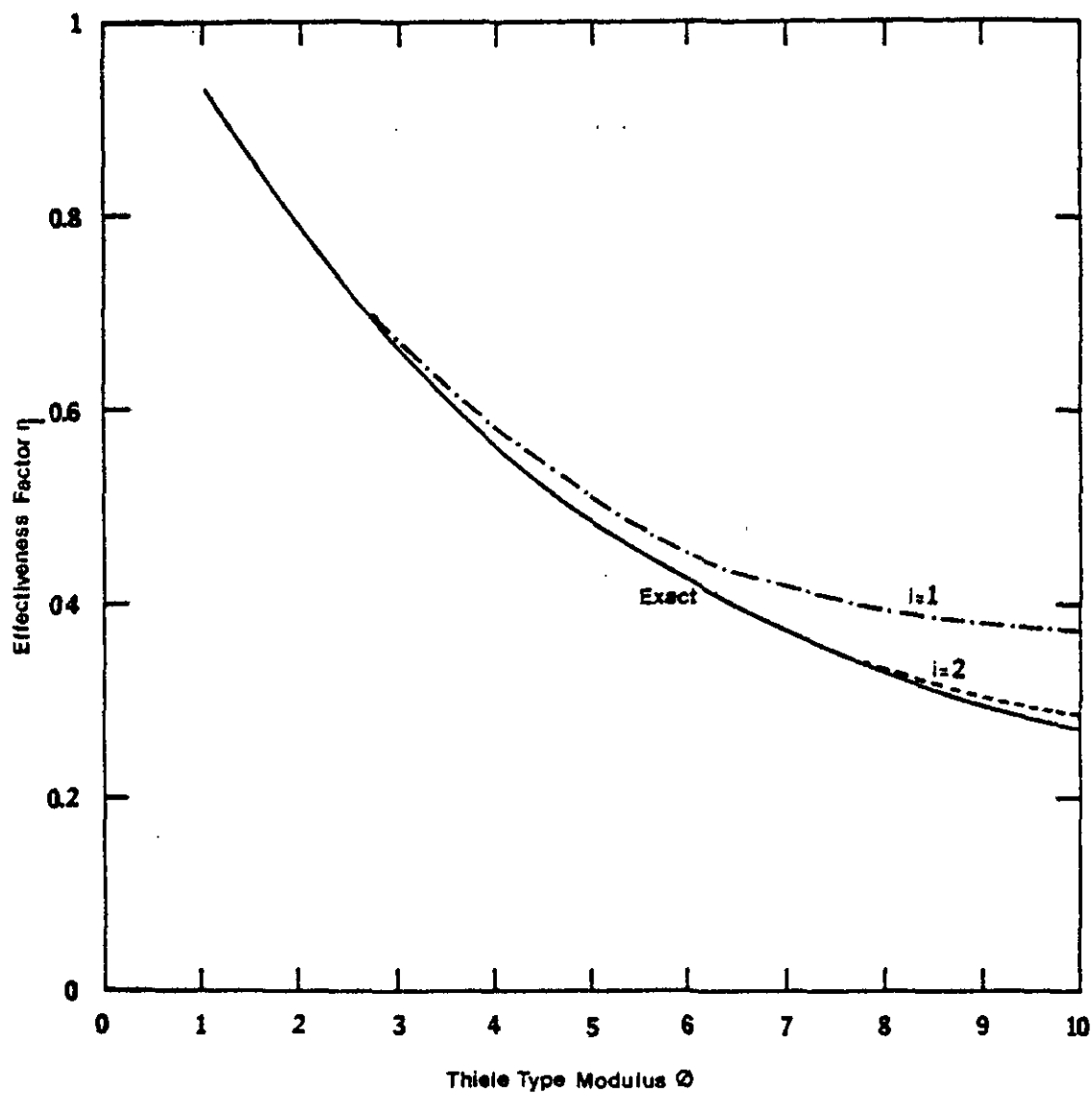
Figure 2-6 Comparison of the Exact and Approximate Values of

η as a Function of φ for 1 and 2 Collocation Points.

First Order Reaction

collocation approximation is adequate. This means that instead of the original differential equation a simple algebraic equation needs to be solved. For most applications a two-point approximation is sufficiently accurate[3, 95]. The error is only 4% when $\phi = 10$, whereas the computational procedure is greatly simplified without significant loss in accuracy.

When a two-point approximation is used, both Eqs. (2-33) and (2-34) are reduced to

$$
\begin{aligned}
B_{11}f(\xi_1) + B_{12}f(\xi_2) + B_{13}f(\xi_3) &= \frac{\phi^2 f(\xi_1)}{1 + \beta f(\xi_1)} \\
B_{21}f(\xi_1) + B_{22}f(\xi_2) + B_{23}f(\xi_3) &= \frac{\phi^2 f(\xi_2)}{1 + \beta f(\xi_2)} \\
B_{31}f(\xi_1) + B_{32}f(\xi_2) + B_{33}f(\xi_3) &= \frac{\phi^2 f(\xi_3)}{1 + \beta f(\xi_3)}
\end{aligned}
\tag{2-37}
$$

$$
\eta = 3(1 + \beta)\{ \frac{w_1 f(\xi_1)}{1 + f(\xi_1)} + \frac{w_2 f(\xi_2)}{1 + f(\xi_2)} + \frac{w_3 f(\xi_3)}{1 + f(\xi_3)} \}
\tag{2-38}
$$

Values of $\bar{B}$ and $\bar{w}$ for $i = 2$ are shown in Eqs. (2-39) and (2-40) respectively. The detailed calculation is shown in Appendix 3.

$$
\bar{B} = \begin{vmatrix}
-15.669962 & 20.034878 & -4.364917 \\
9.965122 & -44.330038 & 34.364917 \\
26.932855 & -86.932855 & 60
\end{vmatrix}
\tag{2-39}
$$

$$\bar{w} = \{0.0949059 \quad 0.1908084 \quad 0.04761905\} \tag{2-40}$$

Significance of Internal Diffusion Resistances on the Overall Rate

The presence of internal diffusion resistances in a heterogeneous reaction system, such as the activated sludge process, always masks the true kinetics of the system. As mentioned previously, the effectiveness factor provides for a convenient means to assess the importance of internal diffusion resistances. Their significance can be easily evaluated when effectiveness factor η is plotted as a function of ϕ^2. Such plots are shown in Figure 2-7. It is clear from these charts that the dependence of η on ϕ^2 becomes less important as β increases, i.e., when zero-order kinetics is approached. In this case, internal diffusion is insignificant for values of $\phi^2 < 100$. On the other hand, as β decreases, η becomes strongly dependent on ϕ which means that the reaction rate is significantly affected by internal diffusion.

Generally speaking, η can be experimentally measured once the true or intrinsic kinetic parameters are determined. In such a case Figure 2-7 is useful in estimating the effective diffusivity D_e for a specific particle size. Additionally, the critical particle size, at which internal diffusion resistances become significant, can be determined.

When the particles are very small the effectiveness factor approaches
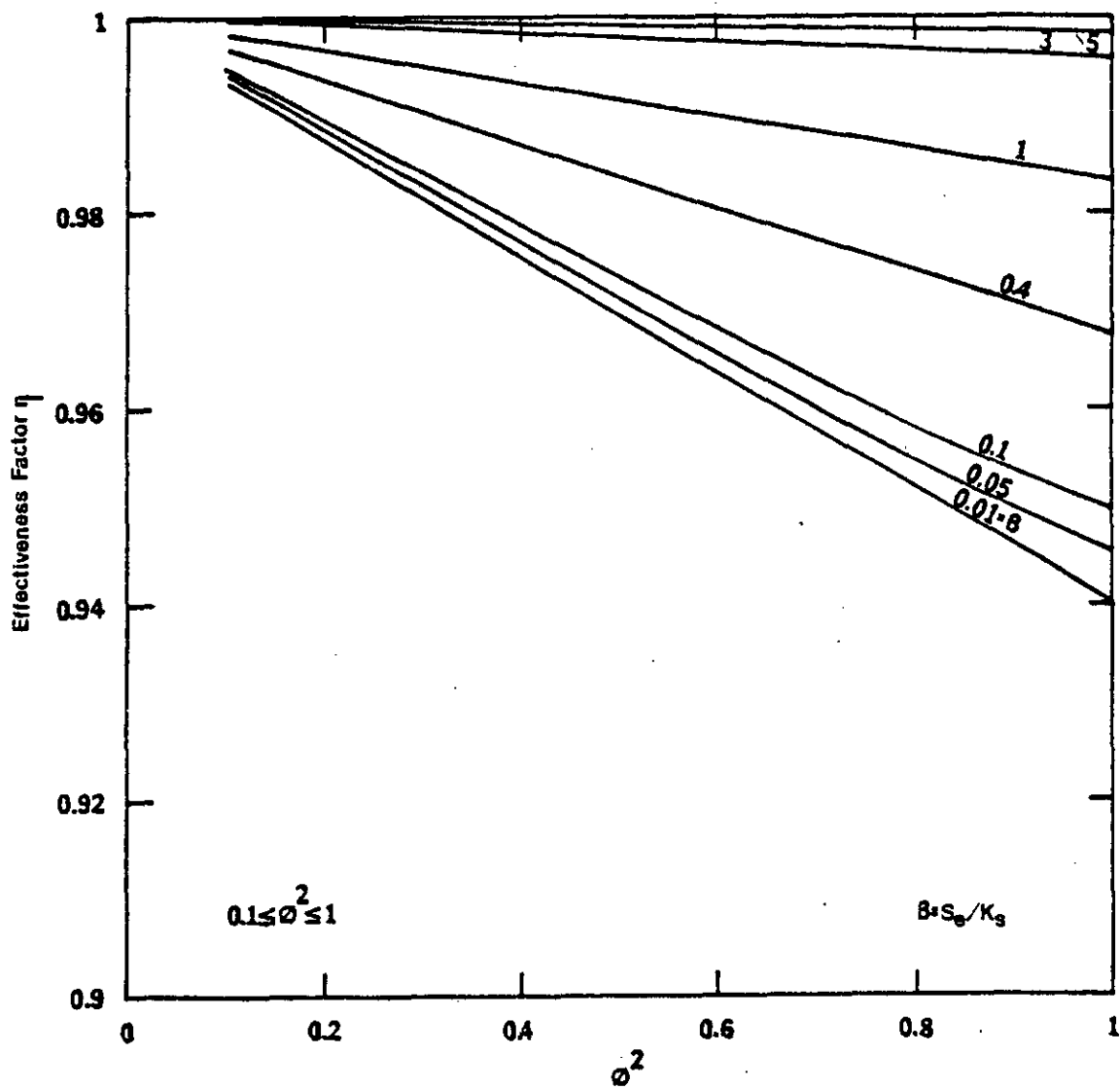
Figure 2-7 Effectiveness Factor Chart for Michaelis-Menten Kinetics, Spherical Particles

$$\phi^2 = R^2(\rho k/D_e K_s)$$
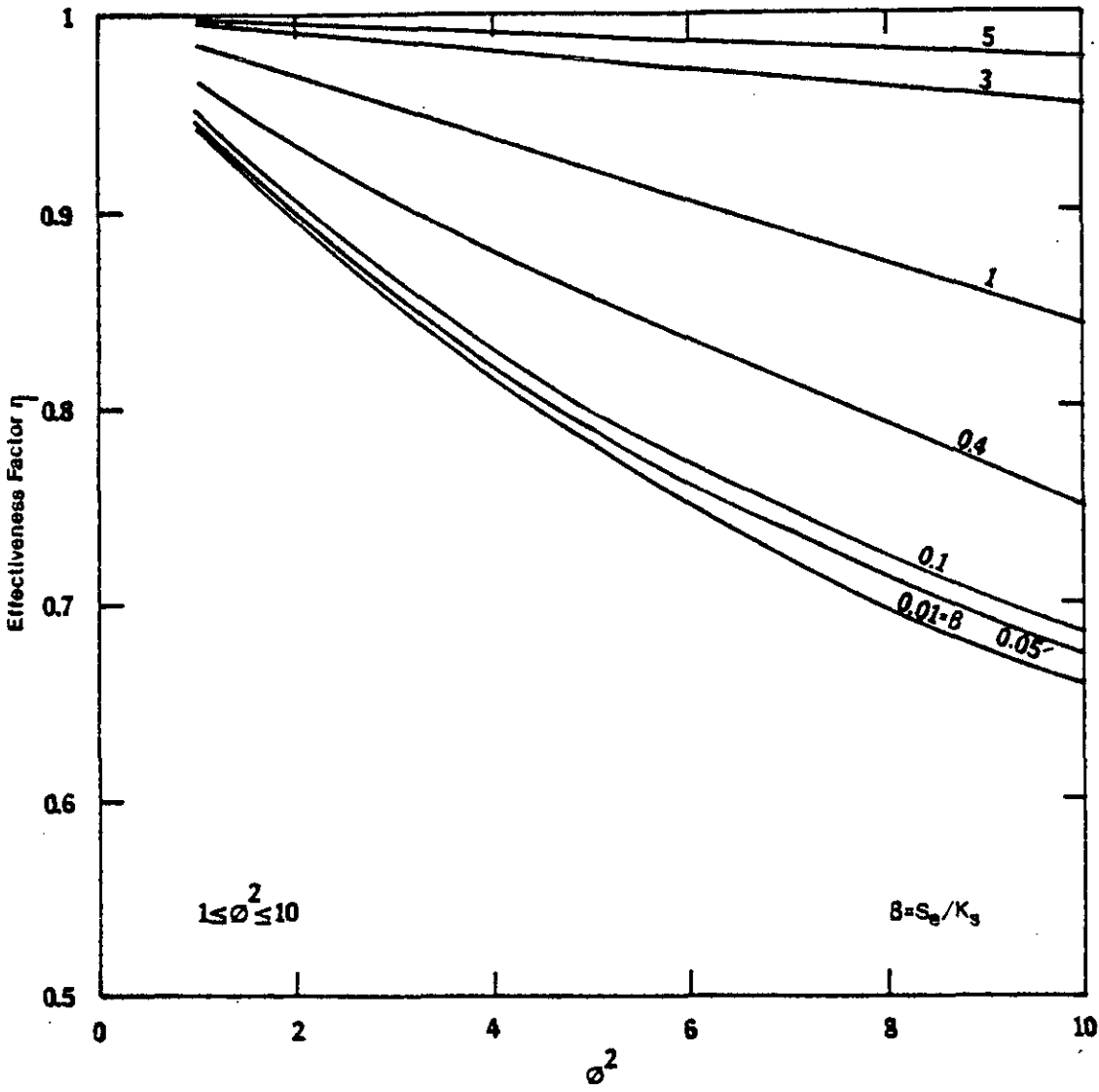
Figure 2-7 Continued
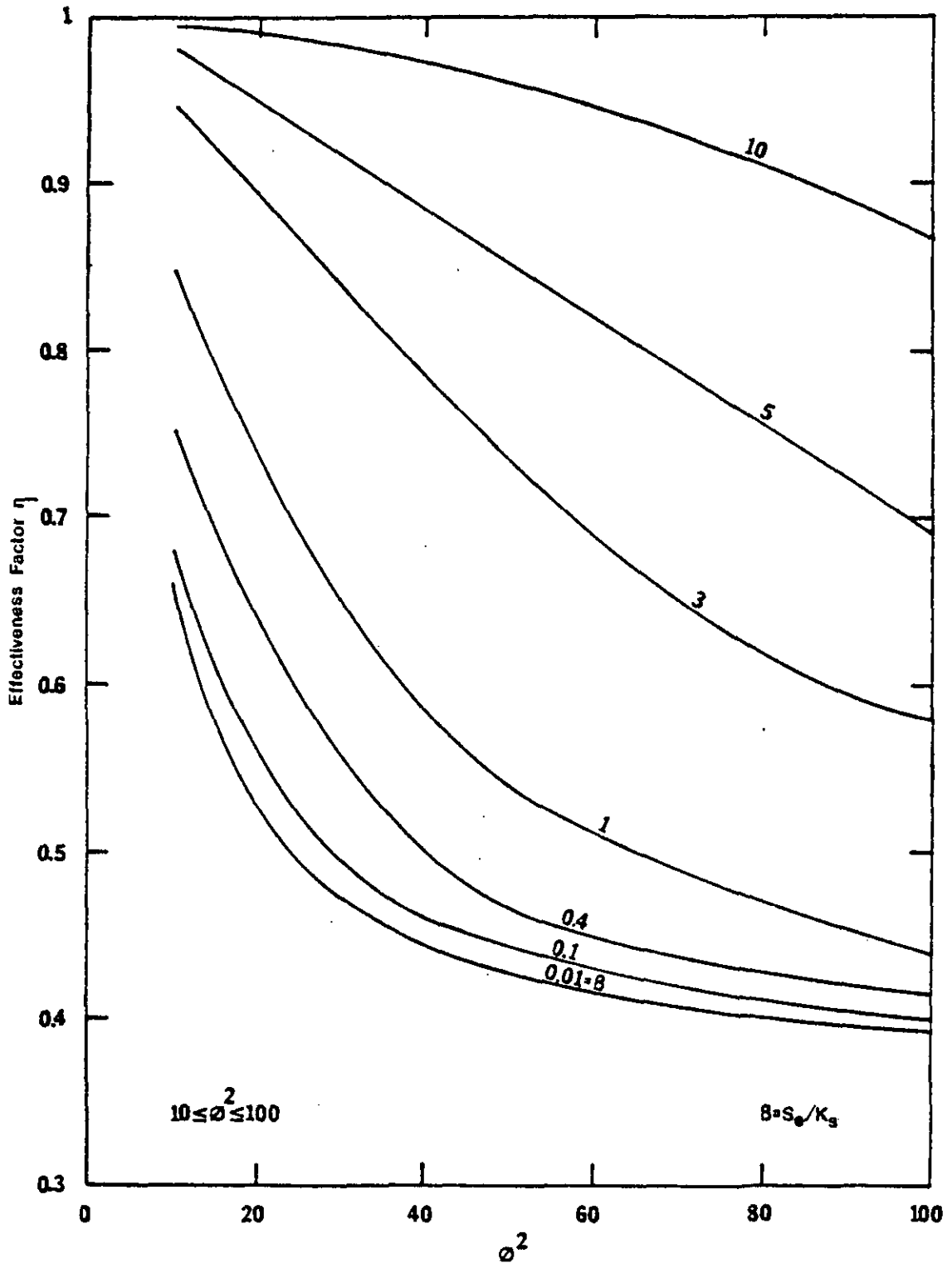
Figure 2-7 Continued
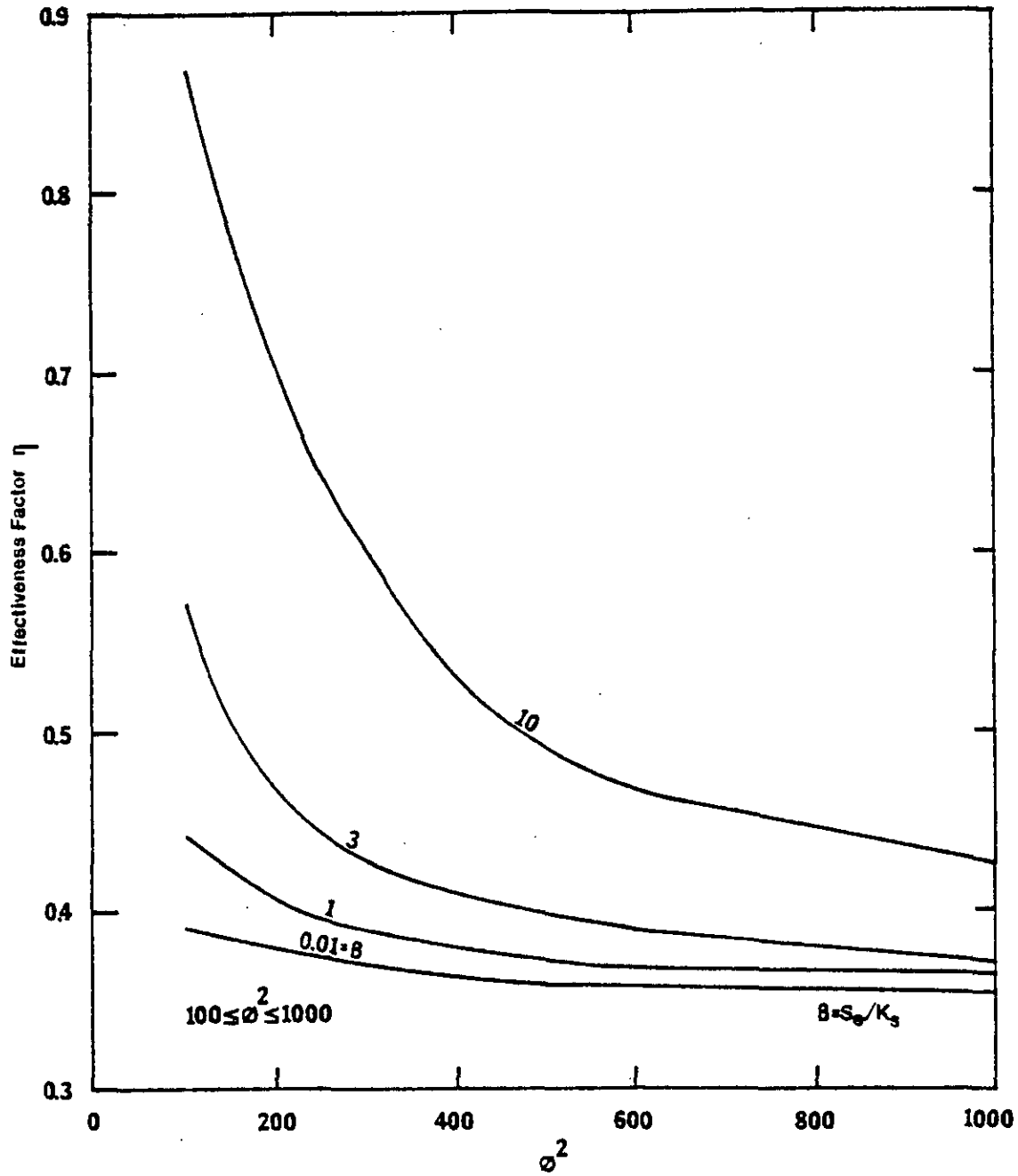
Figure 2-7 Continued

1.0, so it can be safely assumed that the observed rate is the intrinsic one. Rates observed under larger particle sizes will be affected by internal diffusion and will be lower than the intrinsic rate. The ratio of the former to the latter will yield experimental values of the effectiveness factor. Comparison of the theoretical and experimental values of η is an overall measure of the accuracy of the rate data, effective diffusivity, and intrinsic kinetics.

The effect of internal diffusion resistances on the observed reaction order, in biological film systems, has been observed and discussed by various investigators[42, 65, 67]. It is instructive, therefore, to examine such an effect if Michaelis-Menten kinetics is assumed in spherical floc particles. Figure 2-8 shows the curves obtained by plotting the ratio of the observed reaction rate to the saturation utilization rate, k, as a function of β, for different degrees of internal diffusion resistances. These resistances are evaluated through several ϕ^2 values. From these curves it can be seen that, at any given value of the ratio (observed rate/k), and at a fixed substrate concentration, different observed (apparent) values of the Michaelis constant, K_s, will be obtained, depending on the value of ϕ^2. Thus, if internal diffusion resistances are neglected, erroneous kinetic parameters may be obtained.
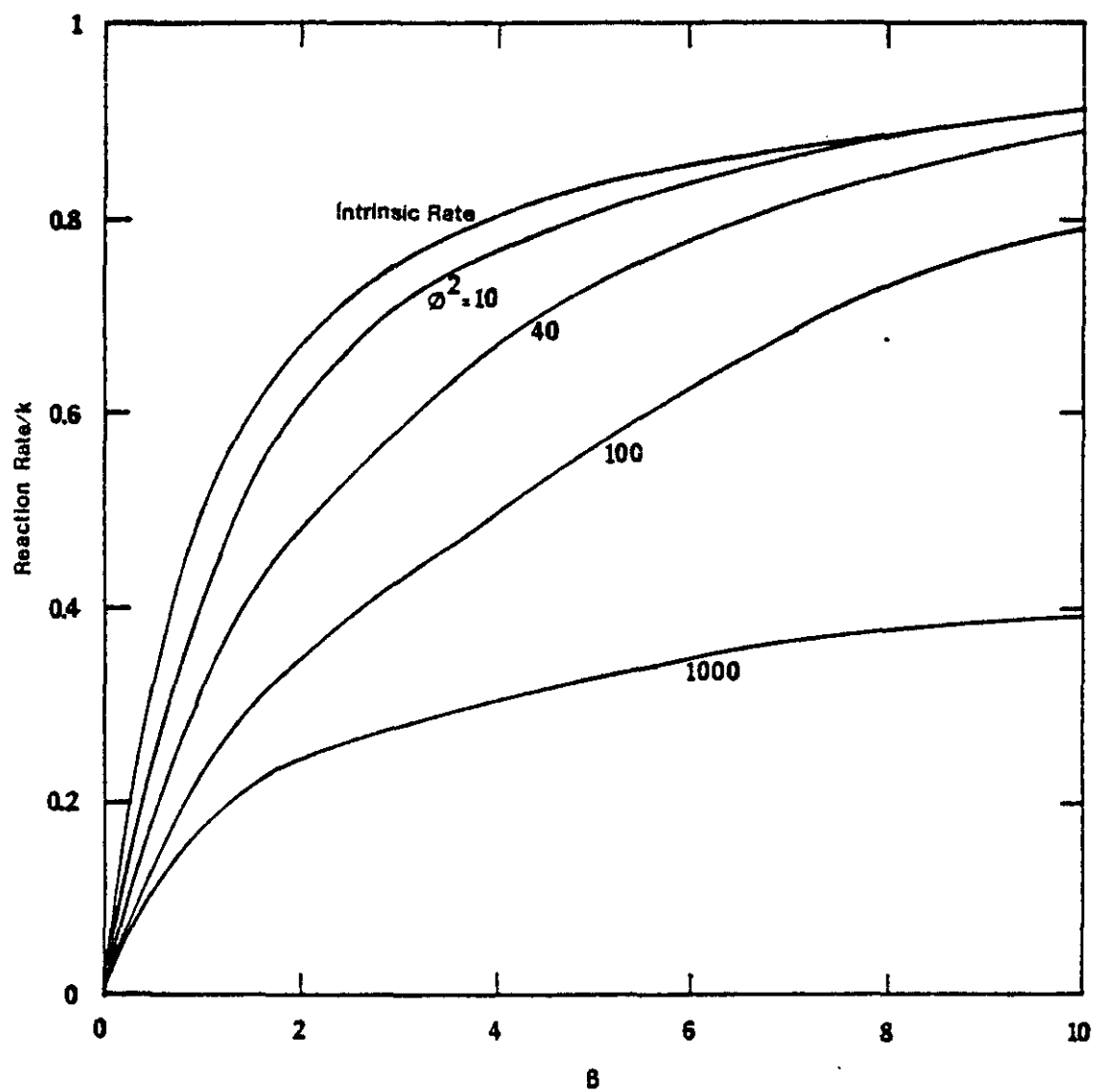
Figure 2-8 The Effect of Internal Diffusion Resistances on the
Observed Kinetics

The Lineweaver-Burk plot, that is, a plot of the reciprocal of the observed reaction rate versus the reciprocal of the steady state ambient substrate concentration, has been used extensively in heterogeneous catalysis and immobilized enzyme kinetics to evaluate both k and K_s from experimental data. Thus it is also instructive to examine the effect of internal diffusion on such a plot. By definition of effectiveness factor

$$\eta = \frac{v_o}{v_i} = \frac{v_o}{\dfrac{kS_e}{K_s + S_e}} \qquad (2\text{-}41)$$

where v_o and v_i are the observed and the intrinsic reaction rates respectively. Thus

$$v_o = \frac{\eta k S_e}{K_s + S_e} \qquad (2\text{-}42)$$

or

$$\frac{k}{v_o} = \frac{1}{\eta} + \frac{1}{\eta}(\frac{K_s}{S_e}) = \frac{1}{\eta} + \frac{1}{\eta}(\frac{1}{\beta}) \qquad (2\text{-}43)$$

Since η is a function of β, a plot of (k/v_o) versus $(1/\beta)$ should not yield a straight line. Such a plot is presented in Figure 2-9 for different degrees of internal diffusion resistances. It can be seen that as $(1/\beta)$ approaches zero (or β approaches infinite), $(1/\eta)$ approaches 1.0 because the reaction rate becomes less dependent on
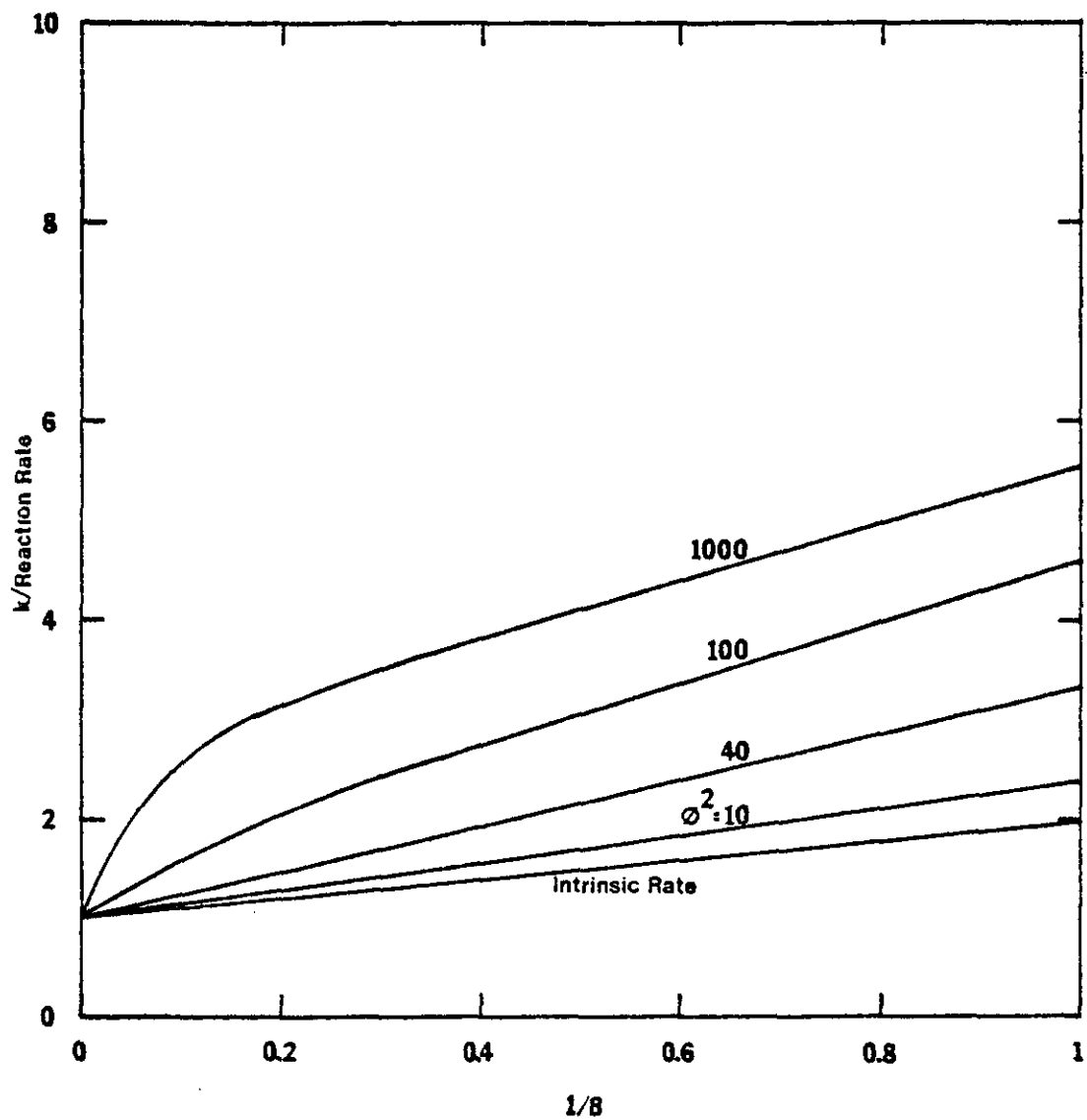
Figure 2-9 The Effect of Internal Diffusion Resistances on the
Lineweaver-Burk Plot

substrate concentration. This means that a single value of (k/v_o) would be obtained regardless of the degrees of internal diffusion resistances. At sufficiently high values of $(1/\beta)$ (or high values of K_s), $(1/n)$ becomes mainly dependent on the degree of internal diffusion resistances because the reaction rate approaches first-order kinetics (see Eq. (A2-9)). Therefore, a curve instead of a straight line would be obtained in the region of low $(1/\beta)$ values when internal diffusion is significant; a straight line is observed only when $(1/\beta)$ is sufficiently high. It is also interesting to note that the slope of the straight portion of the curve increases with increasing values of ϕ^2. Thus a higher value of K_s would be observed when internal diffusion resistances are significant, and a reduced overall rate is obtained. Figure 2-10 shows the effect of internal diffusion on the observed value of Michaelis constant, K_s'. This observed value will obviously mask the true kinetics of the system being studied. However, it is still possible to fit statistically a straight line through experimental data points with acceptable correlation coefficients even though they should not be on a straight line. This was observed and discussed by Regan, et al [96], Gondo, et al [37], Toda and Shoda [124], and Humphrey [52].

Based on the previous discussion, it is important to keep in mind
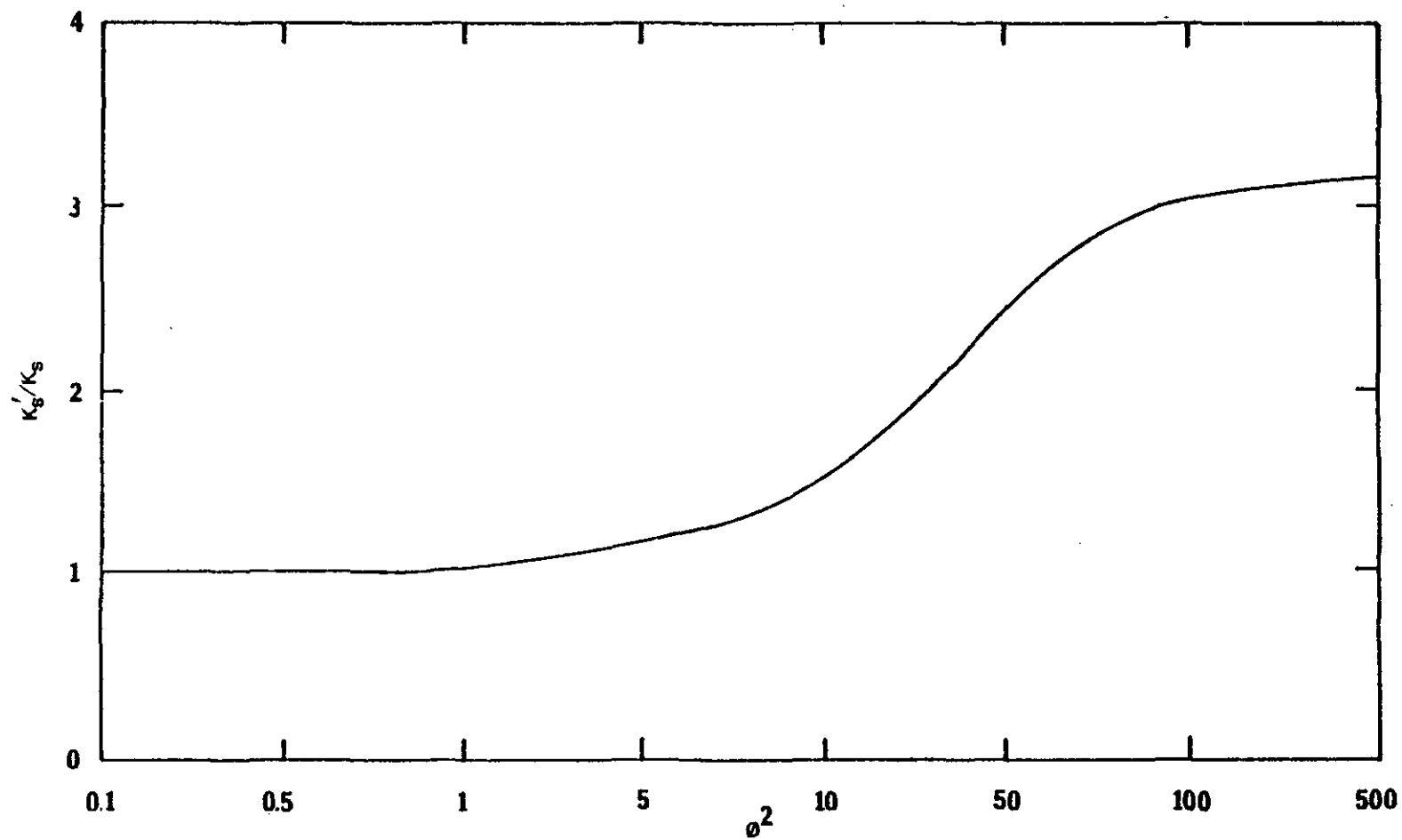
Figure 2-10 The Effect of Internal Diffusion Resistances on the Observed Values of

Michaelis Constant K_s'

that some precautions must be taken to eliminate internal diffusion

resistances when the Lineweaver-Burk plot is used to evaluate both k

and K_s from a limited amount of experimental data.

Kobayashi and Laidler[62], and Satterfield[103, 104] have suggested

that η = 0.95 and η = 0.60 can be taken as criteria for insignificant

and significant internal diffusion resistances respectively. Accordingly,

a plot of β versus ϕ^2 can be prepared as shown in Figure 2-11. Three

regions are formed. Region 1, located at the right side of the curve

corresponding to η = 0.60, corresponds to significant diffusion

resistances. Region 3, at the left side of the curve η = 0.95,

corresponds to intrinsic kinetics, that is, internal diffusion is

insignificant. Region 2 represents the conditions with intermediate

behavior, that is,both internal diffusion and reaction rate are

important. This diagram is helpful in arriving at a preliminary

conclusion on the importance of internal diffusion resistances in a

given system.

Figure 2-11 A Plot of ϕ^2 Against $\beta = S_e/K_s$

3. Region of Insignificant Internal Diffusion Resistances

2. Region of Intermediate Behavior

1. Region of Significant Internal Diffusion Resistances

$\eta = 0.95$

$\eta = 0.60$
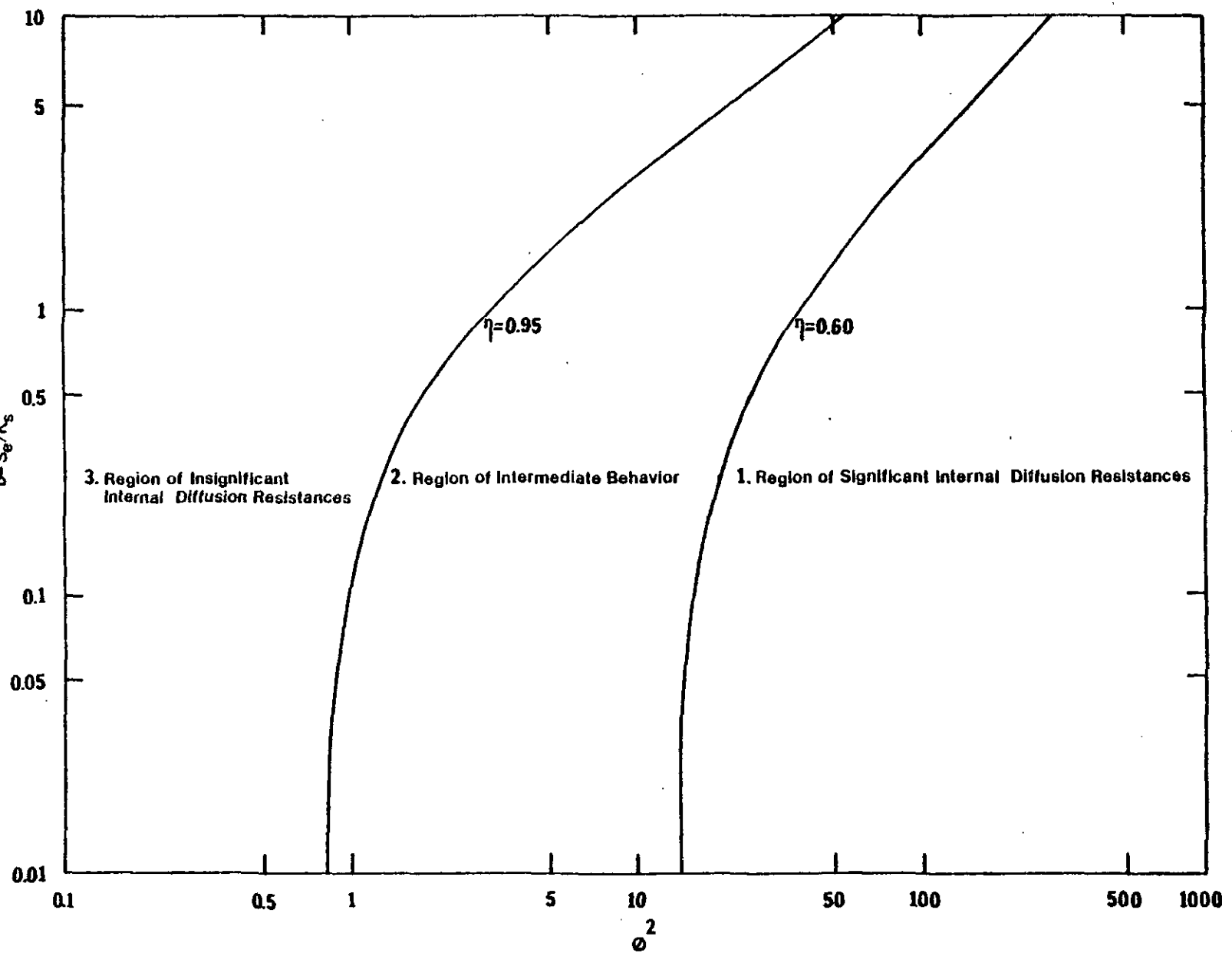
C H A P T E R . I I I

LITERATURE REVIEW

In the past few decades a large amount of research has been done in the area of kinetics of diffusion and reaction in various biological systems. A complete review of all the work accomplished thus far is beyond the scope of this dissertation and therefore only the key papers which are relevant to the objectives of this research have been selected. A literature review of the biological treatment systems available for nitrogen removal is also presented in this chapter.

Mass Transfer Resistances in Biological Systems

As pointed out previously, the biochemical reactions occuring in the biological systems are generally classified as heterogeneous. Therefore, the factors that affect the overall rate of reaction are different from those of homogeneous reactions in which only a single phase is involved. In the latter, temperature, pressure, pH, and composition are important factors. If they are maintained at optimum levels, it is usually found that the biochemical reaction rate becomes rate-limiting. On the other hand, in heterogeneous systems, the rates

of mass transfer become important because materials involved in the

reactions must be transferred from one phase to another. The study of

the overall rate in this system then involves a separation of the

"physical" features, notably mass transfer and fluid mechanical

phenomena, from the "reaction" features, i.e., the biochemical

kinetics[10]. Such a division allows a more detailed appreciation of

the effect of changes of variables and more knowledgeable

interpretation of experimental data.

Transport of substrate from the bulk of liquid to the outer surface

of the biological floc. It has been discussed in Chapter II that the

transport of substrate in the nutrient medium, under laminar flow

conditions, can be described by the continuity equation, namely, Eqs.

(2-2) and (2-3). The predominance of either mechanism (convection

and molecular diffusion) on the overall rate of mass transfer can be

judged by the value of a parameter called Peclet Number, N_{Pe}, which

is defined by Eq. (2-4). It was shown that even under laminar flow

conditions and low flow velocities, the value of N_{Pe} is still very

high, indicating that convective mass transfer predominates over

molecular diffusion. This is true in the activated sludge process

where vigorous agitation is provided by either diffused air or

mechanical systems. It is, therefore, reasonable to assume that the

substrate concentration in the aqueous phase is uniform.

It has been found that the mass transfer coefficient k_{CA} is related to such parameters as reactor size, diffusivity of substrate in the aqueous phase, viscosity of the liquid, relative velocity between the particle and the fluid, etc..

Marangozis and Johnson[75] derived the following correlation of mass transfer data in a solid-liquid system for baffled agitated vessels, with $5000 \leq N_{Re} \leq 60,000$:

$$\frac{k_{CA}d_v}{D} = 0.402(\frac{\mu_\ell}{\rho_\ell D})^{0.333}(\frac{\bar{r}d_r^2\rho_\ell}{\mu})^{0.65} \tag{3-1}$$

where

d_r = rotor diameter, cm

d_v = vessel diameter, cm

D = diffusivity of the solute in the solvent, cm^2/sec

μ_ℓ = viscosity of the fluid, poises

ρ_ℓ = density of the fluid, gm/cm^3

$\bar{r}$ = rpm, rev/sec

An empirical formula was proposed by Sykes and Gomezplata[120] to evaluate k_{CA} in a particle-liquid system in stirred tanks. The value of k_{CA} was found to be affected by the type of agitator used, as indicated below:

$$\frac{k_{CA}d}{D} = 2 + 0.109(N_{Re}^*)^{0.38}(\frac{\nu}{D})^{0.50} \qquad (3\text{-}2)$$

where

d = particle diameter

ν = kinematic viscosity of fluid

$$N_{Re}^* = (\frac{\psi_{imp}}{\psi_{fdt}})^{0.333} (\frac{nd_i^2}{\nu})$$

d_i = impeller diameter

$$\psi = P/\rho_{\ell}n^3d_i^5$$

P = impeller power

n = impeller speed

imp = impeller system

fdt = fan disk turbine system

In their experiments with biological flocs, Mueller[85] and Baillod[13, 14] used Eq. (2-8)[22] to evaluate the significance of external diffusion resistances on the overall oxygen uptake rate in the former, and glucose uptake rate in the latter.

Levin and Glastonbury[71] developed a correlation of mass transfer rate in a stirred tank for a particle-liquid system. They found that k_{CA} was strongly dependent on the density difference between fluid and particle. For particles close to neutral buoyancy, the mass transfer

correlation can be represented by

$$\frac{k_{CA}d}{D} = 2 + 0.47\left(\frac{d^{0.75}\varepsilon^{0.33}}{\nu}\right)^{0.62}\left(\frac{d_i}{d_v}\right)^{0.17}\left(\frac{\nu}{d_v}\right)^{0.36} \tag{3-3}$$

where ε is the energy dissipation rate per unit mass of fluid.

For particles with significantly different density, then

$$\frac{k_{CA}d}{D} = 2 + 0.44\left(\frac{dv_f}{\nu}\right)^{0.5}\left(\frac{\nu}{d}\right)^{0.38} \tag{3-4}$$

Based on the above discussion it can be concluded that there is sufficient information to calculate the external mass transfer coefficient. However, its experimental evaluation has been attempted by relatively few investigators.

External diffusion in biological waste treatment systems. Maier, et al[74] presented a theory which considered external mass transfer of substrate and the growth of microorganisms as the underlying phenomena prevailing in the trickling filter. They observed that the liquid feed rate had a marked effect on the rate of glucose uptake at low flow rates; however, at high flow rates, glucose uptake became independent of the feed rate. Unfortunately, Maier, et al[74] used the inclined plate reactor, which does not allow clear differentiation between kinetic and diffusion regimes. Therefore, their conclusions

are questionable.

The analogy between a microbial floc and a porous catalyst particle was observed by Atkinson and Daoud[7, 8]. They proposed a mathematical model for the flux of reactant through the interface between the microorganisms and the adjacent solution, both for biological films and suspended growth systems. This mathematical model was similar to those which had been applied in heterogeneous catalysis, and was found to be in general agreement with available experimental data. Their results also showed that liquid phase diffusion had considerable influence on the performance of continuous flow film reactors.

In his study with a biological film reactor, using glucose as the substrate, La Motta[65] was able to show that external diffusion resistances could be eliminated when the linear velocity exceeded 0.8 m/sec.

Sylvester and Pitayagulsarn[121] derived an analytical model for the trickling filter process which included the effect of liquid-phase mass transfer (external diffusion resistances) on the BOD removal efficiency. It was shown that liquid-phase mass transfer resistances could significantly affect BOD removal for a given trickling filter. The solutions which were presented could be used to determine the

kinetic rate constant if the BOD removal and the external mass transfer effect were known. Additionally, if the kinetic constant and the mass transfer coefficient are known, the charts they presented allow the prediction of the required filter depth for a given BOD removal efficiency. It is important to note that internal diffusion resistances were not considered in their analysis. Their model is not applied to such a situation when liquid velocity becomes high enough to eliminate the external diffusion resistances.

A mathematical model was formulated by Harris and Hansford[43] to describe the mechanism of substrate removal by microbial slime. Their system consisted of a flat plate over which a liquid film containing substrate was flowing. Basic chemical engineering principles of interfacial mass transfer, diffusion and biochemical reactions were used in the formulation of the model. Good agreement between the experimental data and the model predictions was obtained.

Rickard and Gaudy[99] studied the effect of mixing energy on sludge yield and cell composition. By expressing mixing energy in terms of velocity gradient, G, they showed that the oxygen uptake rate of activated sludge increased with increasing G values (from 0 to 1400 sec^{-1}). Although they mentioned that there were five possible mechanisms which could be advanced to explain the increasing oxygen

uptake rate, they concluded that the higher rates they observed when the turbulence was increased probably resulted from reduction in the cell-liquid interfacial resistance to oxygen transfer. However, based on the analysis presented in Chapter II of this dissertation, it seems unlikely that this conclusion is valid because external diffusion resistances are insignificant in the activated sludge system.

External diffusion in enzyme systems. The kinetics of catalysis of whole-cell E.Coli lactose, immobilized on spherical agar gels, was determined by Toda[125] under the influence of external diffusion resistances in a fixed bed reactor. Within the limited conditions of the experiments, it was observed that the apparent Michaelis constant K_s' (Michaelis-Menten kinetics was assumed) was notably influenced by the low flow rate and increased significantly when the velocity was decreased below 0.05 cm/sec, while with flow rates higher than 0.1 cm/sec, the value of K_s' was close to the intrinsic one, K_s. On the other hand, the apparent saturation utilization rate k' was practically equal to the intrinsic value. It was concluded that the influence of flow rate on K_s' at low flow rates was brought about by external diffusion resistances.

Rovito and Kittrell[100] reported quantitatively the effect of external diffusion on the reaction rate of glucose oxidase immobilized

on porous glass in a continuous, tubular, packed bed reactor. Their

results showed that external diffusion resistances are significant

when Reynolds Number, N_{Re}, defined by the relative velocity between the

fluid and the glass, ranged from 0.2 to 25.

Ramachandran[94] developed a comprehensive model including the effect

of both kinetic and physical parameters for a packed bed encapsulated

enzyme reactor. The significance of external diffusion resistances on

the overall performance of the process was clearly demonstrated.

In summary, external diffusion resistances of substrate can be

significant when the relative velocity between fluid and biomass is

relatively low and when the particles are large. In the activated sludge

process, where sufficient agitation is provided to keep the flocs in

suspension, and the floc particles are relatively small, external

diffusion resistances are negligible. However, in the case of biological

film systems, external diffusion is important. In kinetic studies, the

predominance of external diffusion resistances will mask the true kinetics

of the reaction unless high mass transfer rates are introduced.

Transport of substrate within the biomass. The diffusion of substrate

in the biomass will establish a concentration gradient within it, and

therefore, the interior part of the biomass will be exposed to lower

substrate concentrations than the part near the surface[65, 103, 104].

If the reaction rate is a function of the local substrate concentration, then the overall reaction rate will be less than that which would be observed if all the internal active sites were exposed to the substrate concentration at the outer surface. The significance of internal diffusion on the overall rate has received a great deal of attention in the kinetics of immobilized enzyme and in heterogeneous catalysis. However, the similar problem occurring in the biological waste treatment process has received very little attention until recently. Only in the last decade various investigators have demonstrated its importance in the interpretation of the observed kinetic data.

Internal diffusion in biofilms.

(a) Glucose:

Atkinson and Daoud[7, 8] developed a mathematical model that takes into account internal diffusion and reaction in biological film systems. Later they applied this model to a film reactor, using glucose as the substrate[9, 11, 12]. With this model, and experimentally determined kinetic constants, they were able to predict the performance of the biological film reactor under different operating conditions. One interesting conclusion drawn by the authors was that the same functional expression was applicable to both microbial flocs and films.

Thus, in the authors' opinion, this model provided a convenient and useful basis to experimentally determine kinetic parameters, since biomass geometry has no significant effect on reaction kinetics.

Kornegay and Andrews[64] presented a kinetic model to describe the substrate utilization in fixed-film biological reactors. By recognizing the fact that the entire mass of the attached microorganisms was not active in the removal of soluble substrate, the model was applied to the active portion of the biomass only. Their experimental results showed that the substrate removal rate increased with increasing film thickness until a critical value was reached, beyond which no further increase in substrate removal rate was observed. The agreement between the theoretical curve and the observed results supported the validity of the proposed model. However, no explicit term accounted for diffusion effects. The inclusion of an active thickness in this model considered indirectly the effect of internal diffusion resistances on the observed substrate removal rate.

La Motta[65, 67] presented a theoretical model describing diffusion of substrate and simultaneous zero-order substrate consumption in biological films. The model predicted that the substrate removal rate was proportional to film thickness up to a certain value, beyond which the rate becomes constant. His experimental

data confirmed the theoretical predictions. It is worthwhile

emphasizing that both models suggested by Kornegay and Andrews[64],

and La Motta[65, 67] reached similar conclusions although different

types of kinetic expressions were proposed. La Motta's model was able

to confirm the observations of Hoehn[48, 49], Sanders[101], and

Tomlinson and Sneddon[126], as well as Kornegay and Andrews[64].

La Motta's model also demonstrated that if the intrinsic kinetics is

zero-order, the observed reaction rate will be half-order when internal

diffusion effects are significant. Similar conclusions were arrived at

by Harremoes[41, 42] in his experiments with biological film systems.

(b) Oxygen:

Bungay, et al[25] used a microprobe technique to measure the

diffusivity of oxygen in a microbial slime system. With a dilute

substrate medium, the oxygen profile was found to remain at a high and

uniform concentration within the film, indicating substrate-limited

respiration. A more concentrated medium caused the oxygen profile

to fall to low levels within the film, thus indicating oxygen-limited

respiration. Based on well-known internal diffusion equations, the

diffusivity of oxygen within the film was estimated to be 4.0×10^{-7}

cm^2/sec, while the corresponding value in medium was $8.3 \times 10^{-6} cm^2/sec$.

Bungay and Harold[26] developed a model to describe oxygen

transfer from a flowing nutrient medium into a biological film.
Oxygen concentration profiles were generated at several distances
downstream from the start of the slime. The nutrient medium was
assumed rich and thus the oxygen transfer rate limited microbial
respiration. The model predictions agreed reasonably well with the
experimental data.

An equation describing the fate of a substrate, under oxygen and
substrate limiting conditions was derived by Sanders and Bazin[102]
for a packed column reactor. When oxygen was limiting the observed
reactions obeyed zero-order kinetics, while in the substrate-limited
process, half-order kinetics occured. The model developed demonstrated
clearly the effect of diffusion of substrate on the observed reaction
kinetic order, in agreement with the observations of other
investigators[41, 42, 65, 67].

Based on the analysis of mass transfer of oxygen through both a
liquid film and the biological slime in trickling filters, Schroeder
and Tchobanoglous[105] calculated the maximum expected oxygen flux for
a standard plastic-media trickling filter. From this expected value,
the maximum allowable influent bulk substrate concentration was
determined. They concluded that the appropriate maximum applied
ultimate BOD should be around 400 mg/ℓ. The mass transfer rate of

oxygen might become limiting if the applied BOD is in excess of 500 to 600 mg/ℓ. This is especially important when the process is used to treat high strength BOD wastewaters.

(c) Nitrogen:

A mathematical model was presented by Williamson and McCarty[135, 136, 137] in which substrate utilization within biofilms was described as a process of diffusion with simultaneous reactions. Both experimental and predicted results were in reasonable agreement. However, instead of using well developed biological films, they prepared the film by filtering suspended growth cultures through the filter paper. This procedure is questionable because the structure and the inherent properties of both types of films may be different; therefore, the observed experimental data may not represent actual film behavior.

In an attempt to interpret denitrification data obtained from a pilot plant anaerobic filter, Harremoës and Riemer[41, 42] used the pore-diffusion model to describe substrate diffusion and simultaneous zero-order reaction. The model predicted that the observed denitrification rate, under the influence of significant pore-diffusion resistances, should follow half-order kinetics. Model predictions and experimental data agreed reasonably well.

Diffusion in biological flocs.

(a) Glucose:

Baillod[13, 14] was one of the first investigators to demonstrate

that floc size can affect substrate uptake rate. His theoretical

analysis of diffusion and zero-order reaction within the biological

floc predicted reasonably well the experimental data. By blending

his batch culture he was able to observe the intrinsic glucose uptake

rate, which was different from that of flocculated suspensions. He

concluded that the major portion of the difference between the glucose

uptake rate of the flocculated and blended cultures was due to the

diffusion resistances to glucose transfer afforded by the floc matrix

itself.

(b) Oxygen:

Pasveer[91] conducted a theoretical study of the distribution of

oxygen in the activated sludge floc, and demonstrated that the degree

of turbulence in the mixed liquor could be an influential factor in

promoting the transfer of oxygen to the floc and thus increasing the

rate of biochemical oxidation. With high turbulence the floc size

would become smaller and a high concentration of oxygen would be

maintained within the floc. His theoretical analysis showed that for

a floc radius of 100 microns, the oxygen concentration at the floc

center would be 78.1% of that in the bulk liquid under strongly

turbulent conditions, and only 45.5% under slightly turbulent

conditions. As the floc size decreased to 10 microns, the oxygen

concentration at the center would be 99.7%.

Mueller, et al[85] proposed that internal diffusion resistances

limited the overall oxygen uptake rate of pure flocs of Zoogloea

Ramigera when utilizing glucose as substrate. Their experimental data

regarding oxygen uptake rate for both blended and nonblended floc

particles indicated that, at certain D.O. levels, diffusion of oxygen

through the floc matrix was the mechanism controlling the oxygen

utilization rate by the floc.

Matson, et al[77] evaluated the significance of mass transfer

limitations of oxygen and substrate in the activated sludge process

and concluded that the major resistance to oxygen and substrate

transfer was the floc itself; that is, internal diffusion resistances

significantly affected the overall reaction rate. They also suggested

that increased turbulence could stimulate the waste degradation rate by

reducing floc size and increasing the D.O. level. One interesting

conclusion was that biological processes treating soluble wastes were

likely to be rate controlled by oxygen rather than substrate. Their

approach, however, is questionable because they assumed that the ratio

of diffusivity of oxygen to that substrate (glucose) was the same in

both water and floc which may not be true.

Matson and Characklis[78] developed a method to measure the

effective diffusivities of oxygen and glucose through microbial

aggregates grown under various experimental conditions. They found

that diffusivities of oxygen and glucose were affected by the sludge

age of the cultures that had been used to prepare the film. By

filtering the suspended growth cultures through the millipore filter

and using mercuric chloride to kill the viable cells, they claimed the

observed difference of substrate concentrations at both sides of the

film and filter was due to the diffusion mechanism only. Their approach,

similar to that used by Williamson and McCarty[135-137], is also

questionable.

<u>Effect of internal diffusion resistances on the observed values of</u>
<u>kinetic parameters of Michaelis-Menten kinetics in immobilized enzymes.</u>
As pointed out in Chapter II, the Lineweaver-Burk plot has been used to

determine the parameters k and K_s. Strong internal diffusion effects

affect the shape of the plot, which no longer yields straight lines.

However, several researchers have drawn staight lines through the

Lineweaver-Burk plots of their data, obtaining apparent values of k

and K_s.

Kobayashi, <u>et al</u>[63] studied the oxygen transfer rate into

mycelial pellets.assuming Michaelis-Menten kinetics. The experimental results showed that the specific rate of respiration decreased significantly with increasing pellet size. In analyzing the data they drew straight lines on the Lineweaver-Burk plots even when internal diffusion resistances to oxygen transfer were significant. The apparent Michaelis constant was usually larger as internal diffusion became more significant.

Based on the theoretical analysis of the kinetics of solid-supported enzymes in which diffusion effects were significant, Kobayashi and Laidler[62] developed methods for analyzing experimental results. They demonstrated that the Michaelis-Menten law applied to such a system; however, the observed kinetic parameters were only apparent, their values being influenced by diffusion effects. The method suggested by the authors allowed the true parameters to be derived from the experimental data.

Regan, et al[96] developed numerical solutions to the equations describing simultaneous mass transfer and enzymatic reaction within porous spherical particles. These equations were used to examine the effects of enzyme content and other parameters on the kinetics of immobilized enzymes. The effect of internal diffusion resistances on the Lineweaver-Burk plot was examined. They showed that when internal

diffusion limitation was occuring inside the particles, the

Lineweaver-Burk plot of the data could still be almost linear over a

wide range of substrate concentrations, but the values of k and K_s

obtained from such a plot were likely to be very different from the

real values. They concluded that it is necessary to use small

particles to obtain the intrinsic values for k and K_s.

The effect of internal diffusion on both the slope and the

intercept of the straight line obtained in the Lineweaver-Burk plot,

for immobilized enzyme kinetic data, was considered by Gondo, et al[37].

Using a wide range of substrate concentrations, they arrived at similar

conclusions to those obtained by Regan, et al[96].

Toda and Shoda[124] studied sucrose hydrolysis reaction by using

whole-cell invertase of Sacharomyces Pastorianus, entrapped in

spherical agar pellets, in a CFSTR. Their experimental results showed

clearly that mass transfer resistances were significant when particle

size was large. Under such conditions the apparent values of k and K_s

were significantly different from the intrinsic ones. The theoretical

model developed considered internal diffusion resistances and

simultaneous reactions as controlling factors. Predicted and

experimental results were in good agreement over a wide range of

substrate concentration.

Oxygen transfer to and within fungal pellets was studied by Miura, et al[84]. The oxygen uptake rate of the pellets was evidently increased by agitation. They concluded that oxygen was transfered throughout the pellet with an effective diffusivity, D_e, which was enhanced by agitation. The calculated values of D_e varied from the molecular diffusivity in water to infinity. Their approach to analyze the experimental results was obviously wrong. The observed improvement in oxygen uptake rate was contributed by a decrease in internal diffusion resistances, not by the increase in D_e. Ngian and Lin[89] disagreed with their approach and pointed out that the oxygen uptake rate was affected by the internal diffusion resistances as evidenced by the decreasing values of the Michaelis constant as the degree of agitation increased.

Kinetics of Nitrification

Many of the commonly used biological wastewater treatment processes employ bacteria as the primary microorganisms. While the metabolic pathways may be different (e.g. aerobic versus anaerobic), the process of substrate utilization and subsequent microbial growth are quite similar in all biological systems. Therefore, it is possible to develop a general relationship which can be applied to a wide variety

of processes.

Biological nitrification is carried out by two genera of bacteria (nitrifiers) that sequentially oxidize ammonium to nitrate with intermediate formation of nitrite. The first group of bacteria which oxidize ammonium to nitrite is called <u>Nitrosomonas</u>. The second group of bacteria, <u>Nitrobacter</u>, oxidize nitrite to nitrate. The overall oxidation reaction is shown as follows[93].

$$NH_4^+ + 2O_2 \rightarrow NO_3^- + 2H^+ + H_2O \qquad (3-5)$$

This reaction provides the energy required by nitrifiers while the source of carbon is CO_2. If the cell composition formula is assumed to be $C_5H_7NO_2$, then the overall oxidation and synthesis reaction can be represented by[93]

$$NH_4^+ + 1.83O_2 + 1.98HCO_3^- \rightarrow 0.021C_5H_7NO_2 + 1.041H_2O + 0.98NO_3^- +$$

$$1.88H_2CO_3 \qquad (3-6)$$
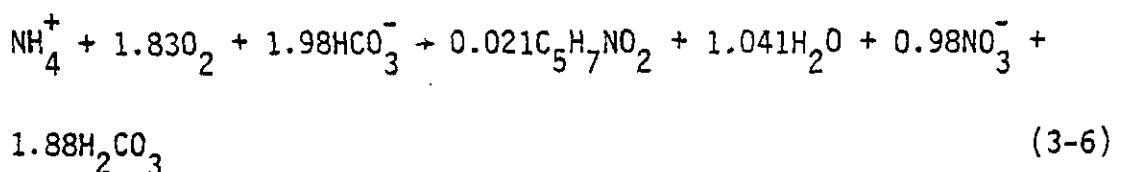
Various investigators[68, 90, 93, 118] have shown that the maximum growth rate of <u>Nitrobacter</u> is considerably larger than that of <u>Nitrosomonas</u>. Thus nitrite does not accumulate in large amounts in biological wastewater treatment systems. For this reason, the rate-limiting step in the biological nitrification is the conversion of ammonium to nitrite.

Environmental engineers often deal with reactor design, for which an understanding of the rate expression is needed. The following discussion is restricted to the rate expressions that have been proposed for the biological nitrification process.

Zero-order kinetics. The reaction can be considered as zero-order kinetics if the reaction rate is independent of the substrate concentration, or

$$\frac{1}{X} v = -k_o \qquad (3-7)$$

where

v = reaction rate, mol/ℓ-day

k_o = zero-order rate constant, mol/mg-day

X = biomass concentration, mg/ℓ

In a pilot plant study of the factors affecting nitrification kinetics, Wild, et al[134] observed zero-order kinetics for nitrification in a batch-type laboratory aeration unit. The sludge was taken from the sludge recycle line of a two-stage activated sludge nitrification unit. At a pH of 8.4 and a temperature of 21°C, the rate constant was calculated to be 1.176 × 10^{-5} mol/mg-day.

Huang and Hopson[50, 51] studied biological nitrification in an inclined film reactor. A zero-order expression provided a good fit to

their experimental data. The influent ammonia concentration in the synthetic wastewater ranged from 7.5 to 110 mg N/ℓ. At a pH of 8.4, and a temperature of 22°C, the rate constant was calculated to be 1.543×10^{-5} mol NH_3-N/ℓ/sec-ft^2.

Srinath, et al[112] studied the nitrification occuring in an oxidation ditch and concluded that the rate of oxidation of NH_4^+ and NO_2^-, at concentrations higher than 10 mg N/ℓ, followed zero-order kinetics, with optimum pH in the range of 7.4 to 7.9.

By performing bench-scale experiments of biological nitrification, Wong-Chong and Loehr[138] have shown that with substrate levels ranging from 100 to 1200 mg N/ℓ, pH ranging from 6.5 to 8.5 and temperature, from 9° to 35°C, both nitrification reactions ($NH_3 \rightarrow NO_2^-$ and $NO_2^- \rightarrow NO_3^-$) were zero-order.

By using a high sludge age contact stabilization process, Zoltek and Lefebvre[141] concluded that the nitrification rate was zero-order with respect to ammonia concentration, under different MLVSS concentrations. The raw wastewater ammonia concentrations were in the range of 16 to 21 mg N/ℓ and TKN, 28 to 36 mg N/ℓ. Temperature was kept at 25 ± 1°C during this study. An average rate constant of 7.857×10^{-7} mol/mg-day was obtained.

In testing the proper kinetic model for nitrification in the

rotating biological contactor (RBC), Murphy, et al[88] concluded that a zero-order model, with respect to filterable TKN concentration, was able to describe the data well. The rate constant obtained was 44 mg/m^2-hr with influent filterable TKN of 25 mg/ℓ (domestic sewage).

First-order kinetics. The first-order reaction can be formulated as

$$\frac{1}{X} v = -k_1 S \qquad (3-8)$$

where k_1 is first-order rate constant, ℓ/mg-day; and S is substrate concentration, mol/ℓ.

By evaluating the performance of a trickling filter for the treatment of domestic wastewater, Grantham, et al[39] found that rate of oxidation of nitrogen per interval of depth in a filter bed was proportional to the remaining concentration of oxidizable nitrogen, i.e., a first-order reaction. The rate constants obtained varied from 0.03 to 0.515, depending on loading rates and media used.

Haug and McCarty[44] found that the removal rate of NH_3-N in an upflow submerged filter could be fit by the following empirical expression:

$$r = -aS^b \qquad (3-9)$$

where a and b are empirical coefficients.

Depending on the operating temperature, the values of a and b were shown as follows:

Temperature, °C	a	b
5	0.38	1.10
10	0.99	1.25
15	1.15	0.93
25	2.59	1.48

It is interesting to notice that two of the values of b are close to 1.0, which would make the resulting model a first-order one with respect to ammonia. Unfortunately, their model is in error, so that the values of a and b are questionable.

In a recent article, Adams and Eckenfelder[1] suggested that the oxidation rate of ammonia in high strength ammonia wastewaters, in the activated sludge process could be formulated as a first-order reaction. Three types of industrial wastewaters were used in their experiments to verify the proposed model: pulp and paper mill, refinery, and phenolic wastes. The experimental results verified the proposed model and indicated the following values of rate constants:

Wastes	k_1 (ℓ/mg-day)	Temperature, °C	pH	Initial NH_3 Concentration (mg/ℓ)
Pulp and paper mill	0.00050	23	7.8	270
Refinery	0.00043	19	7.6	53
Phenolic	0.00039	21	8.2	200

It is interesting to note that although three entirely different wastewaters were used, the calculated values of rate constants were similar.

Michaelis-Menten kinetics. One of the most widely used kinetic expressions in biological wastewater treatment processes is the Michaelis-Menten model[4, 68, 80, 98, 115]. The application of this expression to different types of treatment processes and wastewaters have proven its versatility. Nitrification in biological wastewater treatment is one example. The Michaelis-Menten kinetic expression can be formulated as

$$\frac{1}{X}v = -\frac{kS}{K_s + S}$$ (3-10)

where

k = saturation utilization rate, $\frac{mol/day}{mg}$

K_s = Michaelis constant, mol/ℓ

In their study of the dynamic characteristics of the activated sludge nitrification process, Poduska and Andrews[92] used Michaelis-Menten kinetics for both ammonia and nitrite oxidation. The adequately developed dynamic model described the dynamic response of nitrification in an experimental completely mixed activated sludge process. The kinetic constants determined in their study are summarized below.

$$k_{ammonia} = 1.54 \times 10^{-3} \text{ mol N/mg-day}$$

$$k_{nitrite} = 5.14 \times 10^{-3} \text{ mol N/mg-day}$$

$$K_{s_{ammonia}} = 4.50 \times 10^{-6} \text{ mol N/l}$$

$$K_{s_{nitrite}} = 1.14 \times 10^{-5} \text{ mol N/l}$$

Stratton and McCarty[118] applied the Michaelis-Menten kinetics to predict the effect of nitrification on the D.O. in streams. The agreement between predicted and experimental values showed that this expression was the appropriate one for describing nitrification in streams. The kinetic constant values obtained in their study are presented below:

Temperature, $^{\circ}$C	Initial nitrogen concentration, mg/l	k, mol/mg-day$\times 10^4$	K_s, mol/l$\times 10^4$
25	10.6	1.80	3.99
	5.5	1.19	0.89
20	10.6	1.31	3.28
	5.5	1.19	1.85
15	10.9	0.54	2.70
	5.5	0.75	1.32

Williamson and McCarty[135-137] developed a biofilm model of nitrification using Michaelis-Menten kinetics. The kinetic parameters k and K_s were measured in batch and continuous flow suspended growth reactors respectively. The application of these parameters in the film

model, which also considered internal diffusion resistances, was apparently successful, as indicated by the agreement between predicted and experimental results. The values of k and K_s were found to be

$$k = 7.14 \text{ to } 28.571 \times 10^{-5} \text{ mol N/day/mg TSS}$$

$$K_s = 5 \times 10^{-6} \text{ mol } NO_2^- - N/\ell$$

$$= 3.571 \times 10^{-5} \text{ mol } NH_4^+ - N/\ell$$

$$= 9.375 \times 10^{-6} \text{ mol } O_2/\ell$$

However, the experimental procedure used for obtaining kinetic constants restricts their applicability to the laboratory reactor used by these investigators.

Lawrence and Brown[69] performed a laboratory scale study of nitrification in an activated sludge system. Their experimental results showed that Michaelis-Menten kinetic expression adequately described the rate of nitrification.

Biological Processes for Nitrogen Removal

Many processes have been developed for the removal of nitrogen from wastewaters and polluted streams. Air stripping, ion exchange, breakpoint chlorination, biological nitrification-denitrification, and reverse osmosis are just a few examples. Based on practical

considerations and on operating costs, probably the most common method
of removing nitrogen from wastewater is the biological nitrification-
denitrification process. Reeves[97] and Shindala[109] reviewed the
advantages and disadvantages of different processes for removing
nitrogen, and concluded that biological nitrification-denitrification
process is the most convenient method of nitrogen control.

Based on the physical structure or form of the microbial mass,
biological nitrification-denitrification processes can be divided into
suspended growth and attached growth processes[93]. Suspended growth
processes are those in which the microbial mass is kept dispersed in
the nutrient medium; mixing is provided either by the aerating devices
or by mechanical means. Attached growth processes, on the other hand,
require solid media, on which surface the bulk of the microbial mass
is developed. There are many different configurations of suspended
growth and attached growth processes, which will be discussed in the
next section.

Suspended growth processes. There are two general types of suspended
growth processes that may be employed to remove nitrogen, single-stage
(combined) and two-stage (separated) processes[20, 24]. In the
single-stage process both carbonaceous removal and nitrification occur
in the same reactor. In order to achieve this purpose, the process

must be operated at low loadings. In general, the single-stage process is recommended for low strength wastewaters that are relatively free of toxic materials.

The two-stage process provides for carbonaceous removal and nitrification in separate reactors. The first reactor can be operated at high loadings, which permits smaller reactor volume. The second reactor will be fed with effluent from the first reactor which is low in BOD, thus enabling operation at relatively short detention time. In general, the latter has some advantages in control and resistance to toxic substance.

In 1962, Ludzack and Ettinger[72] proposed the semi-activated sludge process for nitrogen removal. The aeration tank in this process was divided into two zones, an anaerobic zone with low or zero D.O. followed by an aerobic zone. The mixed liquor from the aerobic zone was recirculated to the anaerobic zone to provide dissolved nitrite or nitrate. With ample supply of carbonaceous matter in the influent, the nitrite was reduced to nitrogen gas. The amount of denitrification was controlled by the recycle rate of mixed liquor. The average removal rate of the total nitrogen was about 60%.

Johnson and Schroepfer[58] conducted laboratory studies on the nitrogen removal by activated sludge. In their experiments the F/M

ratio was determined to be a primary factor affecting the degree of nitrification. It was shown that a completely mixed anaerobic activated sludge reactor could be employed as an efficient denitrification unit. The organic carbon required in denitrification was supplied by raw sewage. Reasonable and complete denitrification was obtained with detention times varying from 0.151 to 4.67 hours and loading factors (BOD added/MLVSS) of 0.151 to 0.876. They suggested using the two-stage activated sludge process for complete nitrogen removal.

In their survey, Barth, et al[18] showed that the removal of nitrogen by the conventional activated sludge process was erratic. The total removal of nitrogen varied from 15 to 67%. They recommended that close control of the process was essential for a high degree of nitrogen removal.

Balakrishnan and Eckenfelder[15] proposed using a three-stage system for complete removal of nitrogen. In their approach, settled raw sewage was aerated in the contact-aeration tank (first stage). Following the contact period, the activated sludge was separated by a sedimentation tank and the clarified effluent, low in carbon, was pumped to the trickling filter (second stage) for nitrification. The nitrified effluent and the sludge from the first stage, loaded with

organic materials, were mixed in the denitrification tank (third stage)

for stabilization of the organic matter and denitrification. They

claimed complete nitrification, resulting in an effluent containing

25 to 30 mg/ℓ of NO_3-N. A period of anaerobic digestion of 4 hours

at about $25°C$ and MLSS at 2800 mg/ℓ would bring about a total average

nitrogen removal of 80 to 90%.

In 1972, Matsche reported a significant removal of nitrogen in a

treatment plant at Vienna-Blumental[76]. The activated sludge process

in the treatment plant consisted of two aeration basins in series, the

first one equipped with four rotors and the second basin with two

rotors. Organic nitrogen in the influent was 13.8 mg/ℓ and in the

effluent, 0.4 mg/ℓ. Ammonia was reduced from 21.4 mg/ℓ to 3.8 mg/ℓ.

He reported that in some parts of the second basin the D.O.

concentration became very low, which resulted in complete

denitrification. He estimated that with 35.7 mg/ℓ of TKN in the raw

sewage, 60% being reduced to nitrogen gas through biological

denitrification, 28% being stored in the activated sludge and only 2%

appeared in the final effluent.

Barnard[16, 17] proposed a new modification of the activated

sludge process, called "Bardenpho" sludge process for nitrogen

removal. This process consists of four completely mixed basins in

series, followed by a clarifier from which sludge was recycled back to the first basin. The first and the third basins were stirred gently to keep the solids in suspension while the second and the fourth basins were aerated. Complete nitrification was achieved in the second basin and the mixed liquor from that basin was recycled to the first basin. The nitrate contained in this recycled flow was used by facultative bacteria in the first basin and reduced to nitrogen gas. Mixed liquor not recycled from the second basin passed on to the third basin where nitrate was reduced by the endogeneous respiration of the bacteria. The mixed liquor was then aerated in the fourth basin before reaching the clarifier. About 90 to 95% of the nitrogen could be removed by this process without the use of methanol.

At the Kappalas Lidingo Wastewater Treatment Plant in Sweden, Ericsson[29] conducted a pilot plant study on nitrogen removal by the activated sludge process. The conventional aeration tank was used as the nitrification unit and experimental results showed that nitrification could be accomplished in either combined or separated sludge systems. It was possible to operate the nitrification unit at a sludge age as low as three days. Both the anaerobic completely mixed reactor and the anaerobic filter were evaluated for denitrification. He concluded that the choice depended mainly on cost and operation safety

not on efficiency.

Sutton, et al[119] evaluated both combined and separated sludge alternatives at the pilot plant level. They concluded that under steady-state operating conditions, separated and combined sludge systems, operated for carbon removal and nitrification of a municipal wastewater, would remove equal amounts of filtered TNK at equal system SRT's. They also showed that the nitrification rate was temperature sensitive; however, temperature sensitivity decreased with increasing SRT.

By employing plant-scale experimentation, Beckman, et al[19] were able to demonstrate a combined carbon oxidation-nitrification activated sludge facility was efficient in attaining nitrification. With a temperature of the mixed liquor at 50° to $65^{\circ}F$, optimum F/M ratio was found to be 0.25. Optimum sludge age was greater than 6 days. They also showed that high denitrification could be obtained using clarified nitrified effluent when a detention time of 5 hours, extremely low D.O. levels, and influent COD values greater than 150 mg/ℓ were maintained.

Bishop, et al[23] evaluated a single stage nitrification-denitrification process using an activated sludge reactor-clarifier, with the wastewater as a source of organic carbon for denitrification.

The operation was such that it would provide alternate periods of aerobic and anaerobic conditions within the reactor with sufficiently low F/M values. The reactor was divided into two basins arranged in series. Air was supplied alternately to each basin on a 30-minute cycle. Nitrogen removal data revealed that the alternating nitrification-denitrification process in the winter ($15°C$) produced about 75% nitrogen removal without using methanol. As temperature raised to $25°C$, the removal increased to 84%. At a F/M ratio of 0.1 gm BOD_5/gm MLVSS/day, essentially complete nitrification was achieved. When the D.O. decreased to near zero, denitrification occurred. They claimed the proposed process possessed many advantages, including: (i) reduction of volume of air required, (ii) elimination of supplemental organic carbon sources required for denitrification, (iii) no recycle of mixed liquor and (iv) elimination of intermediate clarifier.

Stover and Kincannon[117] evaluated the performance of a one-stage and a two-stage activated sludge process in laboratory-scale experiments. They found that both processes could be operated and controlled to accomplish complete nitrification. The operation parameter that was important in the performance of the process was SRT. The study showed that the minimum SRT required for complete

nitrification was 6 days for a two-stage unit, and 10 days for a single-stage unit. This study also showed that the two-stage process produced a greater quantity of sludge than the single-stage process.

Voets, et al[129] studied the application of the activated sludge process for treating highly nitrogeneous wastewaters. In their study, total nitrogen concentrations were in the range of 800-1300 mg/ℓ. The liquid retention time (LRT) of the system was kept above 15 days with SRT either 20 days or infinite (no sludge wastage). When treated aerobically at neutral pH, up to 50% of the total nitrogen could be converted to nitrite or nitrate.

Hutton and LaRocca[53] also studied the efficacy of the activated sludge process for treating concentrated ammonia wastewater. The pilot plant used in their study included an equalization basin, pH control equipment, a completely mixed aeration basin, and a clarifier with automatic sludge return. During the study, LRT was varied from 4.5 to 15 days and aeration basin temperature, from 5° to 20°C. The effects of temperature, pH, and SRT were studied. Removal rates dropped about 50% when the temperature was reduced from 20° to 10°C. Optimum pH was found to range from 8.0 to 8.4. The SRT recommended was 30 days.

Zoltek and Lefebvre[141] studied the feasibility of using a high sludge age contact stabilization process for nitrification. They

concluded that unless a high solids concentration was provided the

process was not amenable to providing a substantial degree of

nitrification. In their study, 11 hours of aeration time was required

to achieve 70% depletion of non-oxidized nitrogen with S.S.

concentration of 3000 mg/ℓ. These were too high to be used in the

contact stabilization process because it would produce adverse effects

on the performance of the final clarifier.

Yang and Gaudy[139] studied the feasibility of using the extended

aeration process for nitrogen removal. They found that in general the

the extended aeration process could be expected to produce a nitrified

effluent when the biological solids concentration was rather high.

In his study, Hermann[45] found that stabilization ponds might be

used to reduce high nitrate wastes. Organic wastewaters similar to

domestic sewage and containing NO_3-N concentrations as high as 110 mg/ℓ

were amenable to treatment. He concluded that the upper limit of

nitrate loading was 15 mg NO_3-N/ℓ pond volume/day. The influent

nitrate concentration had no measurable effect on BOD removal.

During a seven-month study of a full-scale oxidation ditch and a

1-acre lagoon system, Jones and Patni[59] concluded that after about

20 weeks of operation, about 80% of the TKN put into the oxidation

ditch had been lost. The pH, temperature and aeration conditions in

the oxidation ditch indicated that ammonia stripping was insignificant. It was concluded that with proper design and operation, the oxidation ditch could be used to effect a high degree of nitrogen removal from high strength ammonia wastes.

The single-stage nitrification-denitrification activated sludge process is currently under investigation at the Pilot Plant at the University of Massachusetts, Amherst, Massachusetts. The effluent from a pilot scale trickling filter (without clarification) is fed into an extended aeration unit which is divided into three zones: nitrification, denitrification, and final aeration zones. The activated sludge recovered in the final clarifier is recycled back to the nitrification zone. 95% removal of total nitrogen has been observed.

Attached growth processes. By using a anaerobic filter with different types of packing media, Tamblyn and Sword[122] have shown that efficient nitrate removal could be accomplished with a hydraulic detention time of 0.5 to 2.0 hours, depending on temperature. Average removal efficiency of 93% was obtained with these media and a hydraulic detention time of 2.0 hours.

Seidel and Crites[106] conducted a pilot-scale experimentation with an anaerobic filter packed with coarse gravel (1" to 1.5") for

nitrogen removal. The nitrified secondary effluent with an average

nitrate of 14 mg/ℓ was fed upward through the filter with a detention

time of 2 hours. The results showed that 90% of the inorganic nitrogen

could be removed with a hydraulic detention time of 1.5 hours. They

also claimed that the anaerobic filter had several advantages over

other processes for denitrification, including low initial and

operating costs, simplicity of operation, absence of sludge recycle,

and others.

Haug and McCarty[44] studied the nitrification in a submerged

filter. Oxygen required was supplied by either preoxygenation or

bubble oxygenation. In general, 90% of the influent ammonia (20 mg

NH_3-N/ℓ) was removed with a detention time based on raw waste flow and

filter void volume of 30 minutes at $25^{\circ}C$, and 60 minutes at $15^{\circ}C$.

Detention times of 90 and 120 minutes were required at temperatures

of 10° and $5^{\circ}C$ respectively. Similar performance was obtained with

both oxygenation systems. The experimental results showed that the

submerged filter is a very stable process for nitrification.

By using unfiltered secondary effluent from the Pomona Water

Renovation Plant, Pomona, California, as the influent, English, et al

[28] employed both sand and activated carbon columns as the reactors

for denitrification. The secondary effluent contained 20 mg NO_3-N/ℓ.

The column contained 20 feet of media and had an empty-bed detention time of 22 minutes. The results showed that both types of media were efficient for denitrification (85% removal). The estimated cost for a 10 MGD denitrification plant using a sand column was $71/MG (1974 dollars).

By evaluating the performance of a 0.5 MGD wastewater treatment plant incorporating the rotating disk process (four stages) for secondary biological treatment, Antonie, et al[5] were able to demonstrate the efficiency of the process for nitrification. During the nine-month period of study, the average effluent ammonia concentration was about 0.4 mg N/ℓ after the fourth stage with an influent concentration of 14.1 mg N/ℓ.

Wen and Molof[132] conducted a bench-scale study of carbon oxidation and nitrification in a biological fixed-film rotating disk system (BFFRD). A six-stage system was used as the experimental device. They claimed that the BFFRD system was an efficient treatment unit for nitrification. They found that there was no significant effect on the nitrification efficiency in the BFFRD system when the detention time per stage was decreased from 96 minutes to 24 minutes at a constant organic and ammonia loadings.

Jeris, et al[54-56] used a granular fluidized bed as the

nitrification unit. They claimed that this process combined the best features of both the trickling filter and the activated sludge processes. They found that the system consistently produced greater than 99% removal of the influent nitrogen in less than 6.5 minutes at a flux rate of 15 gpm/ft^2. They also showed that nitrogen removal efficiency was not affected by diurnal flow variation.

Stenquist, et al[114] conducted a pilot plant study for nitrification at Stockton, California. A trickling filter packed with synthetic medium was used as the reactor. The influent contained 3.5 to 16.4 mg/ℓ of ammonia with a BOD loading of 14 lb/1000 ft^3/day, the trickling filter was able to remove 94% of NH_3-N and 64% of TKN (from 27.8 to 9.9 mg/ℓ). As BOD loading increased to 22 lb/1000 ft^3/day, the unit still removed 89% of the ammonia and 62% of the TKN. Combined carbon oxidation-nitrification could be achieved in plastic media trickling filter when the organic loading was low. A high level of nitrification would occur at an organic loading of approximately 25 lb/1000 ft^3/day.

A pilot plant study was conducted by Young, et al[140] to demonstrate the feasibility of packed-bed reactors (PBR) for both BOD and ammonia removal. The process consisted of two PBR units, 5 feet in diameter and 12 feet high, followed by two 2.0×2.5-ft dual-media

filters. The air was added to each PBR unit through a plastic tube distributor. Sand, crushed coal, and loosely packed plastic were used as the media. With the ammonia concentrations ranging from 5 to 20 mg/ℓ, the ammonia concentration in the second PBR was always less than 5 mg/ℓ. The allowable ammonia loading was estimated to be 6.9 lb NH_3-N/1000 ft^3/day at a detention time of 3.25 hours on an empty-tank basis. It is worthwhile to note that there was no pH adjustment required in the PBR unit.

McHarness, et al[80] conducted comprehensive studies of nitrification with submerged filters. Each filter was 5.5 inches in diameter and 3.5 feet tall and packed with quartzite stone, 1 to 1.5 inches in diameter, to a depth of 3 feet. The oxygen was supplied by either preoxygenation or bubble oxygenation. The process was shown to be not only an efficient nitrification unit, but also an efficient polishing device to reduce BOD, COD, and S.S. from the activated sludge plant effluent. With an influent ammonia concentration of 20 mg/ℓ, the bubble oxygenation unit produced an effluent with 4 mg/ℓ ammonia and the preoxygenation unit, 1 mg/ℓ. The estimated total cost for plants ranging in capacity from 5 to 100 MGD, based on a 5.5% interest rate and a 20-year design period, ranged from $0.048 to $0.028/1000 gal. for a preoxygenation unit and from $0.039 to $0.022/1000 gal. for a

bubble oxygenation unit (1975 dollars).

By using a completely mixed stirred growth reactor (CMSGR) and a submerged filter (SF) for treating concentrated nitrate wastewater, Jewell and Cummings[57] have shown that both processes could efficiently remove concentrations of nitrate and COD as high as 4000 and 14600 mg/ℓ, respectively. They also claimed that at comparable loadings and 80% removal efficiency, the SF unit could remove 30 times as much nitrate as the CMSGR unit at half the liquid detention time.

During the 47- week study at a pilot plant equipped with a rotating disk unit, Lue-Hing, et al[73] found that a high strength ammonia wastewater with an average ammonia concentration of 780 mg N/ℓ could be successfully nitrified by using a four-stage rotating disk system under both ambient summer and winter conditions. At an overall NH_3-N loading to the four-stage rotating disk system of 15.6 lb NH_3-N/1000 ft^3/day at a wastewater temperature of 10°C, 99.4% of the ammonia was removed, while at an overall loading of 43.5 lb NH_3-N/1000 ft^3/day and at a wastewater temperature of 20°C, 99.8% of the ammonia was removed.

After reviewing the performance of two types of supported growth reactors (rotating biological contactor, RBC, and the submerged packed column, SPC) for nitrogen removal, Murphy, et al[88] concluded that

the RBC process was capable of providing efficient and predictable

removal of nitrogen under all temperature conditions normally

encountered in municipal wastewater treatment. The SPC process, with

high porous media, could also provide efficient removal of NO_2+NO_3-N

from wastewater. However, the buildup of biological solids in this

process caused inconsistent and unpredictable denitrification

efficiencies. This type of reactor, as recommended by the authors, was

not suitable for situations where a high quality of effluent was

important.

C H A P T E R I V

EXPERIMENTAL MATERIALS AND METHODS

Research Objectives

The significance of internal diffusion resistances on the overall

rate of substrate utilization was discussed in detail in previous

sections of this dissertation. The literature review in this study

has shown that adequate information regarding the relative importance

of various steps in the nitrification process is very limited. Since

information of this kind is needed for the rational design of reactors

in which biological nitrification is to take place, the investigation

reported herein was performed with the following broad objectives:

(a) Verification of the proposed kinetic model (i.e., Michaelis-

Menten kinetics) in a separate-stage activated sludge process.

(b) Determination of the intrinsic values of the kinetic parameters

for the nitrification process.

(c) Evaluation of the effect of internal diffusion resistances on

the overall nitrification rate.

Once accomplished, it is hoped that these objectives will provide

information which will be helpful in understanding the kinetics (both

true and apparent) of the activated sludge nitrification process. In addition, this information will be very useful in setting up rational design criteria of the biological nitrification treatment process.

Apparatus

In order to accomplish the objectives described previously, a Multigen convertible culture apparatus (Model F-1000, NBS Co., Inc.) was chosen as the reactor. The apparatus is equipped with the following features:

(a) Vessel: The vessel, constructed of pyrex glass, is 1.0 liter in size with a working volume of 600 ml. Fittings are provided for innoculation and chemical addition, aeration, prevention of vortex, heating, cold water circulation, temperature measurement and control, sampling, pH electrode, and D.O. probe. All materials in contact with the culture medium are non-corrosive.

(b) Agitation System: Agitation is provided by means of a heavy duty motor coupled to a magnet assembly located inside the vessel. Speed is adjustable from 0 to 1000 rpm by means of a solid-state electronic controller. Motor operation is not affected by changes in load or variation in supply voltage.

(c) Aeration System: Metered air is supplied by an internal air pump through an air filter which is packed with non-absorbent glass wool. Air is delivered to the vessel through the air fitting, located in the center of the stopper. From here it passes through the agitator shaft to emerge, via a multiplicity of small holes, at the lower end of the shaft. Air may be metered through a precision-bored variable-area flowmeter. A range of 0.1 to 1.0 liter per minute is provided for in the Model F-1000. The system is also suitable for using other gases such as pure oxygen.

(d) Temperature Control System: Medium temperature from $5^{\circ}C$ to $60^{\circ}C$ above water supply temperature, is controlled by a solid-state temperature controller with a fast response thermowell-mounted thermister sensor which provides an accuracy of $\pm 0.2^{\circ}C$. A heating element, encapsulated in an outer housing, is inserted into a well through the vessel stopper and plugs into the circuit through a socket connection on the console. Ambient temperature may be maintained through the use of a stainless steel water cooler, installed in the stopper. Service water supply connections are made at fittings mounted in the rear of the console.

(e) Sampling System: The hooded sampler is attached to a

sampling tube that extends close to near the bottom of the vessel.

The sampler has a rubber suction bulb to facilitate

collection of representative samples without contamination.

A 30 mℓ screw-capped container serves for collection and

removal of samples.

The assembly of the apparatus is shown in Figure 4-1.

Preparation of Feed Solution

In the separated activated sludge nitrification process most of

the organic matter (BOD) in the influent wastewater is removed in the

first reactor by heterotrophic bacteria. The effluent from the first

reactor is then discharged into a second reactor where nitrification

occurs. Low concentration of BOD is the characteristic of the influent

to the nitrification unit. In order to simulate the actual situation,

therefore, a synthetic feed solution was prepared with no organic

matter and with ammonia as the only substrate. It is reasonable to

assume that the mixed population developing on this solution would

mainly be nitrifiers. The composition of the stock solution is listed

in Table 4-1.

The stock solution was diluted with Amherst tap water and
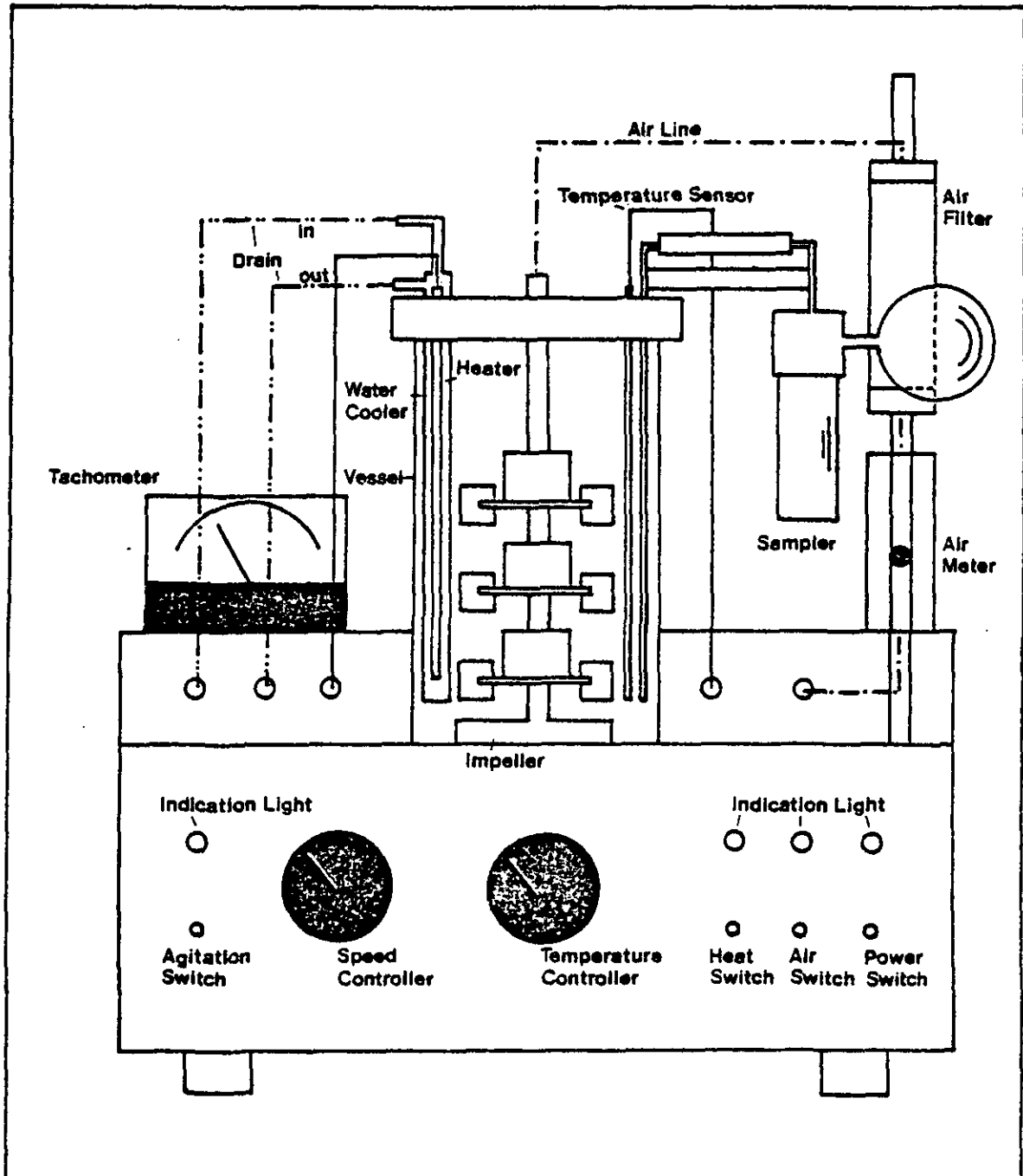
Figure 4-1 Experimental Apparatus

phosphate buffer solution to the desired ammonium concentration for each specific experiment. It is well known that enough alkalinity must be provided in the system for nitrifiers to assimilate ammonium[93]. The alkalinity required was provided by adding sodium bicarbonate to the feed solution. The amount of sodium bicarbonate added was such that for each mole of ammonia (as N) per liter there was about 4.59 equivalent of alkalinity per liter.

The pH of the feed solution was controlled by a phosphate buffer solution (1M KH_2PO_4 and 1N NaOH). The preparation of the phosphate buffer solution is shown in Table 4-2[130].

Preparation of Seed

The seed for this study was taken from the extended aeration unit located at the Wastewater Pilot Plant of the University of Massachusetts, Amherst, Massachusetts. The mixed liquor taken from the aeration unit was concentrated by settling for one hour. The clear supernatant was discarded and the concentrated mixed liquor was then diluted with synthetic feed solution up to three liters. The ammonium concentration in the feed solution was 3.571×10^{-3} mol/ℓ (50 mg/ℓ) as N. The seed suspension was aerated with air. Each day the suspension was allowed to settle for one hour and the supernatant was discarded and

TABLE 4-1

COMPOSITION OF STOCK FEED SOLUTION

Constituent	Concentration	
	gm/ℓ	mol/ℓ
$(NH_4)_2SO_4$	236	1.788
KH_2PO_4	80	0.588
$MgSO_4 \cdot 7H_2O$	20	0.081
$Fe(SO_4)_3 \cdot nH_2O$	85	-
Distilled Water	to 1 liter	

TABLE 4-2

PHOSPHATE BUFFER SOLUTION

pH	x*
6.0	5.6
6.5	13.9
7.0	29.1
7.5	41.1
8.0	46.7
8.5	**
9.0	**

*   50 mℓ 1M KH_2PO_4 + x mℓ 1N NaOH

**   For pH above 8.0, 1N NaOH was added to the buffer

solution with pH = 8.0 until the desired pH is

reached. Final volume of mixture = 1000 mℓ

fresh feed solution was added. The same procedure was repeated for two weeks. During this period, the color of the suspension changed gradually from dark brown to yellow. Then the seed was transferred to a bench-scale CFSTR with cell recycle. The influent ammonium concentration was kept at the same level for two weeks. It was observed that the mixed liquor volatile suspended solids (MLVSS) concentration was low. In order to obtain a higher level of MLVSS, the influent ammonium concentration was increased four times. The pH of the mixed liquor was kept at 8.0 by adding phosphate buffer solution. The ammonium and MLVSS concentrations in the mixed liquor were measured once each day. As the reactor reached a steady state, indicated by the constant ammonium and MLVSS concentrations in the effluent streams, the mixed liquor wasted each day (1440 mℓ) was used as the seed for the Multigen unit. The operation characteristics of the bench-scale CFSTR are shown below:

Reactor volume: 28 liters

Liquid retention time: 1 day

Solid retention time: 28 days

Temperature: 22 ± 2°C

pH: around 8.0

MLVSS: 120 to 140 mg/ℓ

Dissolved oxygen concentration in the mixed liquor: >6 mg/ℓ

Influent ammonium concentration: 1.429×10^{-2} mol/ℓ (200 mg/ℓ) as N

Effluent ammonium concentration: $<7.143 \times 10^{-6}$ mol/ℓ(<0.1 mg/ℓ) as N

Analytical Techniques

Control on several variables was needed to attain the research objectives. These variables are: substrate (ammonium) concentration in both influent stream and the mixed liquor, biomass concentration, and size and density of the floc particles.

Determination of ammonium concentration. The measurement of ammonium was carried out by using an Orion Specific Ion Meter Model 407A equipped with an ammonia probe Model 95-10. The specific ion meter provided a fast, simple and sufficiently accurate method for the measurement of ammonium. A detailed description of the procedure is presented in Appendix 4.

Determination of biomass concentration. Weddle and Jenkins[131] compared different techniques to measure the concentration of active cells in the activated sludge process. Their main conclusion was that "... in the practical operating range of activated sludge plants treating domestic sewage, MLVSS is an excellent index of the viable

organism content of activated sludge. For this reason no further research is necessary for more sophisticated indicators of viable organism content in the practical operating range of the process.".

Thus it seems reasonable that the MLVSS concentration would be a good indicator of the nitrifier concentration. The experimental procedure adopted in this research is the one described in the latest edition of the Standard Methods [113].

Determination of size of the floc particle. In the study of mass transfer of substrate through the activated sludge flocs, it is essential to have an estimate of floc size. Aiba, et al[2] proposed a method to estimate the equivalent size of activated sludge particles by measuring the interfacial settling characteristics of the sludge. Mueller, et al[86] used the Pycnometer to determine the nominal diameter of the floc. Kasaoka, et al[60] suggested that for mixtures of porous solids of various sizes and shapes, the following equation could be used to estimate the average radius of the particles:

$$\bar{R} = \frac{\Sigma V_p}{\Sigma A_p} \tag{4-1}$$

where $\bar{R}$ is the average radius of the particle.

Bird, et al[22] suggested the following equation:

$$\bar{R} = \frac{3V_p}{A_p} \tag{4-2}$$

Obviously there is no standard method which will produce reliable results regarding the floc size. In order to simplify the procedure and obtain reasonable results, a bacterial counter (Petroff-Hausser) was used to measure optically the average size of the floc. The counter consists of molded glass compartment with a rectangular moat with 400 small squares per mm^2. When viewed through a microscope, the ruling appeared as white lines on the dark background. A flat, polished glass covered the moat region 0.02 mm above the ruled surface. Therefore, by counting the number of small squares by each floc particle, the projected area of floc particle, A_p', was determined. The volume of the floc particle is then

$$V_p = A_p' \times depth \tag{4-3}$$

where depth = 0.02 mm.

When a number of measurements were completed, the average volume of the particle was estimated by

$$\bar{V}_p = \frac{depth}{n} \sum_{i=1}^{n} A_{p_i}' \tag{4-4}$$

where

V_p = average volume of the particle

A'_{p_i} = projected area of particle i

n = number of measurements

Assuming that the particle is spherical, then

$$\bar{R} = (\frac{3\bar{V}_p}{4\pi})^{0.333} \tag{4-5}$$

Fifty measurements were used to compute the average radius of the particle through Eq. (4-5) for each specific particle size. Figure 4-2 shows typical floc particles on the Petroff-Hausser Bacterial Counter, as viewed through the microscope.

Determination of floc density. A centrifugation method was used in this study to determine the density of the activated sludge flocs. 50 mℓ of mixed liquor was collected and allowed to settle for one hour. The supernatant was discarded and the concentrated suspension was transferred to a centrifuge where it underwent centrifugation at 2500 rpm for one minute. The accumulated volume of solid was determined and its mass was measured using the same procedure as in the determination of MLVSS. The density was then calculated as the ratio of the mass of solids to its accumulated volume. The experimental results of density determination is presented in Table 1, Appendix 5.
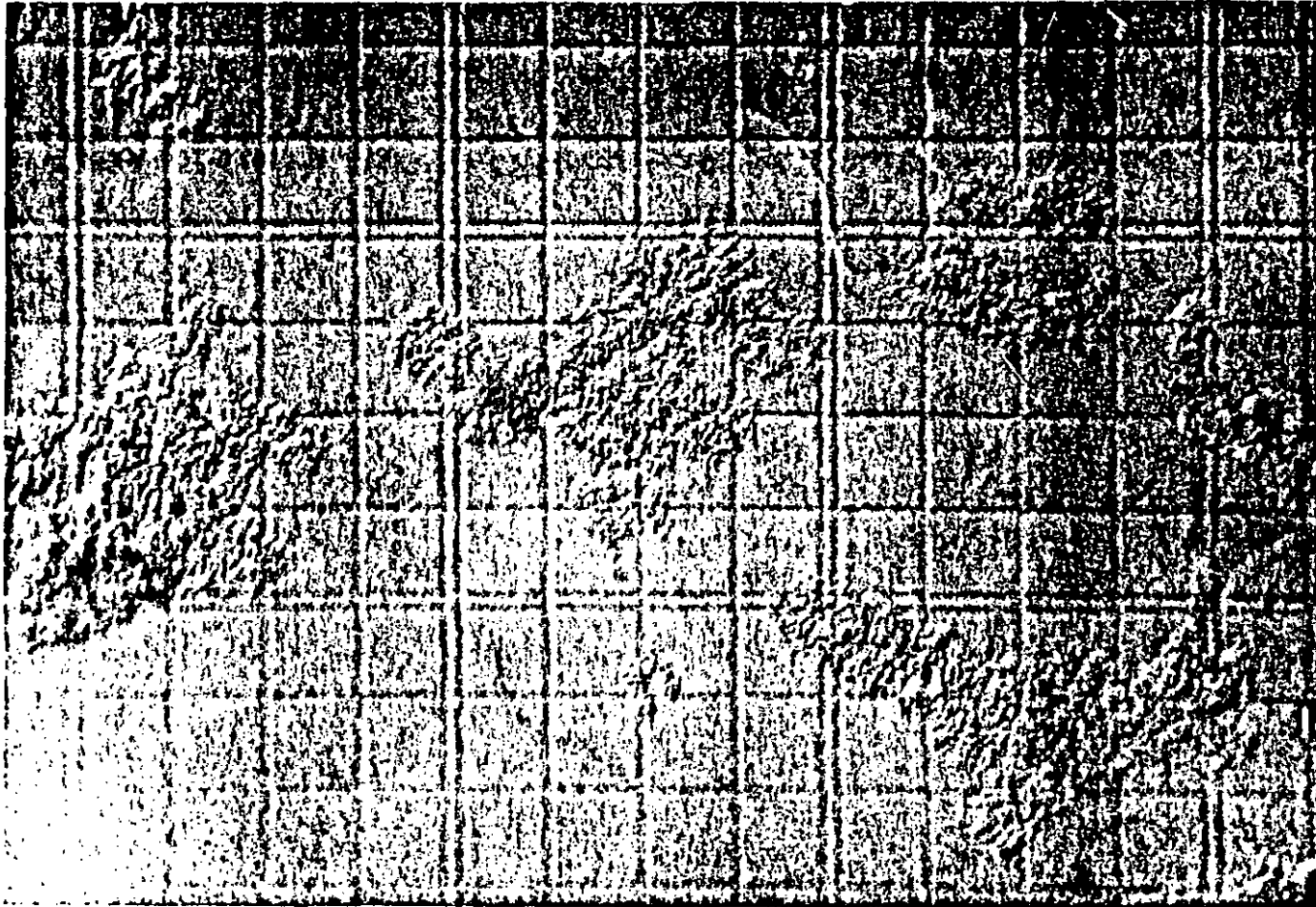
Figure 4-2 Typical Floc Particles on the Petroff-Hausser Bacterial Counter

C H A P T E R   V

BATCH EXPERIMENTS. RESULTS AND DISCUSSION

Introduction

This first stage of the investigation has the following specific objectives:

(a) To determine the optimum operating conditions for observing the intrinsic nitrification rate.

(b) To verify the proposed Michaelis-Menten kinetic expression for the intrinsic rate of nitrification.

(c) To determine the effect of initial substrate (ammonium) concentration on the nitrification rate.

The reasons for performing this first phase of investigation are two-fold. First, in order to observe the intrinsic nitrification rate, not only both external and internal diffusion resistances must be reduced to negligible values, but also optimum environmental conditions must prevail throughout the whole period of the experiment. External diffusion resistances can be eliminated by increasing the rate of external mass transport (e.g. by introducing vigorous agitation), so that the bulk substrate concentration is practically equal to that at

the external floc surface. On the other hand, internal diffusion resistances can be minimized by either decreasing floc size or by maintaining high bulk substrate concentration, thus yielding an effectiveness factor close to 1.0. In this case, a high substrate concentration can be maintained through the center of the floc, and all the microorganisms in the matrix will be able to consume substrate at the highest possible rate.

Since most of the kinetic constants published thus far, which were recently summarized by Lawrence and McCarty[68], and the EPA[93], were observed under the assumption that the microorganisms and the liquid form a single phase, it is reasonable to surmise that some of these observations may have been masked by diffusion resistances. Evidence that internal diffusion resistances may affect the observed rate of carbonaceous substrate uptake in the suspended growth system was presented by Baillod and Boyle[13, 14]. Other investigators [11, 12, 63, 78, 85, 87] observed similar effects on the oxygen uptake rate in suspended growth systems. However, similar information dealing with the nitrification process is scarce.

Various investigators[50, 51, 93, 134] have reported that the nitrification rate depends strongly on such factors as temperature, pH, D.O., and alkalinity. In this investigation, both D.O. and

alkalinity were kept at relatively high levels in the reactor, so
that the number of environmental factors affecting the nitrification
rate could be reduced.

The second reason for carrying out batch experiments is that
there is some experimental evidence suggesting that the kinetic
"constants" in various expressions describing the substrate uptake
rate may be affected by the initial substrate concentration in the
batch experiment. This hypothesis is based on the work of Gaudy,
et al[35, 36], La Motta[65, 66], Benefield and Randall[21], Grady and
Williams[38], and Grau, et al[40] who demonstrated that both
biological growth and substrate uptake strongly depend on initial or
influent conditions.

The fact that batch experiments are simple to perform and can
generate a large amount of experimental data under different conditions
in a relatively short period of time makes the batch reactor a
convinient choice for accomplishing the objectives described previously.
Although there is evidence[27,34] that there is no direct and
interchangable relationship between batch and continuous experimental
data, however, the batch experiment does provide fundamental
information which is important in understanding the kinetics of the
activated sludge process. Continuous flow experiments were also

carried out; the results of this second phase will be reported later.

Theory

If the nitrification kinetics follow the Michaelis-Menten relationship, then

$$v_i = \frac{v}{X} = \frac{dS}{dt} = -\frac{kS}{K_s + S} \tag{5-1}$$

where

v_i = intrinsic substrate uptake rate, mol/mg-day

$\frac{dS}{dt}$ = rate of substrate disappearance, mol/ℓ-day

S = ambient substrate concentration, mol/ℓ

$\dot{X}$ = active biomass concentration, mg/ℓ

k = saturation utilization rate, mol/mg-day

K_s = Michaelis constant, mol/ℓ

t = time, min

The evaluation of the kinetic parameters k andK_s was performed by using the integral method of analysis[70]. Due to the fact that the growth rate of nitrifiers is relatively low[68, 93] it is possible to assume that the biomass concentration remained practically constant during the short experimental runs. Therefore, Eq. (5-1) can be rewritten as

$$\frac{dS}{dt} = - \frac{kS\bar{X}}{K_s+S} \tag{5-2}$$

where $\bar{X}$ is the average biomass concentration during each run.

Integration of Eq. (5-2) with initial condition $S = S_o$ at $t = 0$ yields

$$\frac{K_s}{k\bar{X}} \ln(\frac{S_o}{S}) + \frac{1}{k\bar{X}}(S_o - S) = t \tag{5-3}$$

Graphical evaluation of the parameters k and K_s requires linearization of Eq. (5-3), that is,

$$\frac{\ln(\frac{S_o}{S})}{(S_o-S)} = - \frac{1}{K_s} + \frac{k\bar{X}}{K_s}(\frac{t}{S_o-S}) \tag{5-4}$$

A plot of $\{\ln(S_o-S)\}/(S_o-S)$ versus $t/(S_o-S)$ should yield a straight line; K_s can be determined from the intercept and k from the slope.

used in the respective run.

Initial ammonium concentrations varied from 7.14×10^{-5} mol N/ℓ to about 1.43×10^{-3} mol N/ℓ (1 mg N/ℓ to 20 mg N/ℓ), to cover the range of concentrations normally found in biological wastewater treatment plant influents. Samples were withdrawn at given time intervals, the first sample being collected five minutes after the inoculum was added to the reactor. This was considered to be a reasonable lag period for the cells to adapt to the new environment[135-137]. Thus, time zero starts after this five-minute lag period. The reactor was sealed to minimize the possible stripping of ammonia by agitation.

The optimum operating conditions, i.e., pH, temperature, and particle size were determined first; using these conditions, the effect of initial ammonium concentrations on the nitrification rate was studied.

Experimental Results and Discussion

Determination of the optimum operating conditions. In order to minimize internal diffusion resistances, the floc particles must be reduced in size. This was achieved by increasing the rotational speed of the impeller, which mechanically broke up the larger flocs into smaller particles. Figure 5-1 shows the effect of impeller rotational

speed (RPM) on particle size. It is clear that particle size decreased as the speed increased as high as 500 rpm, beyond which no further reduction in particle size was observed. The minimum average particle radius obtained by this method was 18 μm. Table 2 in Appendix 5 shows the average particle radius at different impeller rotational speeds.

The effect of floc size on the observed nitrification rate was studied at different RPM values. In this experiment, pH and temperature were kept at 8.0 and $30^{\circ}C$ respectively. The initial ammonium concentration was 7.14×10^{-5} mol N/ℓ. Figure 5-2 shows the results obtained in this experiment. The initial uptake rate, k_o', determined by measuring the slope of the tangent to the curve S versus t at t = 0, is seen to increase as rotational speed increases, i.e., as floc size decreases. It can also be seen that speeds higher than 500 rpm did not yield higher rates, thus indicating that the intrinsic nitrification rate was observed. The results shown in Figures 5-1 and 5-2 suggested that rotational speed higher than 500 rpm had to be used in future runs. A rotational speed of 900 rpm was chosen for intrinsic kinetic study. Table 3 in Appendix 5 summarizes the k_o' values obtained at different speeds.

Published data[68, 93, 134] indicate that the optimum pH for
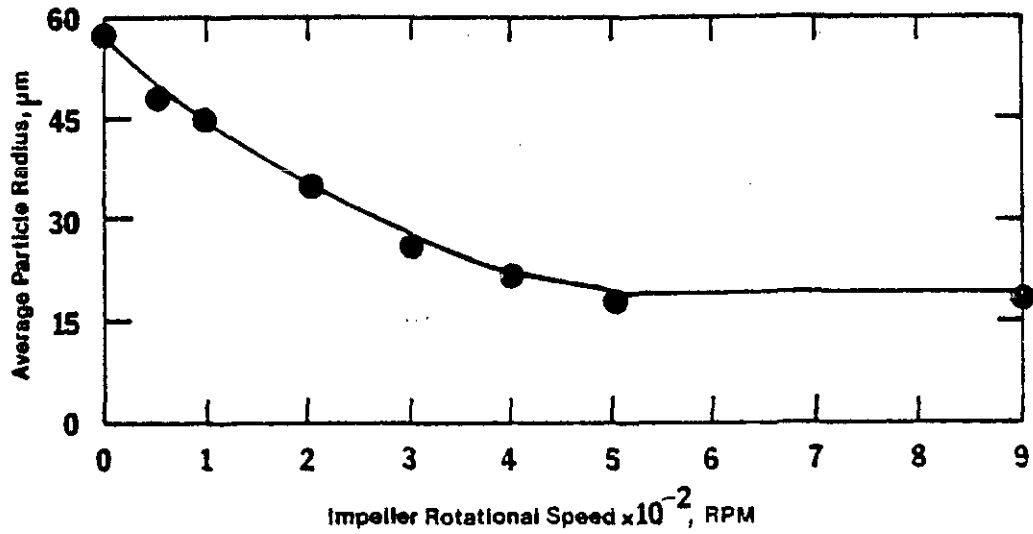
Figure 5-1 *The Effect of Impeller Rotational Speed on Particle Size*
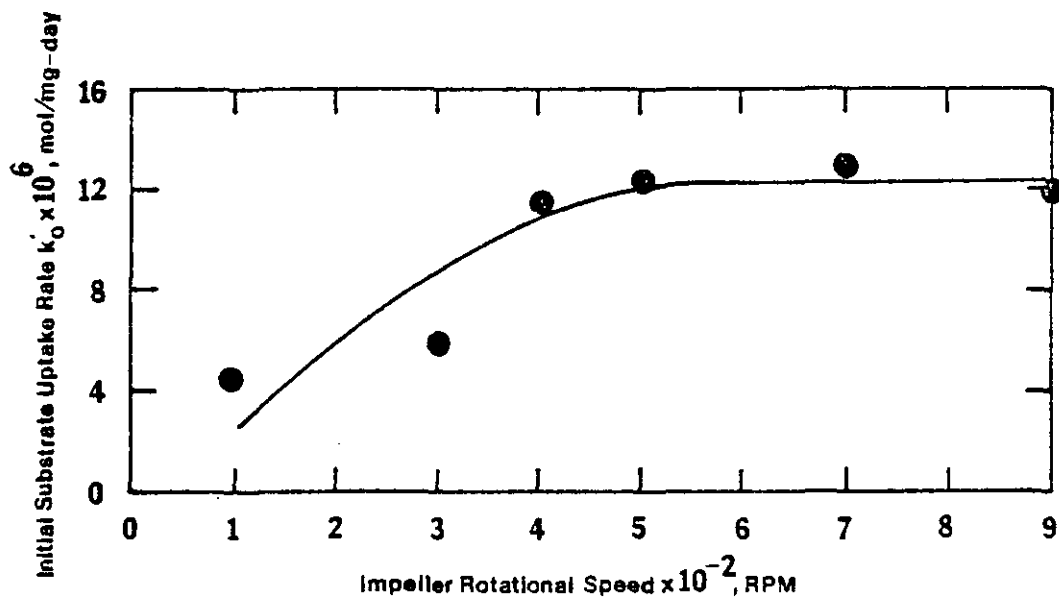
Figure 5-2 The Effect of Impeller Rotational Speed on Initial Substrate

Uptake Rate, k_o'

nitrification is between 7.2 and 9.0, and that the optimum temperature

is between $30°$ and $35°C$. However, it is not clear whether these

values were obtained under diffusion-free conditions. Besides, it is

possible that a portion of the ammonia in water would be stripped out

by vigorous agitation if the pH is above 7.0 and the reactor is exposed

to air. Therefore, a set of experiments was run to determine the

optimum pH and temperature using an impeller rotational speed of

900 rpm to ensure elimination of diffusion resistances; the reactor

was sealed to minimize ammonia stripping by agitation.

In determining the effect of pH on the intrinsic nitrification

rate, the temperature was maintained at $30°C$, and the initial ammonium

concentration was 7.14×10^{-5} mol N/ℓ. Figure 5-3 shows the results of

these experiments. It can be seen that the optimum pH is 8.0 and

that at pH 6.5 nitrification ceased. Table 3 in Appendix 5 lists the

data which was plotted in Figure 5-3.

The optimum temperature was determined in similar experiments by

using the same initial ammonium concentration (7.14×10^{-5} mol N/ℓ).

In these runs, pH was maintained at 8.0. Figure 5-4 depicts that the

maximum initial uptake rate, k_o', was obtained at a temperature ranging

between $30°$ and $35°C$, in agreement with published data[93]. Table 3

in Appendix 5 summarizes the values of k_o' shown in Figure 5-4.
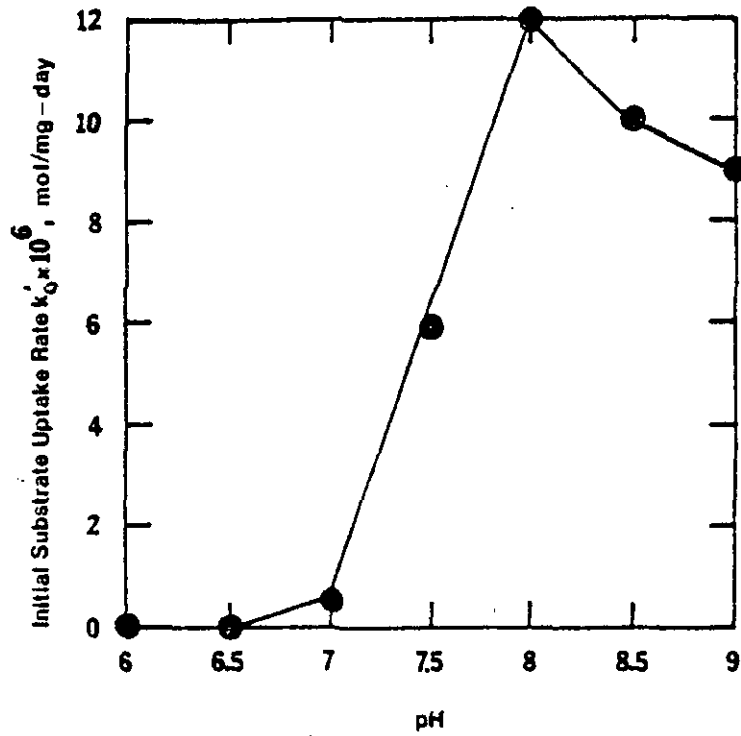
Figure 5-3 The Effect of pH on Initial

Substrate Uptake Rate, k_o'
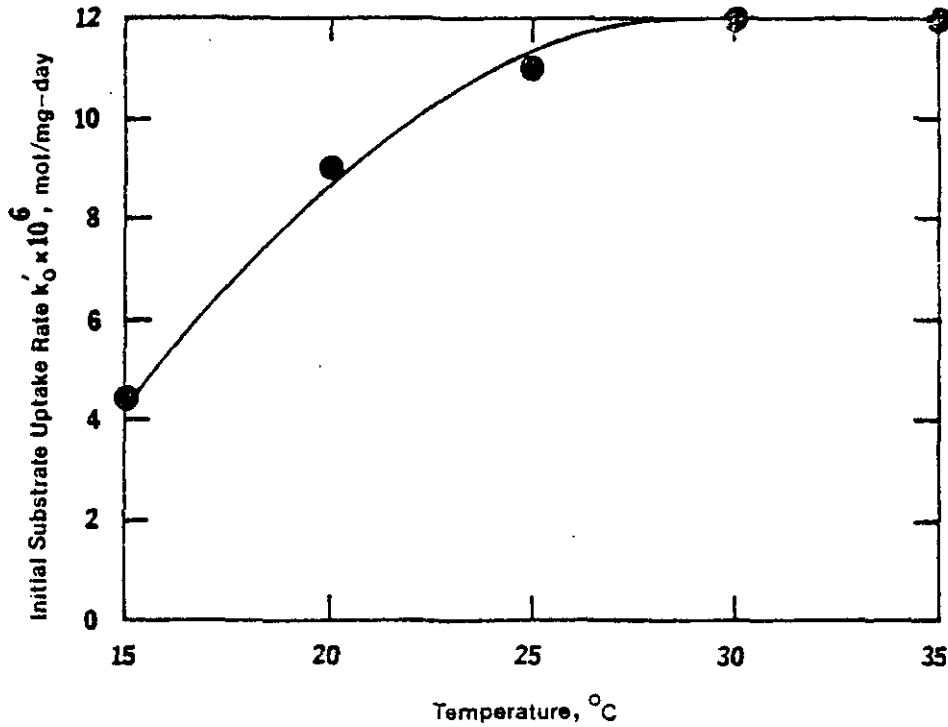
Figure 5-4 The Effect of Temperature on Initial Substrate Uptake Rate, k_o'

The raw experimental data of this part of the investigation are also shown in Table 3, Appendix 5.

The effect of initial ammonium concentration on the rate of nitrification.

Once the optimum operating conditions were determined, the next step of the first phase of the investigation was to observe the effect of initial ammonium concentration on the intrinsic values of both k and K_s. Several ammonium concentrations, ranging from 7.14×10^{-5} mol N/ℓ to about 1.43×10^{-3} mol N/ℓ, were used . Typical plots of the remaining ammonium concentration, S, versus time, t, and their respective linearized forms (cf. Eq. (5-4)) are presented in Figures 5-5 and 5-6 respectively. From these plots it can be concluded that the Michaelis-Menten expression (cf. Eq. (5-2)) fits very well. It is important to mention that the biomass concentration, estimated by the MLVSS test remained practically constant throughout each run, as shown in Figure 5-7. This is due to the low growth rate of nitrifiers and to the relatively short duration of each experiment.

This approach was followed with each one of the fourteen different initial ammonium concentrations. In each case, a plot similar to Figure 5-6 provided the values of the parameters k and K_s. These values were plotted as a function of the initial ammonium concentration, S_o, as shown in Figures 5-8 and 5-9. Table 5 in Appendix 5 lists the
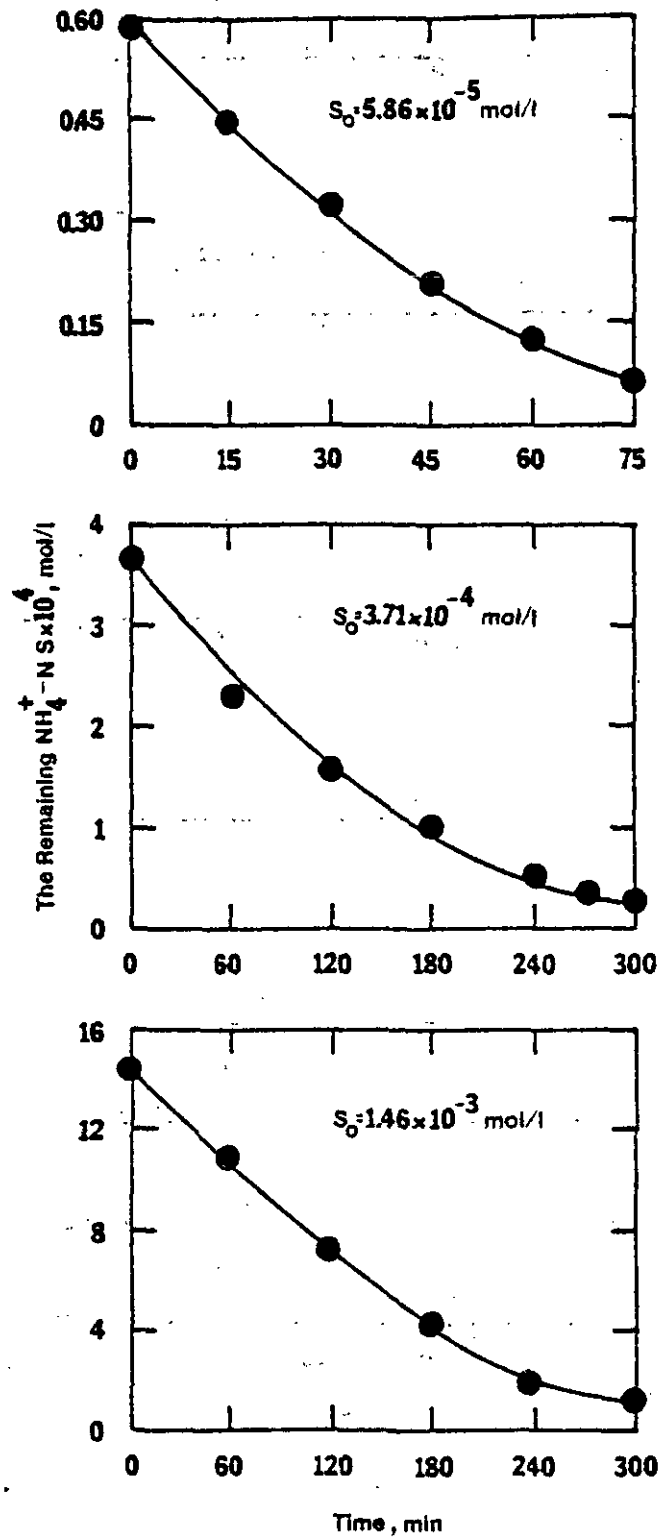
Figure 5-5 Plots of the Remaining
Ammonium Concentration
S versus Time
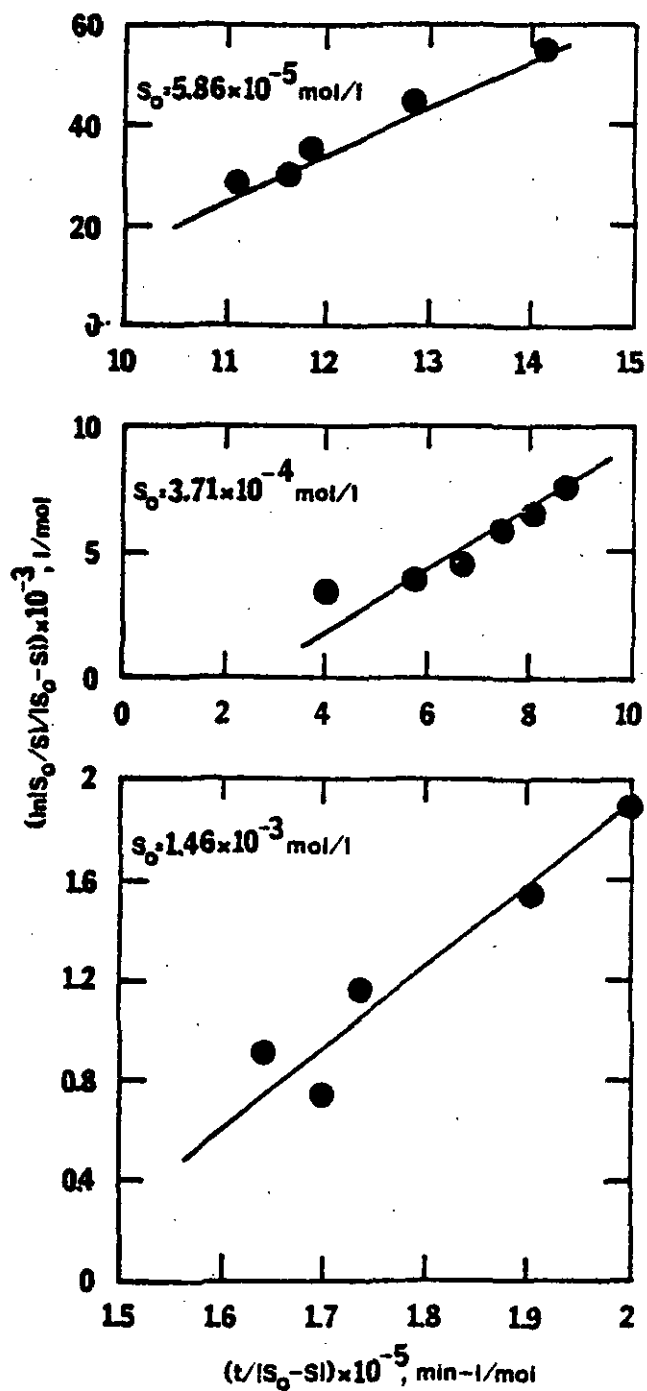
Figure 5-6 Linear Form of Eq. (5-4) of Data Shown in
Figure 5-5
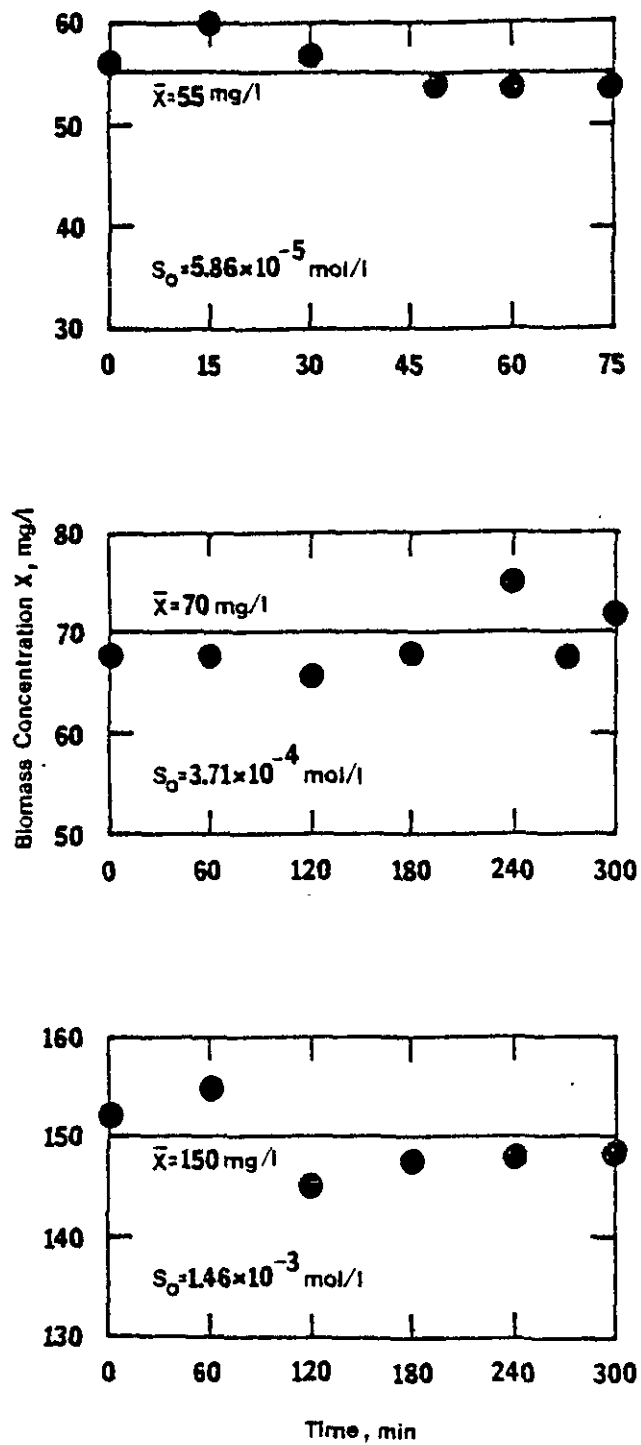
Figure 5-7 Plots of Biomass
Concentration versus
time
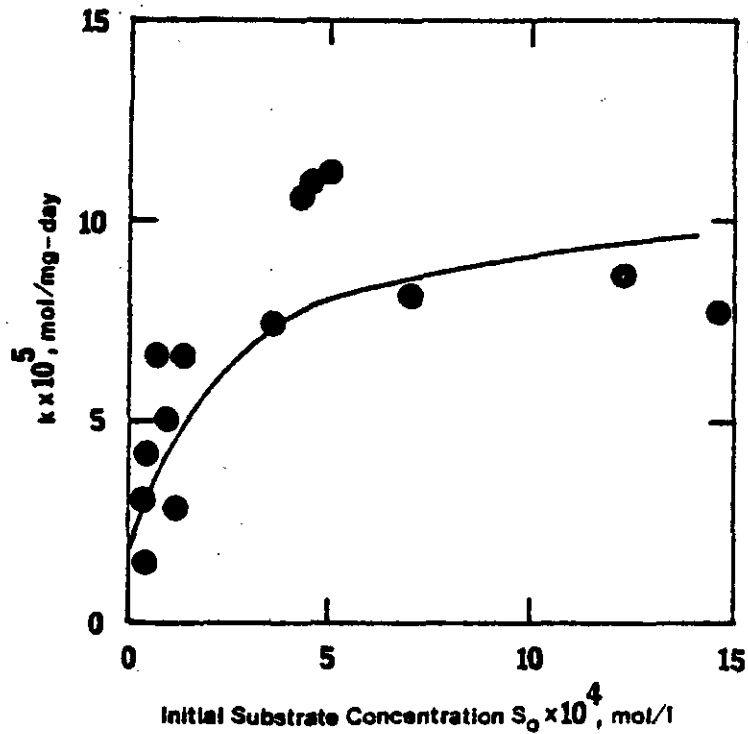
Figure 5-8 The Effect of Initial Ammonium Concentration on k
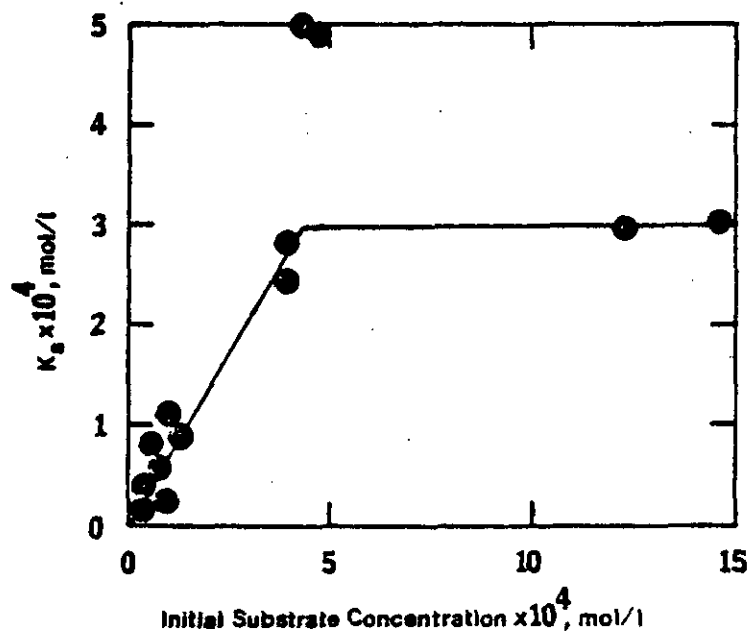
Figure 5-9 The Effect of Initial Ammonium Concentration on K_s

respective data, and Table 4, the raw experimental data of this part of the investigation.

It can be observed that both parameters are strongly dependent on the initial ammonium concentration in the low range of concentrations. However, at sufficiently high concentrations, k and K_s reach a maximum value which is insensitive to increasing initial concentrations.

In the case of the parameter k, an explanation for the behavior shown in Figure 5-9 could be that nitrifiers establish their initial uptake rate level based on the amount of substrate which is externally available. Higher initial substrate concentrations stimulate the activation of new reaction sites, resulting in higher initial uptake rates. However, a saturation of the cell active sites, at high substrate concentrations, would preclude the further increase of the initial uptake rate. A saturation, or maximum initial uptake rate is then observed.

Since the initial rate has a value very close to that of k, the reasoning presented above would apply to the data shown in Figure 5-9. Thus, an equation of the form

$$k = \frac{k_b S_o}{K_m + S_o} \qquad (5-5)$$

would seem to adequately describe the data presented in Figure 5-8.

The curve drawn is Eq. (5-5) and provides a good fit. The values of k_b and K_m, obtained from the Lineweaver-Burk plot (Figure 5-10), are

$$k_b = 9.71 \times 10^{-5} \text{ mol/mg-day, and}$$

$$K_m = 1 \times 10^{-4} \text{ mol/} \ell$$

In the case of the parameter K_s the author is not aware of a theoretical explanation for the observed behavior. The two straight lines drawn through the data points in Figure 5-9 are lines of best fit, and should not be interpreted as a proposed model for such a phenomenon. The lack of sufficient data between initial ammonium concentrations of 4×10^{-4} and 12×10^{-4} mol/ℓ makes it very difficult to arrive at any final conclusion.

Summary

The intrinsic nitrification rate was observed in a batch reactor by eliminating external and internal diffusion resistances. The former were minimized by means of intense agitation, and the latter by mechanical rupture of the floc particles using high impeller rotational speeds. The optimum pH and temperature were found to be 8.0 and 30° to 35°C respectively. The Michaelis-Menten rate equation was found to be an appropriate expression for the nitrification process. However, the intrinsic kinetic parameters k and K_s cannot be considered
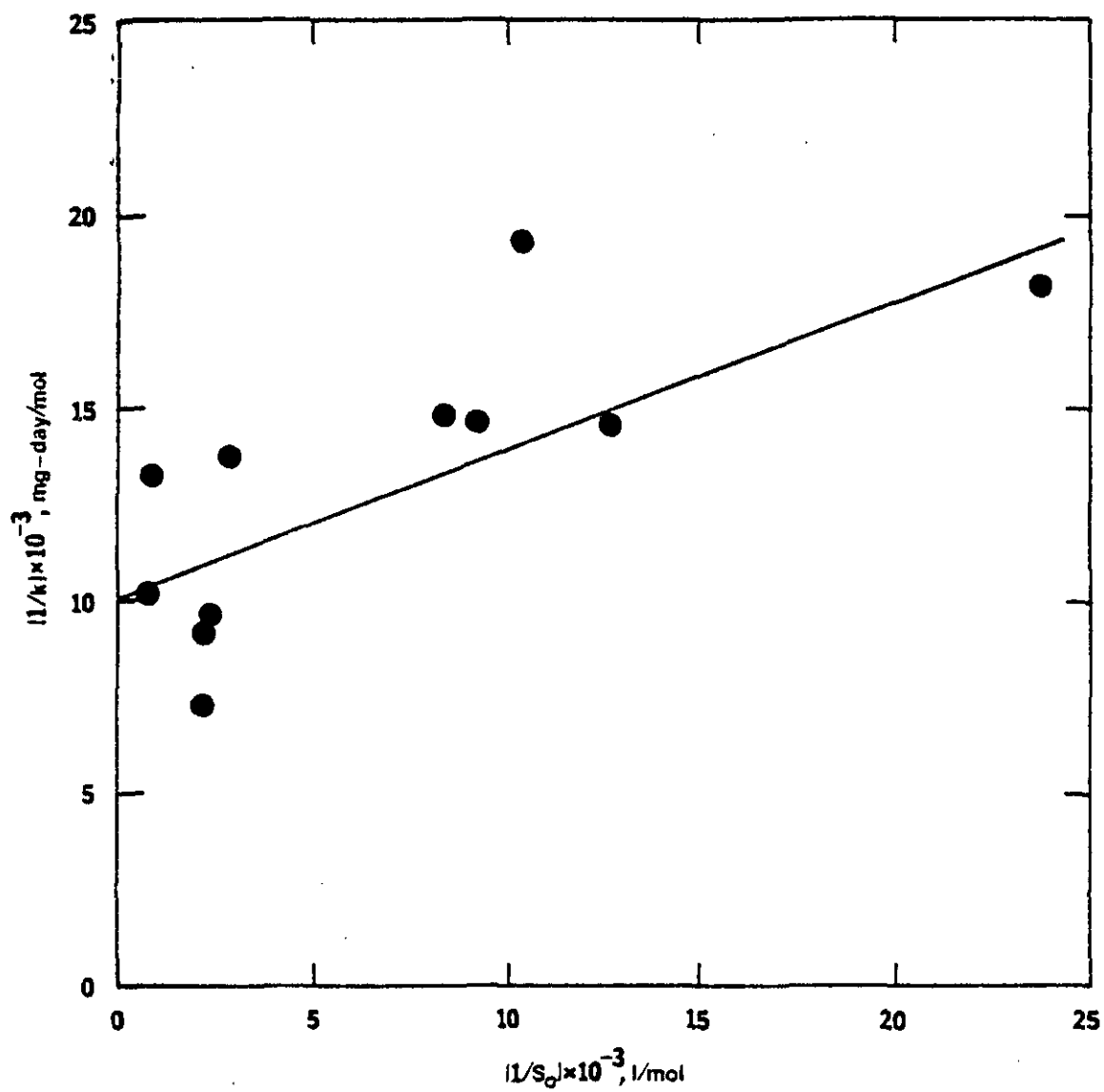
Figure 5-10 Lineweaver-Burk Plot of Data Shown in Figure 5-8

true constants since both of them depend on the initial ammonium concentration. At low ammonium levels, k and K_s strongly depend on the initial ammonium level. At high initial concetrations, k attained a constant maximum value which is independent of the initial ammonium level. Any trend on the dependency of K_s on S_o is difficult to ascertain due to the lack of sufficient experimental data.

CHAPTER VI

CONTINUOUS FLOW EXPERIMENTS. RESULTS AND DISCUSSION

Introduction

The investigation reported in this chapter represents the second phase of the overall study aimed to model the activated sludge nitrification process.

It has been reported in the literature[27, 34] that differences between batch and continuous cultures go beyond physical dissimilarities to the extent that results obtained from batch experiments cannot be directly applied to continuous flow systems. Therefore, this second experimental phase has the following specific objectives:

(a) To verify the applicability of the proposed Michaelis-Menten kinetic expression to the nitrification process in a CFSTR.

(b) To evaluate the effect of detention time on the intrinsic value of the kinetic parameters k and K_s, under continuous flow conditions.

(c) To determine the effect of internal diffusion resistances of substrate on the overall nitrification rate.

The information obtained in these experiments will be of special value in the design of full-scale treatment plants because of the similarity of both types of operation.

As discussed in Chapter V, most of the data published thus far[68, 93] were evaluated under the assumption that the system is homogeneous, that is, the effect of diffusion resistances was neglected. It seems, therefore, necessary to examine the intrinsic kinetics of the continuous flow systems and compare it with the information reported in the literature. It is believed that such information will provide grounds for the sound selection of certain design parameters under specific operating conditions.

Additional information needed to verify the proposed kinetic model is the value of the effective diffusivity, as well as the value of the observed nitrification rate using different floc particle sizes. With this information, it will be possible to assess the effect of internal diffusion resistances on the performance of full-scale systems.

It was shown in Phase I of this investigation that the growth rate of nitrifiers is relatively low, as presented in Figure 5-7. Consequently, it would be necessary to use a long hydraulic retention time to prevent nitrifiers from being washed out from the chemostat.

In addition, elimination of internal diffusion resistances requires mechanical reduction of particle size to appropriate levels. This, however, will significantly affect the settleability of the floc particles, making it necessary to use an unreasonably large settling unit to allow enough time for particle reflocculation. These arguments ruled out the possibility of using a conventional chemostat with cell recycle to perform this study.

A reasonable alternative, which allows maintaining a constant biomass in the reactor, is feeding continuously a suspension of microorganisms of known concentration, and simultaneously, another stream containing the medium. In this way, the hydraulic retention time can be varied at will, regardless of whether the microorganisms can grow under the selected dilution rate. Following this reasoning, activated sludge from the CFSTR seed unit was added continuously to the influent of the Multigen unit as a biomass source. This simulated, to a certain extent, sludge recycling from a final clarifier. The ammonium concentration in the mixed liquor of the seed unit was always less than 7.14×10^{-6} mol N/ℓ (0.1 mg N/ℓ), so that this stream did not contribute any substrate to the Multigen unit. This practice was used throughout the second phase of the investigation. A schematic diagram of the continuous flow setup is shown in Figure 6-1.
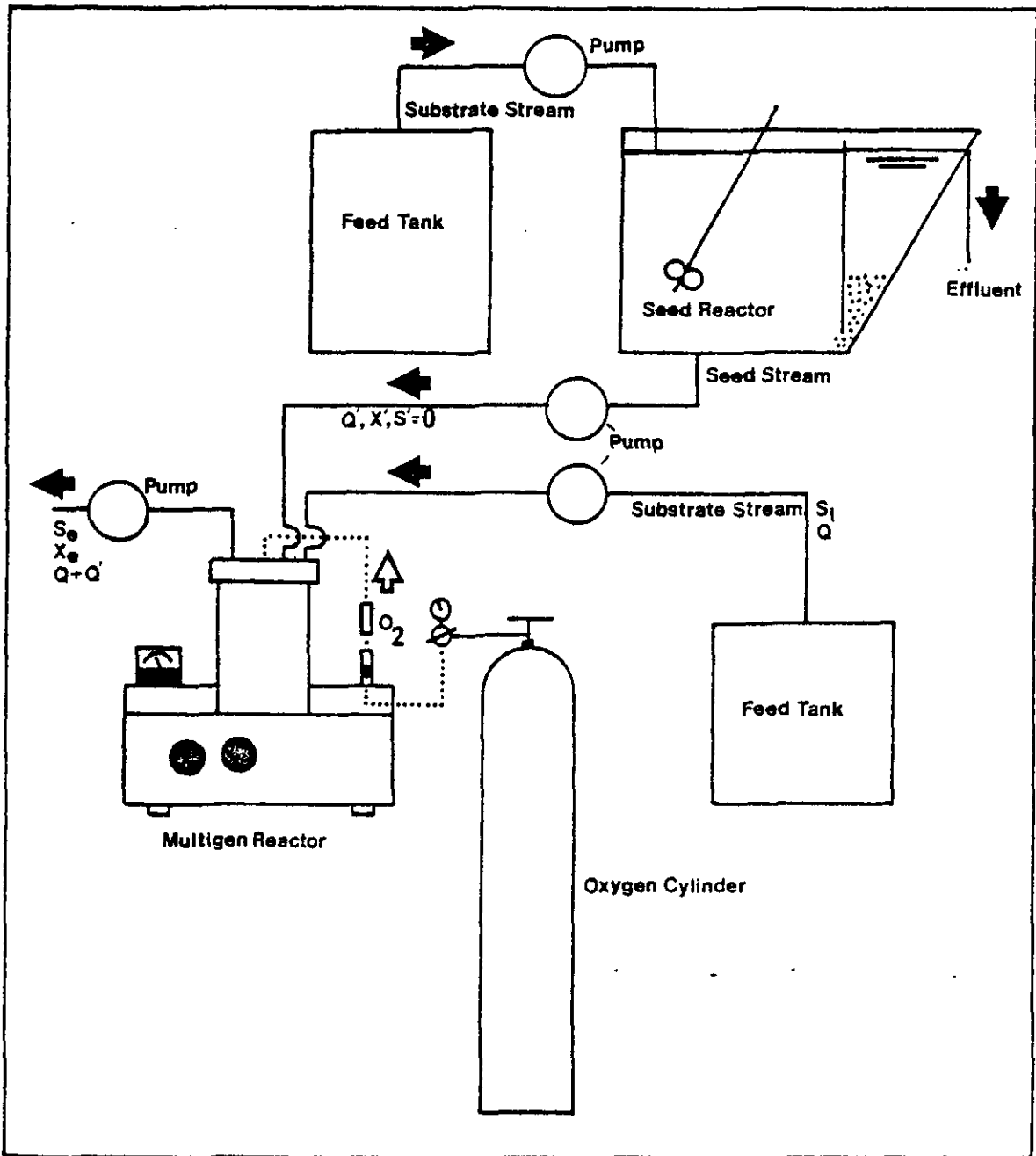
Figure 6-1 Schematic Diagram of the Continuous Flow Experiment Setup

Theory

Intrinsic kinetics. A mass balance of substrate (ammonia) around the

Multigen unit with constant volume yields:

$$V\frac{dS_e}{dt} = Q'S' + QS_i - (Q + Q')S_e - v_i X_e V \tag{6-1}$$

where

V = volume of the Multigen unit, mℓ

Q' = seed flowrate, mℓ/min

Q = influent flowrate, mℓ/min

S' = substrate concentration in seed input flow $\approx$ 0 mol/ℓ

S_i = influent substrate concentration, mol/ℓ

S_e = effluent (or mixed liquor) substrate concentration of the

    Multigen unit, mol/ℓ

t = time, min

v_i = intrinsic removal rate of substrate, mol/mg-day

X_e = concentration of cells in the reactor and in the effluent

    stream, mg/ℓ

Assuming Michaelis-Menten kinetics and steady state conditions, then

$$QS_i - (Q + Q')S_e = \frac{kS_e}{K_s + S_e} X_e V \tag{6-2}$$

or

$$v_i = \frac{QS_i - (Q + Q')S_e}{X_e y} = \frac{kS_e}{K_s + S_e} \qquad (6-3)$$

Rearrangement of Eq. (6-3) yields

$$\frac{1}{v_i} = \frac{X_e V}{QS_i - (Q + Q')S_e} = \frac{K_s}{k} \cdot \frac{1}{S_e} + \frac{1}{k} \qquad (6-4)$$

A plot of $1/v_i$ versus $1/S_e$ should yield a straight line with slope K_s/k and intercept $1/k$, from which the parameters k and K_s can be evaluated.

A steady-state mass balance of biomass around the Multigen unit, in terms of MLVSS, yields

$$Q'X' - (Q + Q')X_e = -v_{mi}V \qquad (6-5)$$

where

X' = biomass concentration in the seed stream, mg/ℓ

v_{mi} = net growth rate of biomass, mg/ℓ-day

If the growth rate of nitrifiers is negligible under the experimental conditions, then $v_{mi} = 0$, or

$$X_e = \frac{Q'X'}{(Q + Q')} \qquad (6-6)$$

Experimental evaluation of the effectiveness factor. If the size of the floc particle is sufficiently large, the observed rate will be

less than the intrinsic one. In this case, the observed rate in the

Multigen unit, at steady state, is

$$v_o = \frac{QS_i - (Q + Q')S_e}{X_e V} \qquad (6-7)$$

The intrinsic rate v_i, at effluent substrate concentration S_e is

$$v_i = \frac{KS_e}{K_s + S_e} \qquad (6-8)$$

The ratio of v_o to v_i is defined as the experimental effectiveness

factor n_e:

$$n_e = \frac{v_o}{v_i} = \frac{\dfrac{QS_i - (Q + Q')S_e}{X_e V}}{\dfrac{kS_e}{K_s + S_e}} \qquad (6-9)$$

Experimental Procedure

Using the results of Phase I of this investigation, a pH of 8.0

and a temperature of $30^{\circ}C$ were selected for the operation of the

continuous flow reactor. The pH of the reactor was continuously

monitored and phosphate buffer solution was added if necessary. The

dissolved oxygen concentration was checked three times a day to assure

it was always kept above 4.7×10^{-4} mol/ℓ. An impeller rotational

speed of 900 rpm was used in the study of intrinsic kinetics to

eliminate internal diffusion resistances. For studying the effect of internal diffusion on the overall rate, different rpm values were used to obtain different floc particle sizes.

The reactor was sealed to minimize ammonia stripping due to oxygenation under intense agitation. In the study of intrinsic nitrification kinetics, five liquid detention times, based on the ratio $V/(Q + Q')$, were used; these ranged from 100 to 300 minutes. Under a fixed flowrate, several influent substrate concentrations, ranging from 5.43×10^{-4} mol N/ℓ to 6.86×10^{-3} mol N/ℓ (7.6 mg N/ℓ to 96 mg N/ℓ) were used. The effluent substrate concentration, S_e, and the MLVSS concentration, X_e, were determined at each influent substrate concentration when steady state was reached. At least three samples were collected and the average values of S_e and X_e were used as the representative values for that specific run. In each case, steady state conditions were reached when S_e and X_e attained constant values.

In the study of the effect of internal diffusion on the overall nitrification rate, a liquid detention time of 150 minutes was used. The range of influent substrate concentrations was the same as that used in the intrinsic kinetics study. Six different rotational speeds, namely 50, 100, 200, 300, 400, and 500 rpm, were used to obtain

different floc particle sizes. The procedure for collecting and analyzing samples were the same as those in the intrinsic kinetics study.

Experimental Results and Discussion

Determination of k and K_s. According to Equation (6-4), evaluation of k and K_s requires observing the intrinsic uptake rate, v_i, under several different effluent concentrations, S_e. This can be done by two procedures, namely, by keeping a constant influent concentration and varying the detention time, or by keeping a constant detention time and varying the influent flow rate.

The first approach has been used by several researchers[1, 33, 68, 83, 98, 115, 116], based on the argument that current kinetic models predict that the effluent organic concentration is not influenced by the influent concentration, nor by the biomass concentration in the reactor. However, recent studies[21, 38, 40, 66] based on the second approach, have demonstrated that reactor performance is significantly affected by the substrate level in the influent stream.

Thus it seemed necessary to use both experimental procedures to observe the effect of both parameters (holding time and influent

substrate concentration), on the value of the kinetic constants k and

K_s. Several sets of continuous flow experiments were performed; each

set was run under a constant detention time, while the influent

ammonium concentration in each run was different. In this way,

intrinsic rates were observed under different ammonium concentrations

for each set of constant detention times.

Figure 6-2 displays the results obtained with a detention time of

150 minutes and shows that the value of the intrinsic rate, v_i,

increases rapidly as S_e increases, in the low range of substrate

concentration, and then levels off at sufficiently high substrate

concentrations. This is a typical characteristic of Michaelis-Menten

kinetics, which was also observed with each one of the detention times

which were tried (the raw data are listed in Table 6, Appendix 5). A

Lineweaver-Burk plot, which according to Eq. (6-4) should yield a

straight line, is presented in Figure 6-3, and shows that the fit is

good. Both k and K_s can be evaluated from the values of the slope and

the intercept of the straight line.

The values of k and K_s, obtained in similar runs, with detention

times of 100, 120, 150, 200, and 300 minutes, are shown in Table 7,

Appendix 5. The magnitude of k was found to be strongly affected by

detention time; Figure 6-4 shows that k decreases as detention time
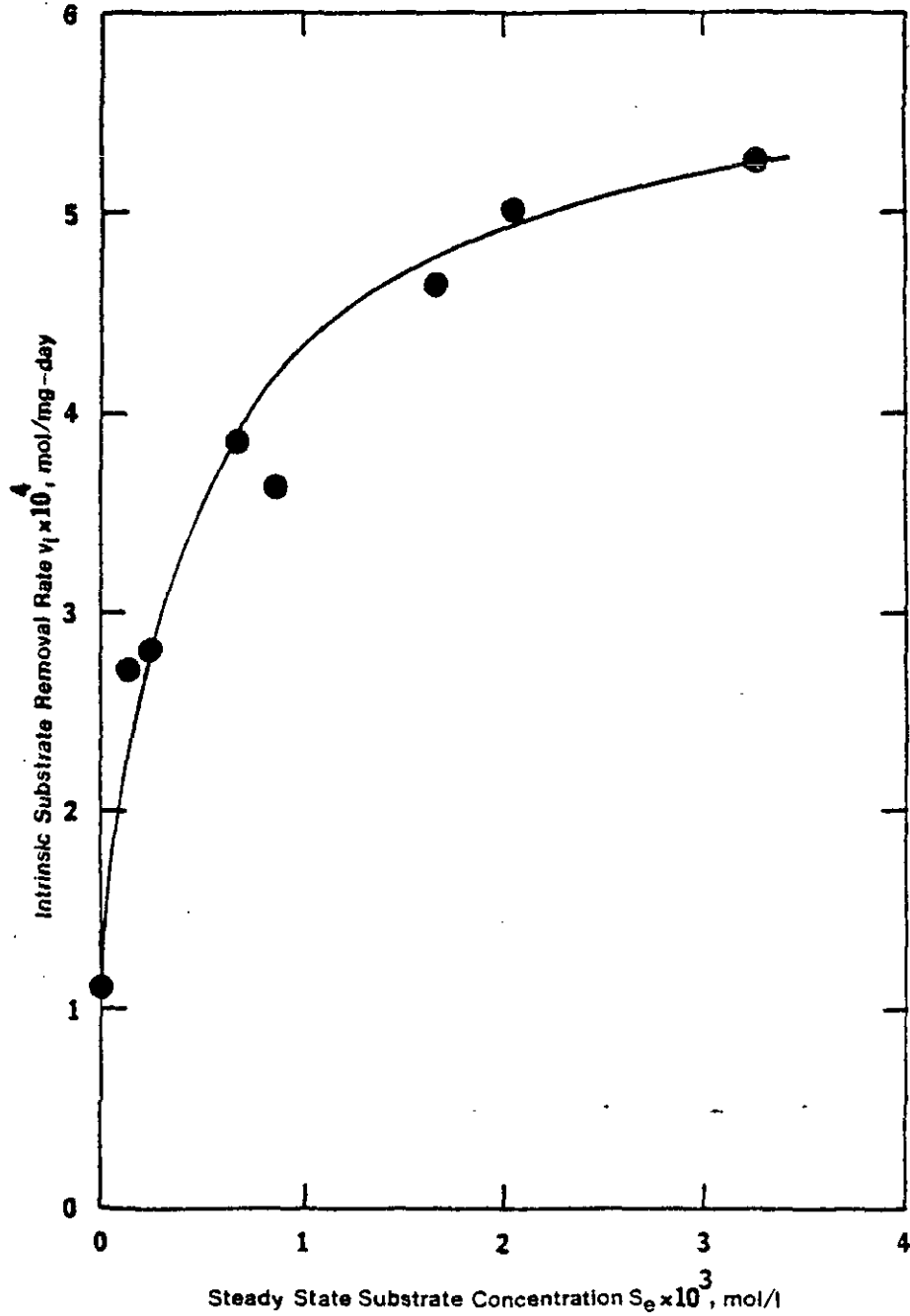
Figure 6-2 Plot of Intrinsic Rate v_i versus Steady
State Substrate Concentration S_e at
Detention Time of 150 minutes
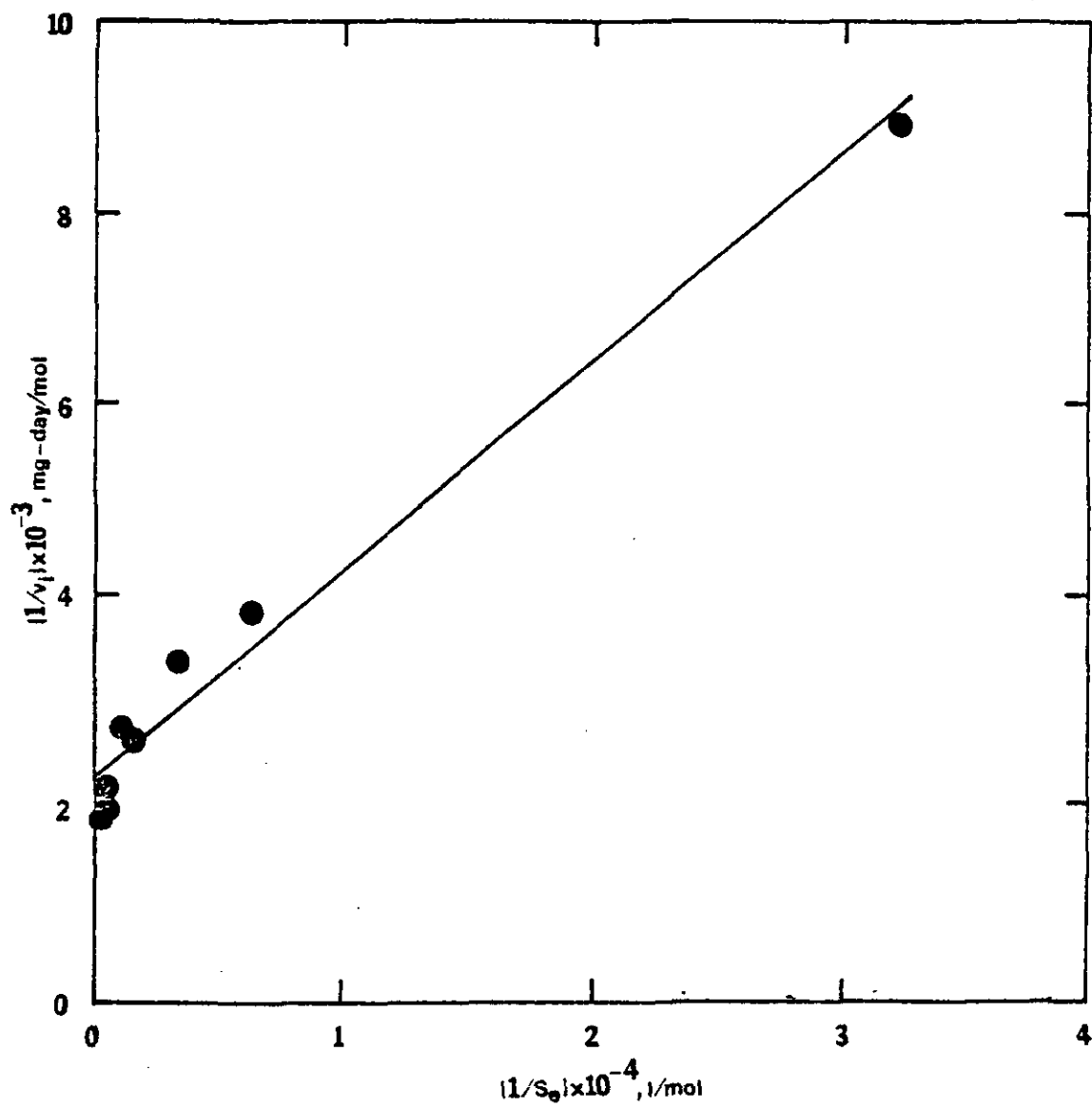
Figure 6-3 Lineweaver-Burk Plot of Data Shown in Figure 6-2
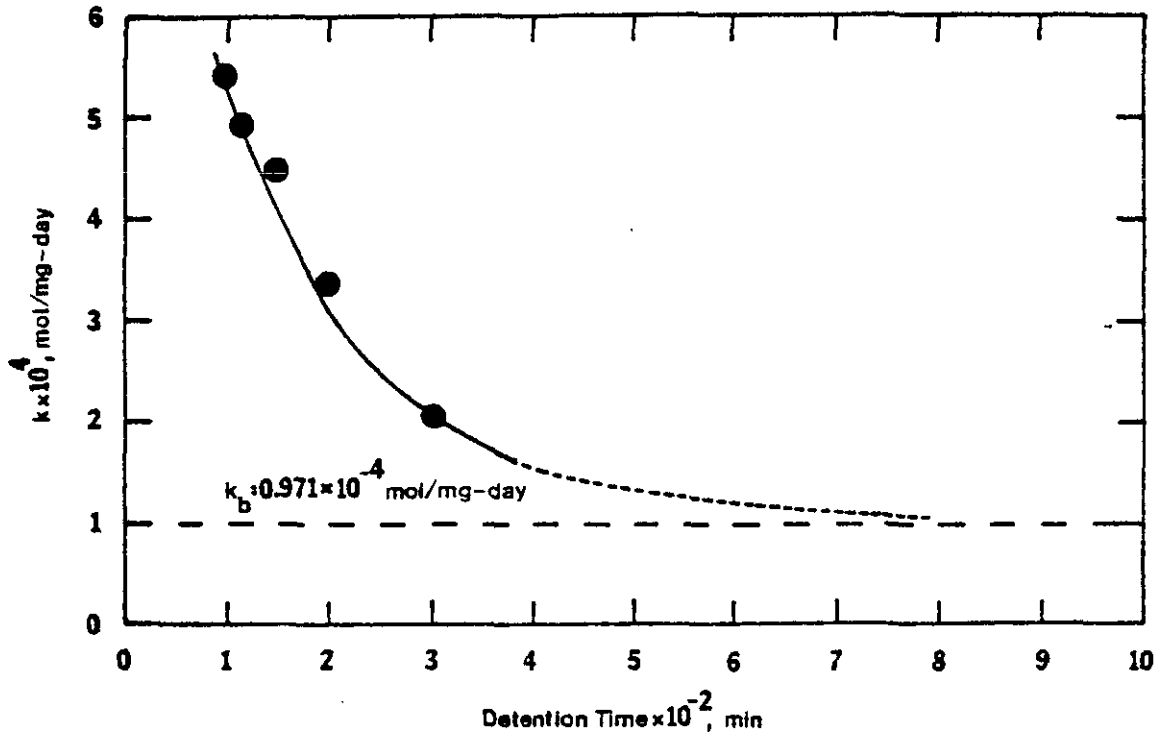
Figure 6-4 The Effect of Detention Time on k
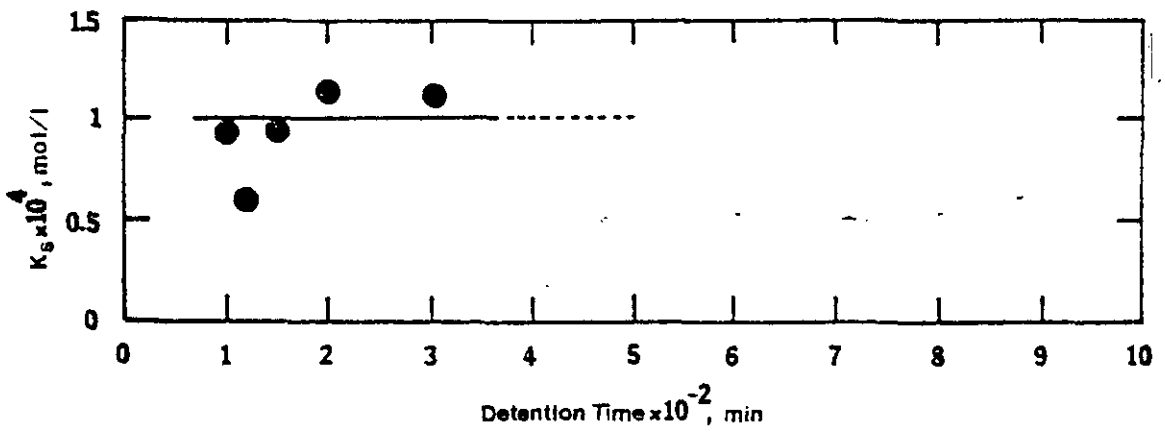
Figure 6-5 The Effect of Detention Time on K_s

increases. At infinite detention time, i.e., under batch conditions, the maximum value of k was found to be $k_b = 0.971 \times 10^{-5}$ mol/mg-day (see Chapter V). It is interesting to see that k would approach this value if the detention time had been increased sufficiently, as indicated by the dotted line.

A reasonable explanation for this phenomenon could be that in a CFSTR under steady state operation, the maximum rate of substrate utilization, at a given influent substrate concentration, is determined by the time the microorganisms are allowed to contact it. Therefore, in order to obtain enough substrate for maintenance and synthesis purposes, the microorganisms will establish higher uptake rates when the contact time with the substrate is shorter.

The observation of this phenomenon is possible only when the microorganisms can always remain in the system, regardless of whether they can grow under the stress of high dilution rates. The method chosen in this investigation, i.e., using a constant input of biomass, is an excellent method to attain this objective. It is believed that for studying the kinetics of biological systems, the correct approach to observe the effect of ambient substrate concentration on the uptake rate is performing the experiments under a constant detention time. The evidence presented above, namely, that the detention time exerts a

strong effect on the saturation utilization rate k, shows the approach

commonly used by many investigators, i.e., maintaining a constant

influent substrate concentration and varying the detention time, may

lead to questionable conclusions with regard to the magnitude of the

kinetic constants.

Figure 6-5 shows the effect of detention time on K_s; it is clear

that K_s is practically unaffected by the detention time values used in

this study.

It is important to note at this point that both batch and

continuous flow experiments have demonstrated the applicability of the

Michaelis-Menten equation to describe the intrinsic kinetics of

nitrification. However, the values of the kinetic constants obtained

with each system, are seen to be completely different. The response

of microorganisms to the changing environment in the batch experiments

differs from that in the steady-state continuous flow experiments, in

which microorganisms are exposed to a constant environment. In

addition, the contact time between microorganisms and substrate in a

continuous flow reactor affects the magnitude of k, to the extent that

reducing the detention time by one half, roughly doubles the value of k.

Additional evidence of the different behavior of microorganisms

under batch or continuous flow conditions was presented by Gaudy, et al

$^{(34)}$ and Chiu, et al$^{(27)}$.

It can be concluded that batch experiments can be used to verify the applicability of a specific kinetic expression. However, the numerical values of the kinetic parameters obtained cannot be applied directly to predict the performance of a continuous flow culture.

The actual biomass concentration in the reactor, X_e, was compared to that calculated by means of Eq. (6-6), to determine whether there was any growth in the reactor over the wide range of influent substrate concentrations used. Table 6-1 shows the results obtained under a detention time of 150 minutes. It is clear that practically no growth of nitrifiers was observed when the influent substrate concentrations varied from 6.0×10^{-4} mol N/ℓ to 6.714×10^{-3} mol N/ℓ (8.4 mg N/ℓ to 94 mg N/ℓ). Similar observations have been reported by some investigators who have found that the yield coefficient of nitrifiers is relatively low (0.02 to 0.084 mg/mg)[68, 93].

Determination of the effect of internal diffusion resistances on the observed nitrification rate. The experiments to determine the effect of internal diffusion resistances on the observed nitrification rate were performed under the same conditions as those in the study of intrinsic kinetics, except for the impeller rotational speed, which was varied to obtain different floc particle sizes. The detention

TABLE 6-1

PREDICTED AND EXPERIMENTAL VALUES OF CONCENTRATION OF MICROORGANISMS. DETENTION TIME, 150 MINUTES

Influent Ammonium Concentration $S_i \times 10^3$ (mol N/ℓ)	Predicted X_e (mg/ℓ)	Experimental X_e (mg/ℓ)
0.60	35	36
1.21	32.5	32
1.75	35	36
2.61	32.5	32
2.79	32.5	32
3.71	30	24
5.00	32	32
6.71	32	32

time used was 150 minutes; therefore, the result obtained must be
compared to those observed under the same detention time in the intrinsic
study.

The observed rate, v_o, was determined using several rotational
speeds, at different effluent substrate concentrations. The results,
shown in Figure 6-6, suggest a common relationship between v_o and S_e,
regardless of rotational speed. Hence a single kinetic expression may
be developed from those experimental data.

As discussed in Chapter II, there are two ways in which internal-
diffusion resistances will affect the observed rate. First, the reaction
order is altered, and the observed kinetic constants include such
parameters as intrinsic kinetic constants, particle dimensions, and
effective diffusivity. This was observed by La Motta[65, 67] and
Harremoës[41, 42] in the case of biological films; they observed that
for a zero-order intrinsic kinetics, the apparent reaction order was
one-half. Second, in the case of complex kinetic relationships, such
as the Michaelis-Menten expression, the effect of internal-diffusion
resistances is manifested on the value of the kinetic parameters k and
K_s.

As discussed in Chapter II, a Lineweaver-Burk plot of data
collected under significant internal diffusion resistances does not
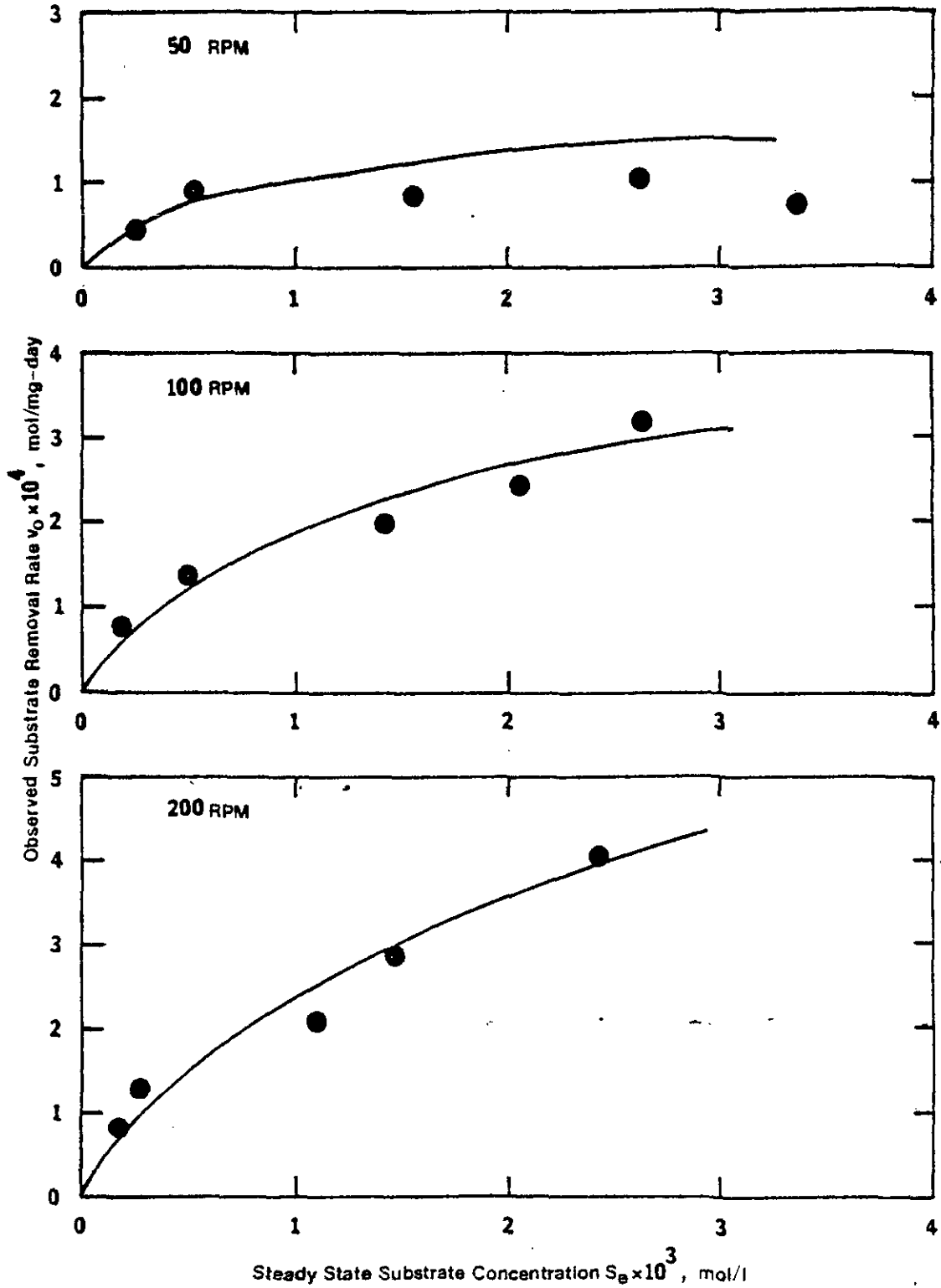
Figure 6-6 Plots of Observed Rate v_o versus Steady State Substrate Concentration S_e at Different Impeller Rotational Speeds
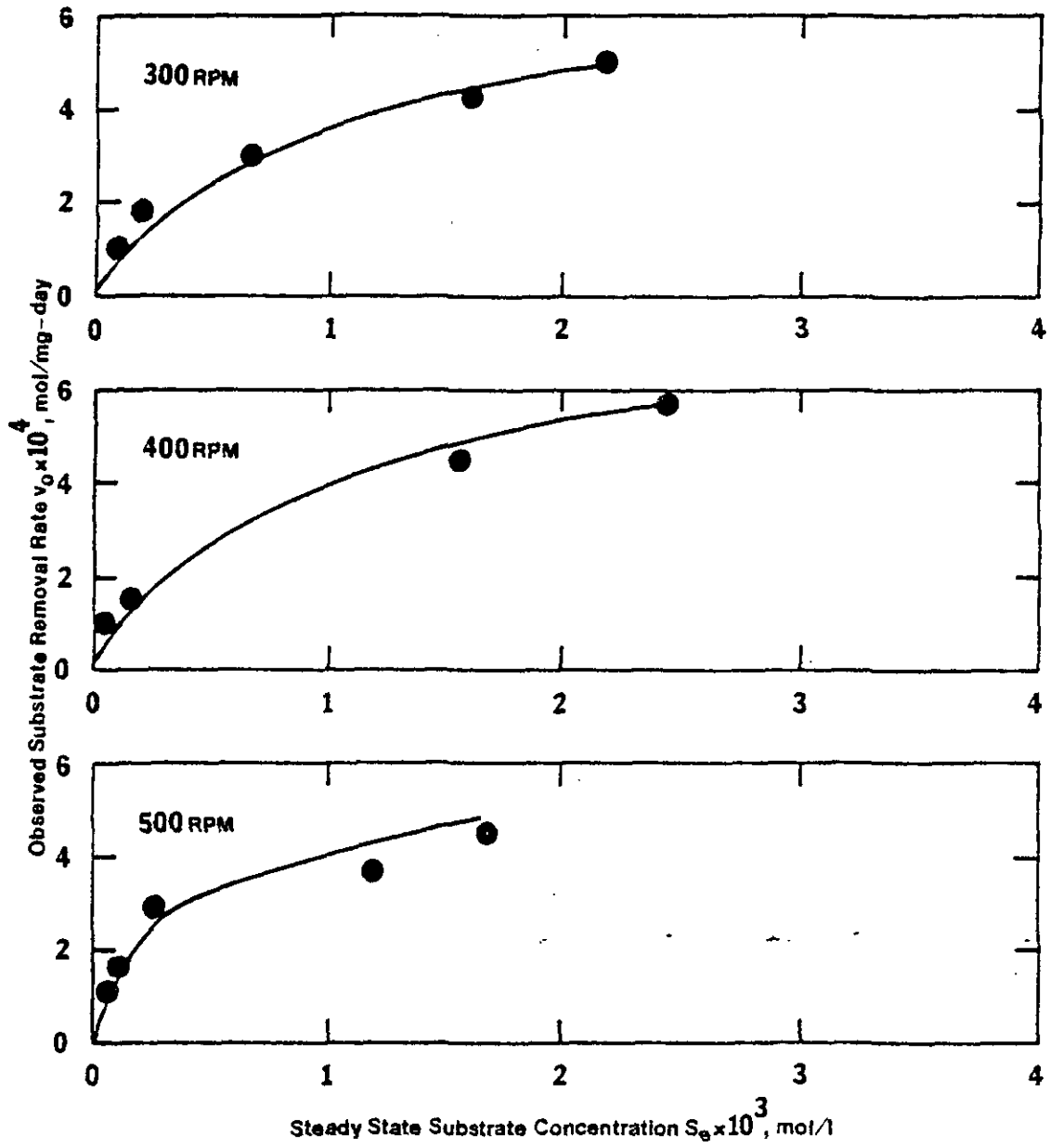
Figure 6-6 Continued

yield a straight line. However, as seen in Figure 2-9, at low

substrate concentrations (i.e., at high values of $1/\beta$) the curves do

not deviate significantly from straight lines; this has led several

investigators[28, 40, 41, 43] to the conclusion that apparent kinetic

coefficients k' and K'_s can be obtained from the slope and intercept of

straight lines of best fit drawn through the experimental data points.

For illustrative purposes, Lineweaver-Burk plots of all data

collected in this phase were prepared. This is shown in Figure 6-7;

it can be seen that straight lines can be drawn through each set of

points. It is also clear that, as expected, both the slope and the

intercept increase as rpm decreases. However, the values of k and K_s

obtained from this analysis are pseudo-constants, the intrinsic ones

being observed only when internal-diffusion resistances are negligible.

This explains the wide variation of the reported values of k and K_s

for the activated sludge nitrification process, since different apparent

constants will be observed in the same system under different particle

sizes.

The ratio of the apparent kinetic constants k' and K'_s to their

respective intrinsic values are plotted in Figures 6-8 and 6-9 as a

function of both rpm and particle size. Table 8 in Appendix 5 lists

the numerical values of k' and K'_s.
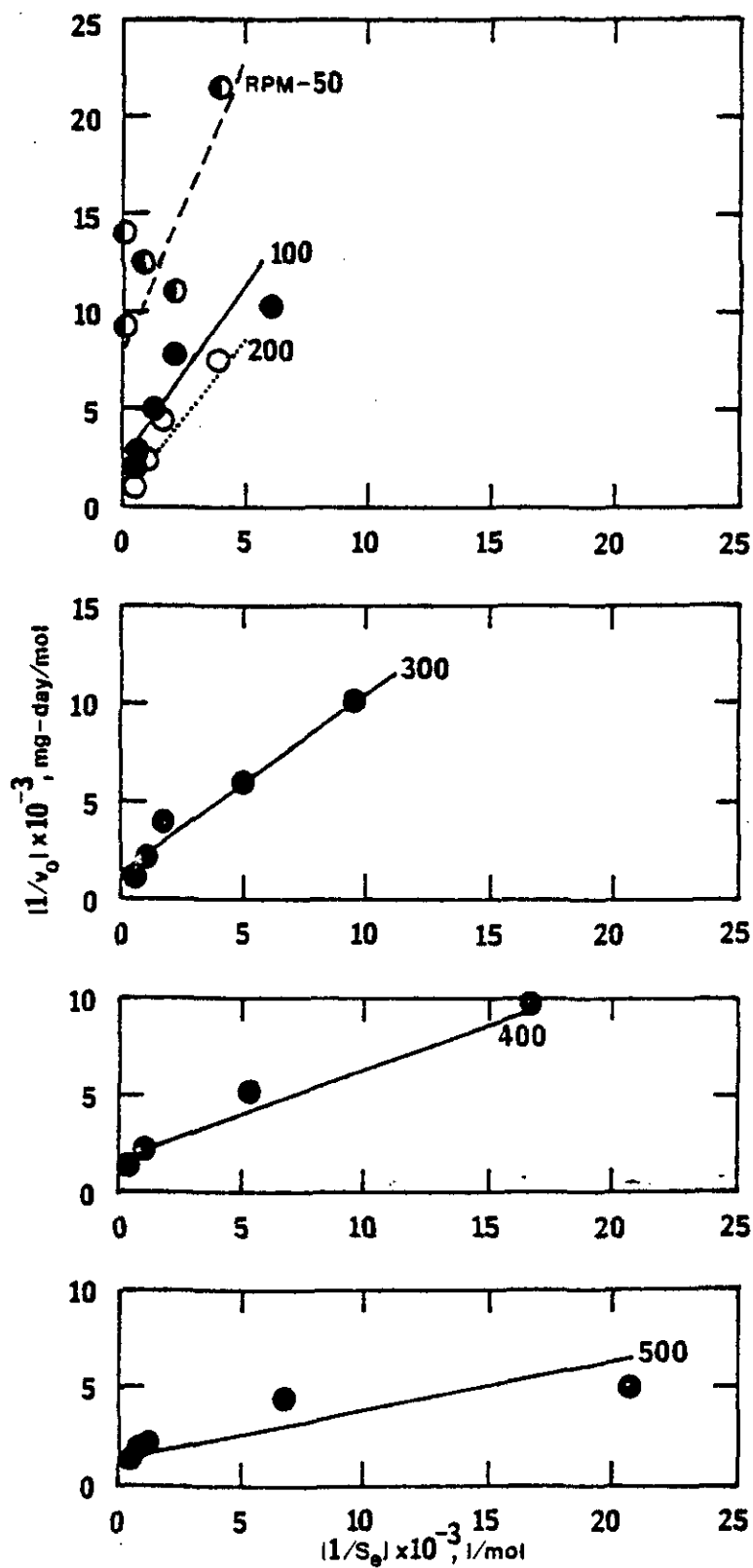
Figure 6-7 The Effect of Internal Diffusion Resistances on Lineweaver-Burk Plots.
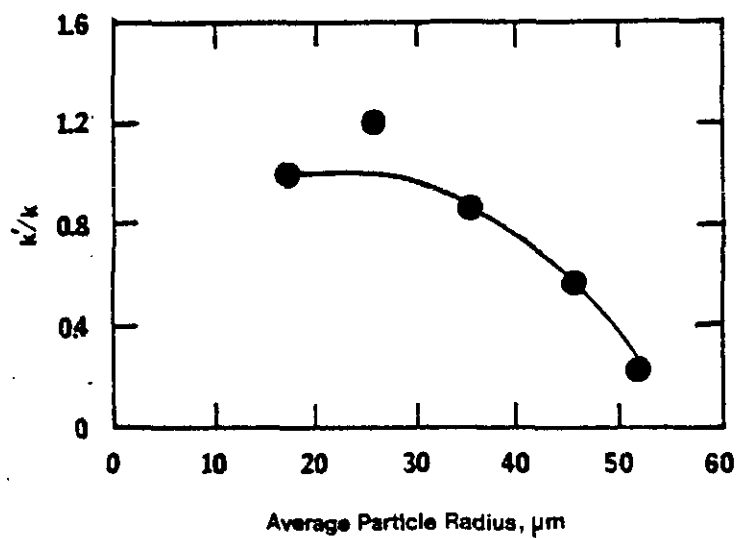
Figure 6-8(a) Values of k'/k at Different
Particle Sizes
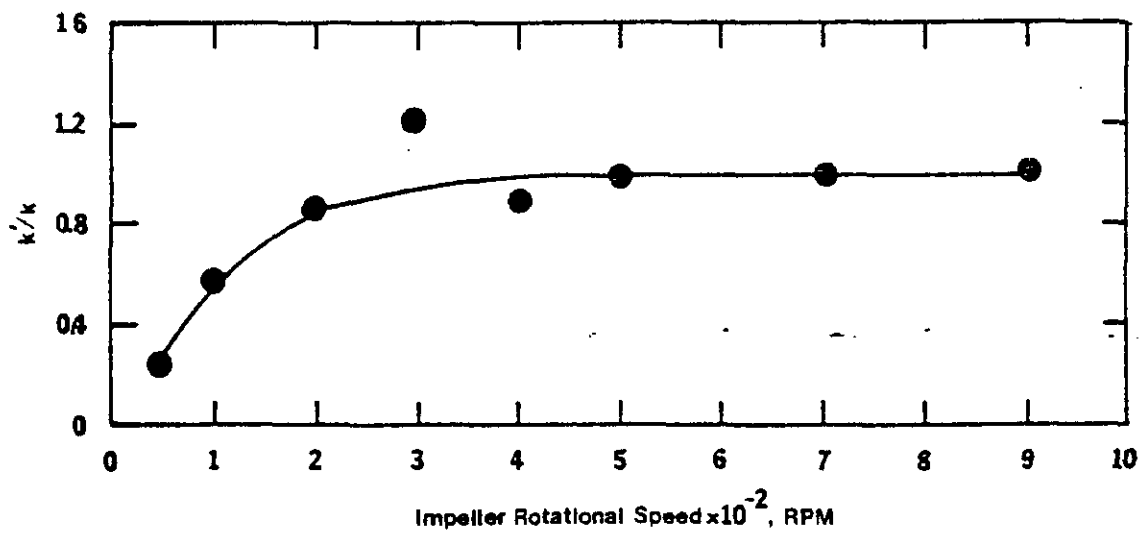
Figure 6-8(b) Values of k'/k at Different Impeller Rotational
Speeds
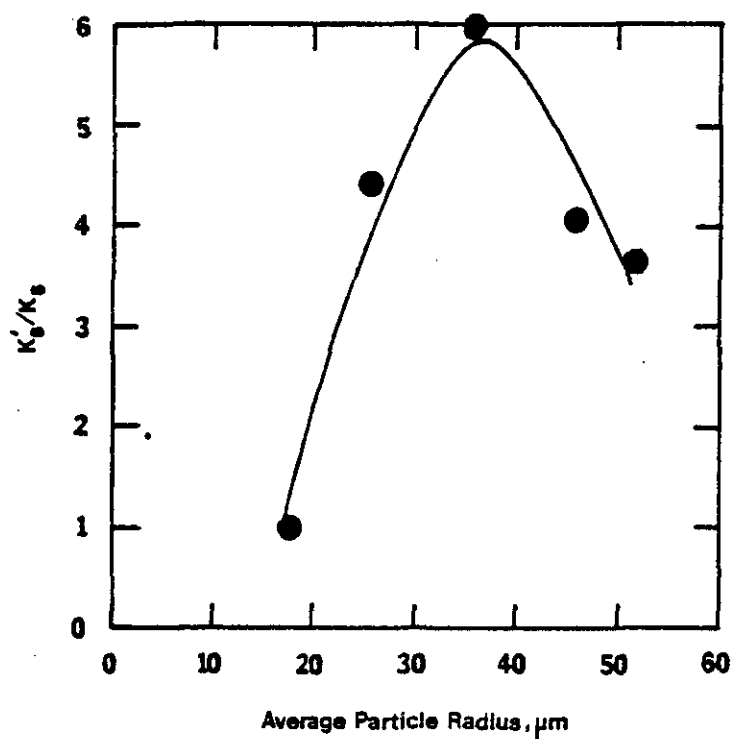
Figure 6-9(a) Values of K'_s/K_s at Different Particle Sizes
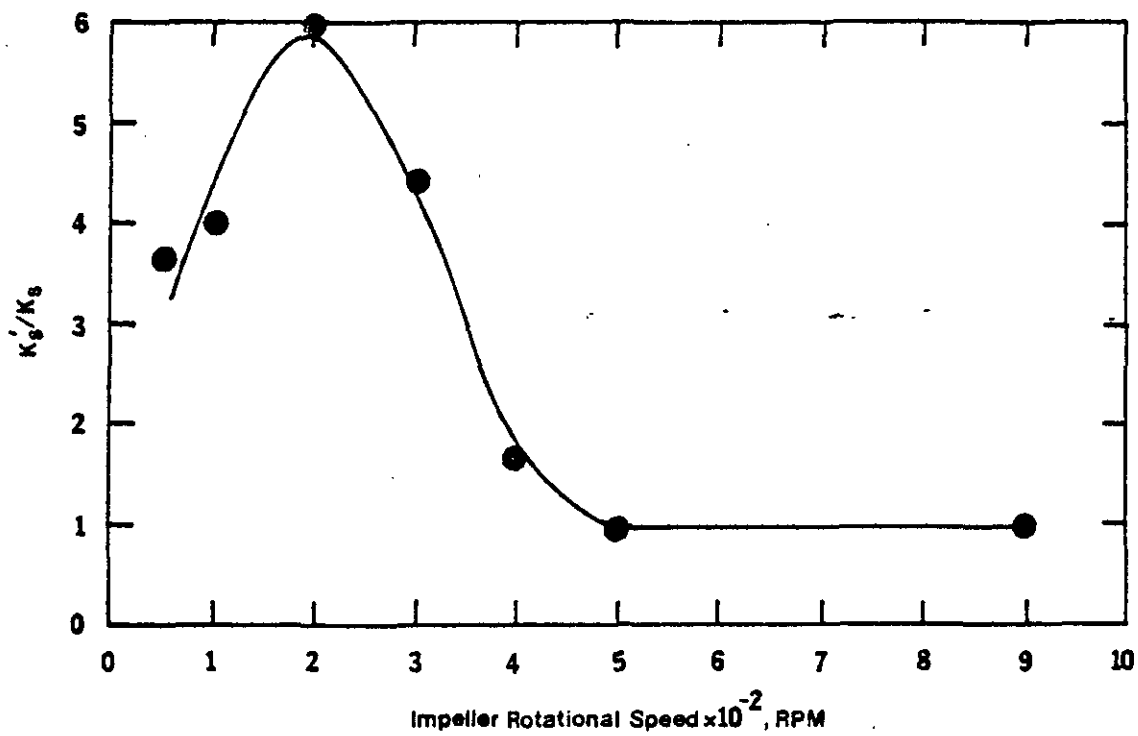
Figure 6-9(b) Values of K'_s/K_s at Different Impeller Rotational Speeds

In the case of k', the ratio k'/k increases as particle size decreases; the lower values correspond to significant internal diffusion resistances. The value of k' approaches the intrinsic value as floc size is reduced to 36 μm, in which the effectiveness factor is 1.0.

In the case of K_s', higher values of K_s'/K_s were observed at larger floc sizes. A value of K_s'/K_s of 6.0 was observed at a particle size of 72 μm, showing that K_s is strongly affected by internal diffusion resistances. This may explain why the reported values of K_s in the literature vary so widely[68, 93]. As in the case of k', K_s' becomes equal to the intrinsic value as floc size approaches 36 μm.

An important conclusion from the analysis presented above is that erroneous interpretation can be made regarding the true kinetics of the system, unless proper account of the effect of floc size on the uptake rate is made. This is particularly important in the case of the Michaelis-Menten expression, since this rate equation apparently maintains its form regardless of the significant internal diffusion resistances. It is also important to point out that the results obtained in this phase of investigation are in agreement with the predictions of the modified model presented in Chapter II.

The experimental effectiveness factor n_e, which can be evaluated by Eq. (6-9), were calculated from the experimental data collected

at specific rpm values. Figure 6-10 shows the relationship between n_e

and S_e with rpm as a parameter. Based on the theoretical considerations

presented in Chapter II, internal diffusion resistances can be minimized

by either reducing the floc size or by maintaining high ambient

substrate concentrations. Reduction of floc size increases the depth

of penetration of substrate within the floc, and thus results in a higher

utilization rate. Maintenance of high ambient substrate concentration

results in a greater concentration gradient inside the floc and thus

a higher mass flux through the biomass. Therefore larger values of n_e

should be obtained at either higher rpm's or higher ambient substrate

concentrations. This is clearly demonstrated in Figure 6-10, thus

showing the reasoning presented above is valid. The experimental data

for the evaluation of n_e is shown in Table 9, Appendix 5.

It will be useful to know the critical particle sizes which define

significant and insignificant diffusion resistances under specific

operating conditions. As discussed previously, the magnitude of the

ambient substrate concentration, S_e, has a significant effect on defining

such critical sizes. Figure 6-11 shows the computed critical floc sizes

for significant and insignificant diffusion resistances, which are

arbitrarily defined by $n_e = 0.60$ and $n_e = 0.95$ respectively, at different

S_e values. Both curves demonstrate that the higher the ambient substrate
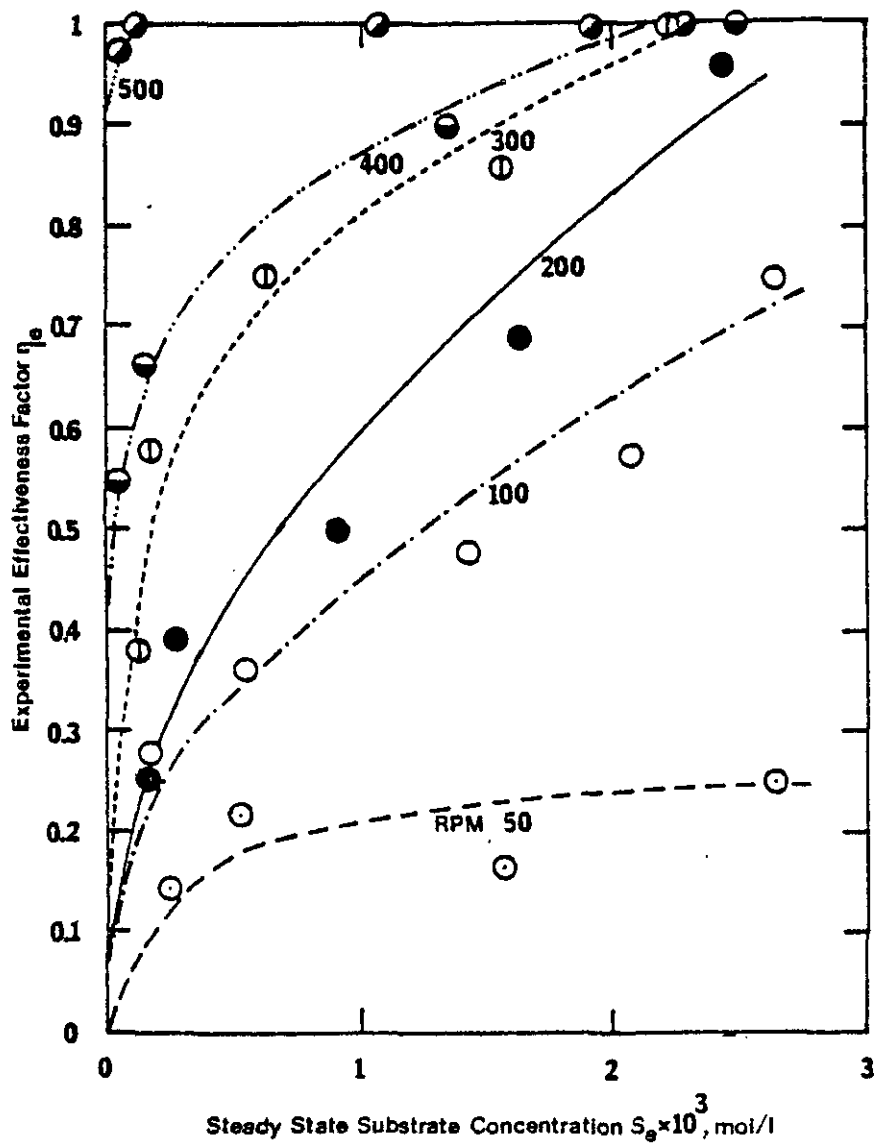
Figure 6-10 Experimental Effectiveness Factor η_e
as the Function of Steady State Substrate
Concentration S_e, for the Indicated
Impeller Rotational Speeds
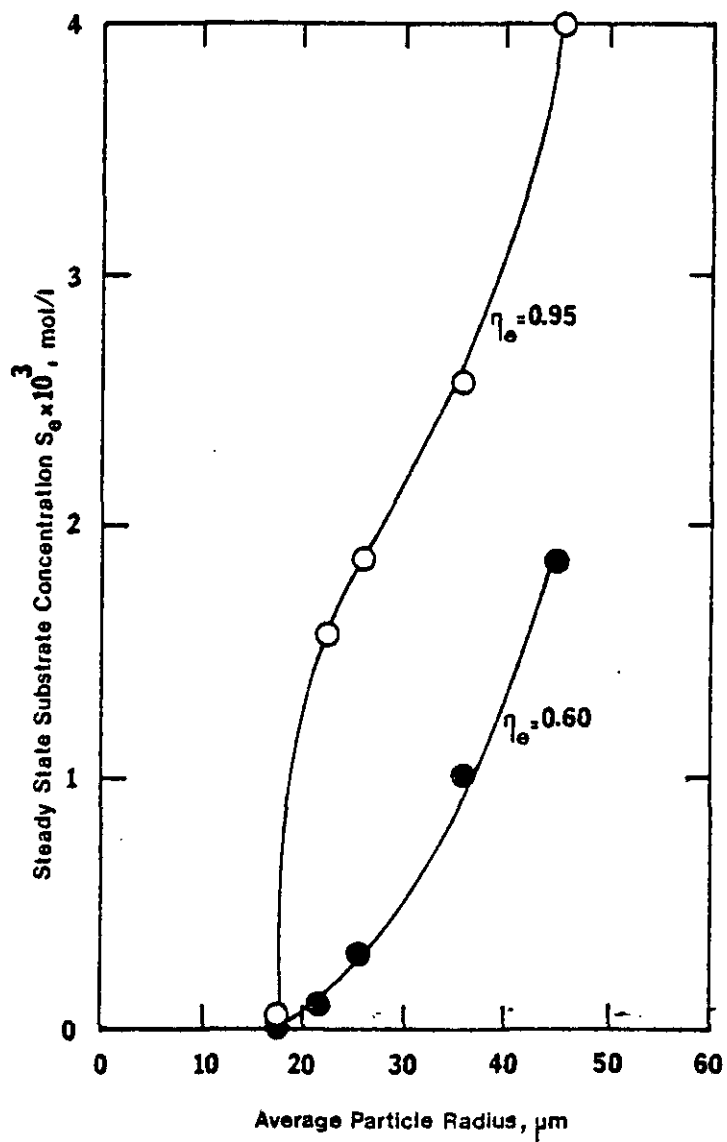
Figure 6-11 Critical Floc Sizes as the
Function of Steady State
Substrate Concentration S_e
for η_e = 0.95 and η_e = 0.60

concentration, the larger the floc that can be maintained in the system without significant internal diffusion effects. These curves also indicate that it is possible to run intrinsic kinetic studies under normal operating conditions (such as in a diffused air unit) as long as the ambient substrate concentration is maintained at relatively high levels.

Evaluation of the effective diffusivity. The effective diffusivity, D_e, can be estimated from the experimental effectiveness factor. The approach used here is similar to that suggested by Kawakami, et al[61]. Using the effectiveness factor charts shown in Figure 2-7, the following procedure can be used to determine D_e. First, the experimental effectiveness factor is determined by means of Eq. (6-9). From this value, and with the parameter β, which is defined as the ratio of the steady state substrate concentration S_e to the intrinsic K_s, the corresponding modulus ϕ^2 is read on the abscissa. The value of D_e is then calculated from ϕ^2, provided both biomass density ρ and floc particle radius R are known.

The biomass density was measured following the procedure described in Chapter IV. The average of thirty measurements is 57.35 mg/cm^3 (see Table 1, Appendix 5 for the individual measurements). The floc radius was obtained through Figure 5-1. With these data, the estimated

values of D_e were found to range from 0.61 to 3.543 × 10^{-7} cm^2/sec, which represent about 0.04 to 2% of the molecular diffusivity of the ammonium ion in water at 30^OC.

One of the possible explanations for the wide variation of the calculated values of the effective diffusivity could be that in these calculations an estimated average particle radius was used, while the particle size distribution was unknown. Had the latter been available, a more accurate estimate of the mean particle radius could have been obtained.

Table 6-2 presents values of effective diffusivities of several substrates in both biological flocs and biofilms. It can be seen that the range of variation of D_e found in this study compares well with that found by other investigators. Nevertheless, it is necessary to point out that the values of D_e reported herein are considerably lower than those obtained by Williamson and McCarty[135-137]

Summary

The intrinsic nitrification rate was observed in a continuous flow reactor under the same optimum operating conditions as in the batch experiments. The Michaelis-Menten relationship proved to be an appropriate expression for describing the intrinsic nitrification rate.

TABLE 6-2

EFFECTIVE DIFFUSIVITIES OF VARIOUS SUBSTRATES
IN DIFFERENT BIOLOGICAL SYSTEMS

Researcher	Substrate	Effective Diffusivity $\times 10^5$, cm^2/sec	Type of Biomass
Tomlinson and Snaddon[126]	Oxygen	1.5	Bacterial slime of sewage
Bungay, et al[25]	Oxygen	0.04(26°C)	Bacterial slime from polluted stream
Williamson and McCarty[135-137]	Oxygen	2.55	Nitrifier culture
	NH_3	1.50	
	NO_2	1.39	
	NO_3	1.62	
Mueller, et al[85]	Oxygen	0.18(20°C)	Zoogloea Ramigera
		0.04(26°C)	
Matson and Characklis[78]	Oxygen	0.4 - 2.0	Mixed culture
	Glucose	0.06 - 0.21	
La Motta[65]	Glucose	0.28	Biofilm
Atkinson and Daoud[8]	Glucose	0.07(25°C)	Biofilm
Baillod, et al (13, 14)	Glucose	0.048	Zoogloea Ramigera
Pipes[78]	Glucose	0.06 - 0.6	Activated sludge
Toda and Shoda[124]	Sucrose	0.67(47.5°C)	Agar gel

The effect of internal diffusion resistances on the overall rate was studied at different floc sizes. It was shown that the existence of significant internal diffusion resistances resulted in smaller k and larger K_s, which in turn reduced the overall rate.

The experimental effectiveness factor, n_e, was found to increase by either reducing floc size or increasing ambient substrate concentrations. The experimental results were in good agreement with those predicted by the model.

The effective diffusivity of ammonium was found to vary from 0.61 to 3.543×10^{-7} cm^2/sec. These values represent about 0.04 to 2% of the molecular diffusivity of ammonium in water at $30^\circ C$.

CHAPTER VII

ENGINEERING APPLICATIONS

The significance of internal diffusion resistances on the overall nitrification rate has clearly been demonstrated by the experimental results presented in this investigation. Although it was shown that the observed kinetic expression apparently maintains the same form regardless of internal diffusion effects, the value of the apparent kinetic parameters are different from the intrinsic ones. The presence of internal diffusion resistances in the system will reduce the efficiency of nitrification, even if the optimum operating conditions are maintained through the system. In addition, the application of apparent kinetic information will result in overdesign of a full-scale plant, which means higher capital, operating and maintenance costs.

For practical purposes, the information presented in Figures 6-8 and 6-9 is very useful in assessing the effect of floc size on the performance of a full-scale treatment plant. With a knowledge of the prevailing floc size in the plant, the expected values of both k'/k and K_s'/K_s can be estimated from these figures. By selecting a desired effluent substrate concentration S_e, the effectiveness factor can be

156

calculated by the following equation:

$$\eta = \frac{k'}{k} \times \frac{K_s + S_e}{K_s' + S_e} \qquad (7-1)$$

The value of K_s could be estimated to be approximately 1×10^{-4} mol/ℓ.

An engineering judgement can be made based on the calculated η value. If the system is under strong influence of internal diffusion resistances, say $\eta < 0.60$, a suitable reduction of floc size without sacrificing its settling properties, would be desirable, or some modifications of the process could be attempted.

One possible modification of the process to improve its performance is to divide the aeration tank into two zones. The first zone could be used as a high-rate reactor, that is, it would provide a very short detention time (say, one to two hours) and a high degree of agitation. This practice would yield not only a high value of k (cf. Figure 6-4), but also a high effectiveness factor (smaller floc particle and high ambient substrate concentration). The overall effect is that a very high removal rate of substrate would be obtained. A high air supply should be provided in this zone.

The second zone would be the reflocculation zone. Low air supply and longer detention time could be provided to allow floc particles to reflocculate and to grow, thus improving the settling characteristics

of the activated sludge. The sludge recovered from the final clarifier would be recycled back to the first zone as a biomass source.

This arrangement can be applied directly to the existing aeration tank without increasing the power cost or affecting the performance of the final clarifier. Zoning of the tank and redistribution of both power input and air supply are the only modifications required. A proposed schematic diagram of this modification is presented in Figure 7-1.

Another possible alternative is to use a high-rate reactor similar to the one described previously, followed by an upflow clarifier. The upflow clarifier provides a long cell detention time which allows reflocculation and growth of the cells. The cells recovered are recycled back to the high-rate reactor as the biomass source. In order to prevent denitrification from occurring in the clarifier with the resulting problem of floating sludge, pure oxygen instead of air may have to be used in the high-rate reactor. The residual D.O. concentration in the effluent from the reactor should be high enough to meet the requirement of nitrifiers in the upflow clarifier. It is believed that such an arrangement will reduce both the plant size and initial cost. An arrangement of this modification is shown in Figure 7-2.
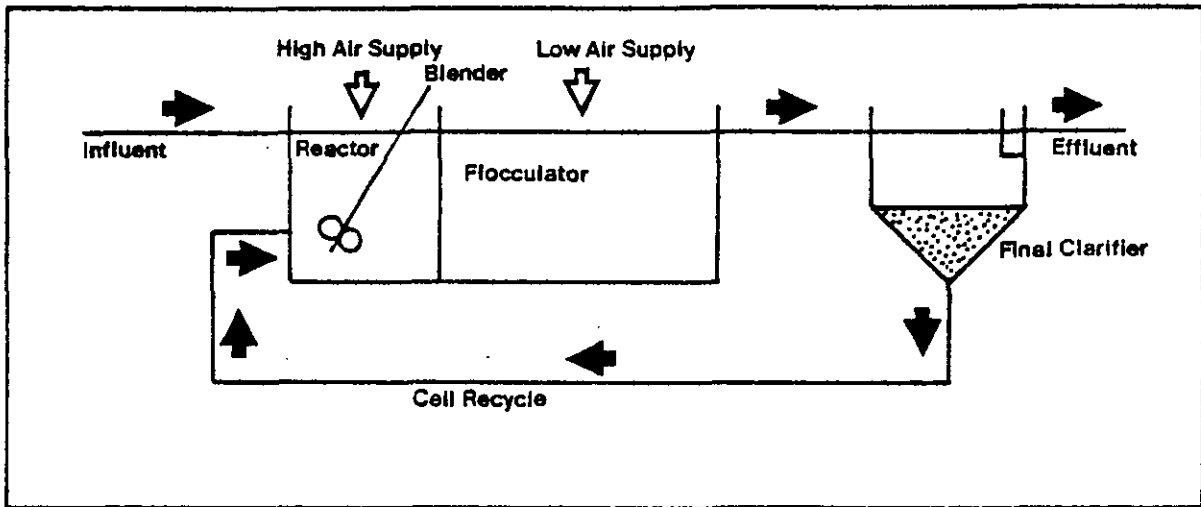
Figure 7-1 An Arrangement of Aeration Tank for High-Efficiency
Nitrification
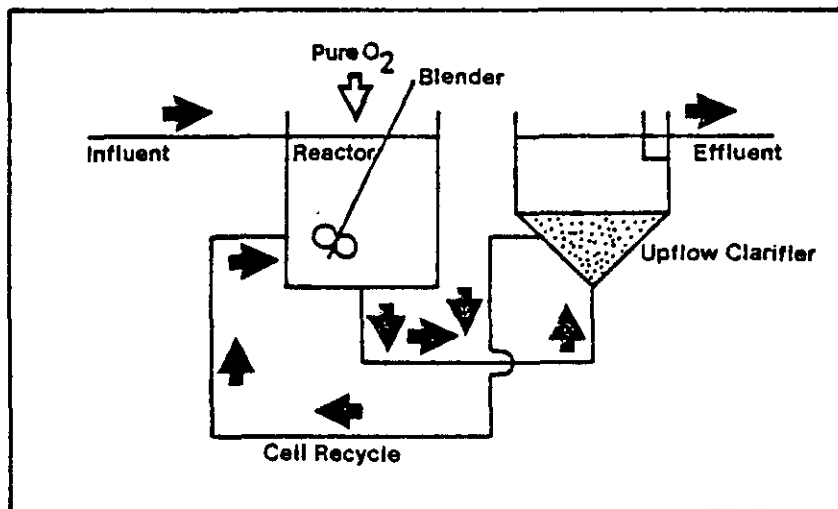
Figure 7-2 An Arrangement of a High-Rate Reactor Followed
by an Upflow Clarifier for High-Efficiency
Nitrification

CHAPTER VIII

CONCLUSIONS

From the results of this investigation, the following conclusions can be made:

(a) A modified model, which incorporates the consideration of internal diffusion and simultaneous biochemical reactions as controlling factors, provides an adequate description of the performance of the activated sludge nitrification process.

(b) It was shown mathematically that both mass transfer resistances in the bulk liquid and in the boundary layer surrounding the floc particle are insignificant as long as a high degree of agitation is provided in the system. Aeration in the activated sludge process is sufficient to provide the required agitation.

(c) The intrinsic nitrification study was conducted under such conditions that both external and internal diffusion resistances were eliminated and optimum operating conditions were prevailed. A pH of 8.0 and a temperature of $30^\circ C$ were found to be the optimum values for nitrification.

(d) The Michaelis-Menten kinetic relationship of the form

$v = kS_e/(K_s + S_e)$ is an appropriate expression for describing the intrinsic nitrification rate occurring in the activated sludge process. However, as shown in the batch experiments, both k and K_s were strongly affected by initial substrate concentration in the low range of concentrations. At sufficiently high initial substrate concentration, k becomes insensitive to increasing initial concentrations.

(e) The presence of significant internal-diffusion resistances affects the value of the pseudo-kinetic parameters k' and K_s'. Smaller values of k' and larger values of K_s' are observed as floc size increases beyond the critical value. A reduced overall rate was observed under such conditions.

(f) The experimental effectiveness factor n_e was found to increase when floc size was reduced or when the ambient substrate concentration was increased. This is in agreement with the results predicted by the kinetic model proposed in this investigation.

(g) The effective diffusivity, D_e, which was estimated from the experimental effectiveness factor calculations, varied from 0.61 to 3.543×10^{-7} cm^2/sec. These are about 0.04 to 2% of the corresponding values in water at $30^\circ C$.

(h) Although both batch and continuous flow experiments :
demonstrated the applicability of Michaelis-Menten kinetic
expression to the activated sludge process, the information
obtained from both experiments is not interchangable. The
behavior of both systems differs significantly, to the extent
that the kinetic constants k and K_s are entirely different.

(i) The saturation utilization rate k in the Michaelis-Menten
kinetic expression was found to vary with detention time in
the continuous flow experiments; that is, larger values of k
were observed under shorter detention times. The values of
k approached asymptotically the respective value corresponding
to the batch experiments. The Michaelis constant K_s remains
practically constant regardless of the detention time.

CHAPTER IX

RECOMMENDATIONS FOR FUTURE RESEARCH

(a) The investigation reported here demonstrated that internal
diffusion and simultaneous biochemical reactions can be
adequately described by the modified kinetic model developed
in Chapter II. However, only a single soluble substrate
(ammonia) was used. Similar studies are required for single
carbonaceous substrate and multisubstrate systems containing
colloidal substrate such as lipids, starch, etc.

(b) The accurate determination of particle size distribution
requires a particle size analyzer, such as the Coulter
Counter. Such a distribution is required to determine the
average particle size, which in turn is a key parameter to
estimate the effective diffusivity.

(c) The study of the effect of mass transfer resistances on the
overall substrate uptake rate should be conducted in modified
activated sludge processes, such as contact stabilization,
step aeration, etc. Such study would yield information which
can be used in improving plant performance.

(d) The effect of substrate concentration on the values of the

kinetic parameters should be conducted with other types of substrates to observe if a similar behavior to that reported herein is observed.

(e) The modifications suggested in Figures 7-1 and 7-2 should be tried at the bench scale, to study the feasibility of adapting them to full-scale plant operation.

(f) Further study of the effect of detention time on the values of the kinetic parameters should be conducted with different types of substrates and processes.

BIBLIOGRAPHY

(1) Adams, C. E. Jr., and W. W. Eckenfelder, Jr., "Nitrification Design Approach for High Strength Ammonia Wastewaters", J. Water Poll. Control Fed., Vol. 49, 413 (1977)

(2) Aiba, S., et al., Biochemical Engineering, Univ. of Tokyo Press, Tokyo, Japan (1965)

(3) Ames, W. F., Nonlinear Partial Differential Equations in Engineerings, Academic Press, New York (1965)

(4) Andrews, J. F., "Dynamic Model of the Anaerobic Digestion Process", J. San. Eng. Div., ASCE., Vol. 95, 95 (1969)

(5) Antonie, R. L., et al., "Evaluation of a Rotating Disk Wastewater Treatment Plant", J. Water Poll. Control Fed., Vol. 46, 498 (1974)

(6) Aris, R., Elementary Chemical Reactor Analysis, Prentice-Hall, Englewood Cliffs, N.J., (1969)

(7) Atkinson, B., and I. S. Daoud, "The Analogy Between Microbiological 'Reaction' and Heterogeneous Catalysis", Trans. Instn. Chem. Engr., Vol. 46, T19 (1968)

(8) Atkinson, B., et al., "A Theory for the Biological Film Reactor", Trans. Instn. Chem. Engr., Vol. 46, T245 (1968)

(9) Atkinson, B., and I. S. Daoud, "The Overall Rate of Substrate Uptake Reaction by Microbial Films, Part II - Effect of Concentration and Thickness with Mixed Microbial Films", Trans. Instn. Chem. Engr., Vol. 52, 260 (1974)

(10) Atkinson, B., Biochemical Reactors, Pion, London (1974)

(11) Atkinson, B., and I. S. Daoud, "Diffusion Effects within Microbial Films", Trans. Instn. Chem. Engr., Vol. 48, T245 (1970)

(12) Atkinson, B., and I. S. Daoud, "The Overall Rate of Substrate Uptake Reaction by Microbial Films, Part I - A Biological Rate Equation", <u>Trans. Instn. Chem. Engr.</u>, Vol. 52, 248 (1974)

(13) Baillod, C. R., <u>et al.</u>, "An Experimental Valuation of the Intra-Particle Resistance in Substrate Transfer to Suspended Zoogloeal Particles", <u>Proc. of the 24th Industrial Waste Conf.</u>, Purdue Univ., 302 (1969)

(14) Baillod, C. R., and W. C. Boyle, "Mass Transfer Limitations in Substrate Removal", <u>J. San. Eng. Div., ASCE.</u>, Vol. 96, 525 (1970)

(15) Balakrishnan, S., and W. W. Eckenfelder, Jr., "Nitrogen Removal by Modified Activated Sludge Process", <u>J. San. Eng. Div., ASCE.</u>, Vol. 96, 501 (1970)

(16) Barnard, J. L., "Cut P and N without Chemicals", <u>Water and Wastes Eng.</u>, Vol. 11, 33 (1974)

(17) Barnard, J. L., "Cut P and N without Chemicals", <u>Water and Wastes Eng.</u>, Vol. 11, 41 (1974)

(18) Barth, E. E., <u>et al.</u>, "Removal of Nitrogen by Municipal Wastewater Treatment Plants", <u>J. Water Poll. Control Fed.</u>, Vol. 38, 1208 (1966)

(19) Beckman, W. J., <u>et al.</u>, "Combined Carbon Oxidation-Nitrification", <u>J. Water Poll. Control Fed.</u>, Vol. 44, 1916 (1972)

(20) Behrman, B. W., "Nitrogen Removal Depends on Form Nutrient Takes", <u>Water and Wastes Eng.</u>, Vol. 13, 27 (1976)

(21) Benefield, L. D., and C. W. Randall, "Evaluation of a Comprehensive Kinetic Model for the Activated Sludge Process", <u>J. Water Poll. Control Fed.</u>, Vol. 49, 1636 (1977)

(22) Bird, R.B., <u>et al.</u>, <u>Transport Phenomena</u>, Wiley, New York (1960)

(23) Bishop, D. F., <u>et al.</u>, "Single-Stage Nitrification-Denitrification", <u>J. Water Poll. Control Fed.</u>, Vol. 48, 520 (1976)

(24) Braunscheidel, D. E., and R. C. Gyger, "UNOX System for Waste

Water Treatment", _Chemical Engineering Progress_, Vol. 72, 72 (1976)

(25) Bungay, H. R. III, _et al._, "Microprobe Techniques for Determining Diffusivities and Respiration Rates in Microbial Slime Systems", _Biotechnol. Bioengr._, Vol. XIII, 569 (1971)

(26) Bungay, H. R. III, and D. M. Harold, Jr., "Simulation of Oxygen Transfer in Microbial Slimes", _Biotechnol. Bioengr._, Vol. XIII, 569 (1971)

(27) Chiu, S. Y., _et al._, "Kinetic Behavior of Mixed Population of Activated Sludge", _Biotechnol. Bioengr._, Vol. XIV, 179 (1972)

(28) English, J. N., _et al._, "Denitrification in Granular Carbon and Sand Column", _J. Water Poll. Control Fed._, Vol. 46, 28 (1974)

(29) Ericsson, B., "Nitrogen Removal in a Pilot Plant", _J. Water Poll. Control Fed._, Vol. 47, 727 (1975)

(30) Finlayson, B. A., _The Method of Weighted Residuals and Variational Principles_, Academic Press, New York (1972)

(31) Finlayson, B. A., "Orthogonal Collocation in Chemical Reaction Engineering", _Cat. Rev. - Sci. Eng._, 10(1), 69 (1974)

(32) Fuhs, G. W., "Nutrients and Aquatic Vegetation Effects", _J. Env. Eng. Div., ASCE._, Vol. 100, 269 (1974)

(33) Gates, W. E., _et al._, "A Rational Model for the Anaerobic Contact Process", _J. Water Poll. Control Fed._, Vol. 39, 1951 (1967)

(34) Gaudy, A. F. Jr., "Kinetic Behavior of Heterogeneous Populations in Completely Mixed Reactor", _Biotechnol. Bioengr._, Vol. IX, 387 (1967)

(35) Gaudy, A. F. Jr., _et al._, "Control of Growth Rate by Initial Substrate Concentration at Values Below Maximum Rate", _Appl. Microbiol._, Vol. 22, 1041 (1971)

(36) Gaudy, A. F. Jr., _et al._, "Exponential Growth in Systems Limited by Substrate Concentration", _Biotechnol. Bioengr._, Vol. XV, 589 (1973)

(37) Gondo, S., et al., "Effects of Internal Diffusion on the Lineweaver -Burk Plots for Immobilized Enzymes", Biotechnol. Bioengr., Vol. XVII, 423 (1975)

(38) Grady, C. P. N. Jr., and D. R. Williams, "Effects of Influent Substrate Concentration on the Kinetics of Natural Microbial Populations in Continuous Culture", Water Res., Vol. 9, 171 (1975)

(39) Grantham, G. R., et al., "Progress Report on Trickling Filter Studies", Sewage and Industrial Wastes, Vol. 22, 867 (1950)

(40) Grau, P., et al., "Kinetics of Multicomponent Substrate Removal by Activated Sludge", Water Res., Vol. 9, 637 (1975)

(41) Harremoes, P., and M. Riemer, "Report on Pilot Experiments on Down-Flow Filter Denitrification", Rept. from Dept. of Sanitary Engineering, Technical Univ. of Denmark, Lyngby (1975)

(42) Harremoes, P., "The Significance of Pore Diffusion to Filter Denitrification", J. Water Poll. Control Fed., Vol. 48, 377 (1976)

(43) Harris, N. P., and G. S. Hansford, "A Study of Substrate Removal in a Microbial Film Reactor", Water Res., Vol. 10, 935 (1976)

(44) Haug, R. T., and P. L. McCarty, "Nitrification with the Submerged Filter", Technical Report No. 149, Dept. of Civil Engineering, Stanford Univ. (1971)

(45) Hermann, E. R., "Stabilization Pond as a Nitrate Reducing Reactor", J. San. Eng. Div., ASCE., Vol. 88, 1 (1962)

(46) Hershey, D., Transport Analysis, Plenum Publishing Corporation, New York (1974)

(47) Hildebrand, F. B., Introduction to Numerical Analysis, 2nd Edition, McGraw-Hill, New York (1974)

(48) Hoehn, R. C., "The Effects of Thickness on the Structure and Metabolism of Bacterial Films", Ph.D. Dissertation, Univ. of Missouri (1970)

(49) Hoehn, R. C., and A. D. Ray, "Effects of Thickness on Bacterial

Film", J. Water Poll. Control Fed., Vol. 45, 2302 (1973)

(50) Huang, C. S., "Kinetics and Process Factors of Nitrification on a Biological Film Reactor", Ph.D. Dissertation, State Univ. of New York at Buffalo (1973)

(51) Huang, C. S., and N. E. Hopson, "Nitrification Rate in Biological Process", J. Env. Eng. Div., ASCE., Vol. 100, 409 (1974)

(52) Humphrey, A. E., "Current Developments in Fermentation", Chemical Engr., Vol. 26, 98, December 9 (1974)

(53) Hutton, W. C., and S. A. LaRocca, "Biological Treatment of Concentrated Ammonia Wastewaters", J. Water Poll. Control Fed., Vol. 47, 989 (1975)

(54) Jeris, J. S., et al., "High Rate Biological Denitrification Using a Granular Fluidized Bed", J. Water Poll. Control Fed., Vol. 46, 2118 (1974)

(55) Jeris, J. S., and R. W. Owens, "Pilot-Scale, High-Rate Biological Denitrification", J. Water Poll. Control Fed., Vol. 47, 2043 (1975)

(56) Jeris, J. S., et al., "Biological Fluidized Bed Treatment for BOD and Nitrogen Removal", J. Water Poll. Control Fed., Vol. 49, 816 (1977)

(57) Jewell, W. J., and R. J. Cummings, "Denitrification of Concentrated Nitrate Wastewaters", J. Water Poll. Control Fed., Vol. 47, 2281 (1975)

(58) Johnson, W. K., and G. J. Schroepfer, "Nitrogen Removal by Nitrification and Denitrification", J. Water Poll. Control Fed., Vol. 36, 1015 (1964)

(59) Jones, P. H., and N. K. Patni, "Nutrient Transformations in a Swine Waste Oxidation Ditch", J. Water Poll. Control Fed., Vol. 46, 366 (1974)

(60) Kasaoka, K., et al., "Unsteady State Diffusion within Porous Solid Particle", J. Chem. Engr. Japan, Vol. 1, 32 (1968)

(61) Kawakami, K., et al., "The Effectiveness Factor of a Catalyst Pellet in the Liquid-Phase Hydrogenation of Styrene", J. Chem. Engr. Japan, Vol. 9, 392 (1976)

(62) Kobayashi, T., and K. J. Laidler, "Kinetic Analysis for Solid-Supported Enzymes", Biochemica et Biophysica Acta, 302 (1973)

(63) Kobayashi, T., et al., "Oxygen Transfer into Mycelial Pellets", Biotechnol. Bioengr., Vol. XV, 143 (1973)

(64) Kornegay, B. H., and J. F. Andrews, "Kinetics of Fixed-Film Biological Reactor", J. Water Poll. Control Fed., Vol. 40, Part 2, R460 (1968)

(65) La Motta, E. J., "Evaluation of Diffusional Resistances in Substrate Utilization by Biological Films", Ph.D. Dissertation, Univ. of North Carolina (1974)

(66) La Motta, E. J., "Kinetics of Growth and Substrate Uptake in a Biological Film System", Appl. Env. Microbiol., Vol. 31, 286 (1976)

(67) La Motta, E. J., "Internal Diffusion and Reaction in Biological Films", Environ. Sci. Technol., Vol. 10, 765 (1976)

(68) Lawrence, A. W., and P. L. McCarty, "Unified Basis for Biological Treatment Design and Operation", J. San. Eng. Div., ASCE., Vol. 96, 757 (1970)

(69) Lawrence, A. W., and C. G. Brown, "Design and Control of Nitrifying Activated Sludge Systems", J. Water Poll. Control Fed., Vol. 48, 1779 (1976)

(70) Levenspiel, O., Chemical Reaction Engineering, Wiley, New York (1972)

(71) Levin, D. M., and J. R. Glastonbury, "Particle-Liquid Hydrodynamics and Mass Transfer in a Stirred Tank", Trans. Instn. Chem. Engr., Vol. 50, 132 (1972)

(72) Ludzack, F. J., and M. B. Ettinger, "Controlling Operation to Minimize Activated Sludge Effluent Nitrogen", J. Water Poll. Control Fed., Vol. 34, 920 (1962)

(73) Lue-Hing, C., et al., "Biological Nitrification of Sludge
Supernatant by Rotating Disks", J. Water Poll. Control Fed.,
Vol. 48, 25 (1976)

(74) Maier, W. J., et al., "Simulation of the Trickling Filter Process",
J. San. Eng. Div., ASCE., Vol. 93, 91 (1967)

(75) Marangozis, J., and A. I. Johnson, "A Correlation of Mass Transfer
Data of Solid-Liquid Systems in Agitated Vessels", The Canadian
J. Chem. Engr., Vol. 40, 231 (1962)

(76) Matsché, N., "The Elimination of Nitrogen in the Treatment Plant
of Vienna-Blumental", Water Res., Vol. 6, 485 (1972)

(77) Matson, J. V., et al., "Oxygen Supply Limitations in Full Scale
Biological Treatment Systems", Proc. of the 27th Industrial Waste
Conf., Purdue Univ., 894 (1972)

(78) Matson, J. V., and W. G. Characklis, "Diffusion into Microbial
Aggregates", Water Res., Vol. 10, 877 (1976)

(79) McCabe, W. L., and J. C. Smith, Unit Operation of Chemical
Engineering, 3rd Edition, McGraw-Hill, New York (1976)

(80) McHarness, D. D., et al., "Field Studies of Nitrification with
Submerged Filters", J. Water Poll. Control Fed., Vol. 47, 291
(1975)

(81) McKinney, R. E., Microbiology for Sanitary Engineers, McGraw-Hill,
New York (1962)

(82) McKinney, R. E., "Mathematics of Complete-Mixing Activated Sludge",
J. San. Eng. Div., ASCE., Vol. 88, 87 (1962)

(83) Middlebrooks, E. J., and C. F. Garland, "Kinetics of Model and
Field Extended-Aeration Wastewater Treatment Units", J. Water
Poll. Control Fed., Vol. 40, 586 (1968)

(84) Miura, Y., et al., "Oxygen Transfer within Fungal Pellet", J. Chem.
Engr. Japan, Vol. 8, 300 (1975)

(85) Mueller, J. A., et al., "Oxygen Diffusion Through a Pure Culture

Floc of Zoogloeal Ramigera", Proc. of the 21st Industrial Waste Conf., Purdue Univ., 964 (1966)

(86) Mueller, J. A., et al., "Nominal Diameter of Floc Related to Oxygen Transfer", J. San. Eng. Div., ASCE., Vol. 92, 9 (1966)

(87) Mueller, J. A., et al., "Oxygen Diffusion Through Zoogloeal Flocs", Biotechnol. Bioengr., Vol. X, 331 (1968)

(88) Murphy, K. L., et al., "Nitrogen Control: Design Considerations for Supported Growth Systems", J. Water Poll. Control Fed., Vol. 49, 549 (1977)

(89) Ngian, K. F., and S. H. Lin, "Diffusion Coefficient of Oxygen in Microbial Aggregates", Biotechnol. Bioengr., Vol. XVIII, 1623 (1976)

(90) Painter, H. A., "A Review of Literature on Inorganic Nitrogen Metabolism in Microorganisms", Water Res., Vol. 4, 393 (1970)

(91) Pasveer, A., "Research on Activated Sludge, III Distribution of Oxygen in Activated Sludge Floc", Sewage and Industrial Wastes, Vol. 26, 28 (1954)

(92) Poduska, R. A., and J. F. Andrews, "Dynamics of Nitrification in the Activated Sludge Process", J. Water Poll. Control Fed., Vol. 47, 2599 (1975)

(93) Process Design Manual for Nitrogen Control, U.S. Environmental Protection Agency, Technology Transfer (1975)

(94) Ramachandran, P. A., "A General Model for the Packed Bed Encapsulated Enzyme Reactor", J. Appl. Chem. Biotechnol., Vol. 24, 265 (1974)

(95) Ramachandran, P. A., "Solution of Immobilized Enzyme Problems by Collocation Methods", Biotechnol. Bioengr., Vol. XVII, 311 (1975)

(96) Regan, D. L., et al., "Influence of Intraparticle Diffusional Limitation on the Observed Kinetics of Immobilized Enzymes and Catalyst Design", Biotechnol. Bioengr., Vol. XVI, 1081 (1974)

(97) Reeves, T. G., "Nitrogen Removal: A Literature Review", J. Water Poll. Control Fed., Vol. 44, 1895 (1972)

(98) Reynolds, T. D., and J. T. Yang, "Model of the Completely Mixed Activated Sludge Process", Proc. of the 21st Industrial Waste Conf., Purdue Univ., 696 (1966)

(99) Richard, M. D., and A. F. Gaudy, Jr., "Effect of Mixing Energy on Sludge Yield and Cell Composition", J. Water Poll. Control Fed., Vol. 40, Part 2, R129 (1968)

(100) Rovito, B. J., and J. R. Kittrell, "Film and Pore Diffusion Studies with Immobilized Glucose Oxidase", Biotechnol. Bioengr., Vol. XV, 143 (1973)

(101) Sanders, W. M. III, "Oxygen Utilization by Slime Organisms in Continuous Culture", Air & Water Poll. Int. J., Vol. 10, 253 (1966)

(102) Sanders, P. T., and M. J. Bazin, "Attachment of Microorganisms in a Packed Column: Metabolite Diffusion Through the Microbial Film as a Limiting Factor", J. Appl. Chem. Biotechnol., Vol. 23, 847 (1973)

(103) Satterfield, C. N., and T. K. Sherwood, The Role of Diffusion in Catalyst, Addison-Wesley, Reading, Mass. (1963)

(104) Satterfield, C. N., Mass Transfer in Heterogeneous Catalysis, MIT Press, Cambridge, Mass. (1970)

(105) Schroeder, E. D., and G. Tchobanoglous, "Mass Transfer Limitation on Trickling Filter Design", J. Water Poll. Control Fed., Vol. 48, 771, (1976)

(106) Seidel, D. F., and R. W. Crites, "Evaluation of Anaerobic Denitrification Processes", J. San. Eng. Div., ASCE., Vol. 96, 267 (1970)

(107) Sherrard, J. H., and A. W. Lawrence, "Design and Operation Model of Activated Sludge", J. Env. Eng. Div., ASCE., Vol. 99, 773 (1973)

(108) Shindala, A., "Nitrogen and Phosphorus Removal from Wastewaters

- Part 2 - Chemical - Biological", Water and Sewage Works, Vol. 119, 60 (1970)

(109) Shindala, A., "Nitrogen and Phosphorus Removal from Wastewater - Part 1", Water and Sewage Works, Vol. 119, 66 (1972)

(110) Skelland, A. H. P., Diffusional Mass Transfer, Wiley, New York (1974)

(111) Smith, J. M., Chemical Engineering Kinetics, 2nd Edition, McGraw-Hill, New York (1976)

(112) Srinath, E. G., et al., "A Technique for Estimating Active Nitrifying Mass and Its Application in Designing Nitrifying Systems", Proc. of the 29th Industrial Waste Conf., Purdue Univ., 1038 (1974)

(113) Standard Method for the Examination of Water and Wastewater, APHA-AWWA-WPCF (1975)

(114) Stenquist, R. J., et al., "Carbon Oxidation-Nitrification in Synthetic Media Filter", J. Water Poll. Control Fed., Vol. 46, 2327 (1974)

(115) Stensel, H. D., "Biological Kinetics of the Suspended Growth Denitrification Process", Ph.D. Dissertation, Cornell Univ., (1971)

(116) Stensel, H. D., et al., "Biological Kinetics of Suspended Growth Denitrification", J. Water Poll. Control Fed., Vol. 45, 249 (1973)

(117) Stover, E. L., and D. F. Kincannon, "One- versus Two-Stage Nitrification in the Activated Sludge Process", J. Water Poll. Control Fed., Vol. 48, 645 (1976)

(118) Stratton, F. E., and P. L. McCarty, "Prediction of Nitrification Effects on the Dissolved Oxygen Balance of Streams", Environ. Sci. Technol., Vol. 1, 405 (1967)

(119) Sutton, P. M., et al., "Efficacy of Biological Nitrification", J. Water Poll. Control Fed., Vol. 47, 2665 (1975)

(120) Sykes, P., and A. Gomezplata, "Particle Liquid Mass Transfer in Stirred Tanks", The Canadian J. Chem. Engr., Vol. 45, 189 (1967)

(121) Sylvester, N. D., and P. Pitayagulsarn, "Effect of Mass Transport on BOD Removal in Trickling Filters", Water Res., Vol. 9, 447 (1975)

(122) Tamblyn, T. A., and B. R. Sword, "The Anaerobic Filter for the Denitrification of Agricultural Subsurface Drainage", Proc. of the 24th Industrial Waste Conf., Purdue Univ., 1135 (1969)

(123) Theodore, L., Transport Phenomena for Engineers, International Textbook Co., (1971)

(124) Toda, K., and M. Shoda, "Sucrose Inversion by Immobilized Yeast Cells in a Complete Mixing Reactor", Biotechnol. Bioengr., Vol. XVII, 1729 (1975)

(125) Toda, K., "Interparticle Mass Transfer Study with a Packed Column of Immobilized Microbes", Biotechnol. Bioengr., Vol. XVII, 1759 (1975)

(126) Tomlinson, T. G., and D. H. M. Snedden, "Biological Oxidation of Sewage by Films of Microorganisms", Air & Water Poll. Int. J., Vol. 10, 865 (1966)

(127) Tuček, F., et al., "Unified Basis for Design of Biological Aerobic Treatment Processes", Water Res., Vol. 5, 647 (1971)

(128) Villadsen, J. V., and W. E. Steward, "Solution of Boundary-Value Problems by Orthogonal Collocation", Chem. Eng. Sci., Vol. 22, 1483 (1967)

(129) Voets, J. P., et al., "Removal of Nitrogen from Highly Nitrogenous Wastewaters", J. Water Poll. Control Fed., Vol. 47, 395 (1975)

(130) Weast, R. C., Handbook of Chemistry and Physics, 54th Edition, CRC Press, (1973-1974)

(131) Weddle, C. L., and D. Jenkins, "The Viability and Activity of Activated Sludge", Water Res., Vol. 5, 621 (1971)

(132) Wen, C. N., and A. H. Molof, "Nitrification in the Biological Fixed-Film Rotating Disk System", J. Water Poll. Control Fed., Vol. 46, 1674 (1974)

(133) White, G. C., Handbook of Chlorination, Van Notstrand Reinhold, New York (1972)

(134) Wild, H. E. Jr., et al., "Factors Affecting Nitrification Kinetics", J. Water Poll. Control Fed., Vol. 43, 1845 (1971)

(135) Williamson, K. J., "The Kinetics of Substrate Utilization by Bacterial Films", Ph.D. Dissertation, Stanford Univ. (1973)

(136) Williamson, K. J., and P. L. McCarty, "A Model of Substrate Utilization by Bacterial Films", J. Water Poll. Control Fed., Vol. 48, 9 (1976)

(137) Williamson, K. J., and P. L. McCarty, "Verification Studies of the Biofilm Model for Bacterial Substrate Utilization", J. Water Poll. Control Fed., Vol. 48, 281 (1976)

(138) Wong-Chong, G. M., and R. C. Loehr, "The Kinetics of Microbial Nitrification", Water Res., Vol. 9, 1099 (1975)

(139) Yang, P. Y., and A. F. Gaudy, Jr., "Nitrogen Metabolism in Extended Aeration Processes Operating with and without Hydrolytic Pretreatment of Portions of the Sludge", Biotechnol. Bioengr., Vol. XVI, 1 (1974)

(140) Young, J. C., et al., "Packed-Bed Reactors for Secondary Effluent BOD and Ammonia Removal", J. Water Poll. Control Fed., Vol. 47, 46 (1975)

(141) Zoltek, J. Jr., and L. Lefebvre, "Nitrification in High-Sludge Age Contact Stabilization", J. Water Poll. Control Fed., Vol. 48, 2183 (1976)

APPENDICES

APPENDIX 1

EVALUATION OF SIGNIFICANCE OF EXTERNAL DIFFUSION
RESISTANCES OF SUBSTRATE

By Eq. (2-8), and for ammonium ion in water with a temperature of $30^{\circ}C$, then

$$\frac{k_{CA}d}{D} = 2.0 + 51.7713(d)^{0.5}(v_f)^{0.5} \tag{A1-1}$$

If $d = 0.012$ cm, then

$$k_{CA} = 1.4467 \times 10^{-3}(2 + 5.6173v_f^{0.5}) \ (cm/sec) \tag{A1-2}$$

If $d = 0.006$ cm, then

$$k_{CA} = 2.893 \times 10^{-3}(2 + 4.01v_f^{0.5}) \ (cm/sec) \tag{A1-3}$$

The mass flux of substrate, N, across the outer surface of the floc is shown in Eq. (2-9), and if the mass flux of substrate is expressed in terms of mass of substrate per unit mass of particle per unit time, Eq. (2-10) applies.

For spherical particle, $A_p/V_p = 3/R$, where R is the radius of the particle. Thus

$$\Delta S = 0.2082 \times \frac{N'R}{k_{CA}} \tag{A1-4}$$

where ΔS is in terms of mol/ℓ, R in cm, k_{CA} in cm/sec, and N' in mol/mg-day.

APPENDIX 2

CALCULATION OF EXACT VALUES OF EFFECTIVENESS FACTOR FOR THE FIRST ORDER REACTION

If $1 >> \beta f$, then Eq. (2-20) is reduced to

$$\frac{1}{\xi^2} \frac{d}{d\xi} \left(\xi^2 \frac{df}{d\xi} \right) = \phi^2 f \tag{A2-1}$$

where

$$\phi = (\rho k / K_s D_e)^{0.5} R = (\rho k_1 / D_e)^{0.5} R$$

$$k_1 = k/K_s = \text{first order rate constant}$$

Boundary conditions for Eq. (A2-1) are shown in Eq. (2-21).

Differential equations in which the operator $(1/\xi^2)d/d\xi(\xi^2 d/d\xi)$ appears can frequently be simplified by a change of variable of the type $f(\xi) = F(\xi)/\xi$ [11].

By substituting $f(\xi) = F(\xi)/\xi$ into Eq. (A2-1), then

$$\frac{d^2 F}{d\xi^2} = \phi^2 F \tag{A2-2}$$

with boundary conditions

B.C. 1 $F = 1$ at $\xi = 1$

B.C. 2 $\dfrac{d^2 F}{d\xi^2} = 0$ at $\xi = 0$ $\tag{A2-3}$

The general solution of Eq. (A2-2) is

$$F(\xi) = Ae^{\phi\xi} + Be^{-\phi\xi} \tag{A2-4}$$

where A and B are constants.

Substituting Eq. (A2-3) into Eq. (A2-4), then

$$F(\xi) = \frac{1}{e^{\phi} - e^{-\phi}}(e^{\phi\xi} - e^{-\phi\xi}) = \frac{\sinh\phi\xi}{\sinh\phi} \tag{A2-5}$$

By recognizing that $f(\xi) = F(\xi)/\xi$, then

$$f(\xi) = \frac{1}{\xi}\frac{\sinh\phi\xi}{\sinh\phi} \text{ , or}$$

$$S = \frac{S_e R}{r} \frac{\sinh(\rho k_1/D_e)^{0.5}r}{\sinh(\rho k_1/D_e)^{0.5}R} \tag{A2-6}$$

where S is the substrate concentration at distance r from the center of the floc.

The mass flux N across the surface at r = R is

$$N\Big|_{r=R} = -D_e \frac{dS}{dr}\Big|_{r=R} = \frac{D_e S_e}{R}\{1-(\rho k_1/D_e)^{0.5}R\coth(\rho k_1/D_e)^{0.5}R\} \tag{A2-7}$$

The mas flow of substrate across the surface at r = R is

$$NA\Big|_{r=R} = 4\pi R D_e S_e\{1-(\rho k_1/D_e)^{0.5}R\coth(\rho k_1/D_e)^{0.5}R\} \tag{A2-8}$$

If the internal surface of the floc were all exposed to the ambient concentration S_e, the concentration gradient in the r direction would be zero and the substrate would not have to diffuse through the

pores to a reaction site.   In this case the reaction rate will become maximum.

Thus the maximum possible rate is

$$\frac{4\pi R^3}{3}(-\rho k_1 S_e)$$

Therefore, the effectiveness factor η is

$$\eta = \frac{3}{\phi^2}(\phi \coth\phi - 1) \tag{A2-9}$$

APPENDIX 3

EVALUATION OF $\bar{B}$ AND $\bar{w}$ FOR $i = 2$

For $i = 2$

$$\bar{B} = \left\{ \begin{bmatrix} 0 & 6 & 20\xi_1^2 \\ 0 & 6 & 20\xi_1^2 \\ 0 & 6 & 20\xi_1^2 \end{bmatrix} \begin{bmatrix} \xi_1^0 & \xi_1^2 & \xi_1^4 \\ \xi_2^0 & \xi_2^2 & \xi_1^4 \\ \xi_3^0 & \xi_3^2 & \xi_3^4 \end{bmatrix}^{-1} \right. \qquad (A3\text{-}1)$$

$$\bar{w} = \left\{ \int_0^1 \xi^2 d\xi \quad \int_0^1 \xi^4 d\xi \quad \int_0^1 \xi^6 d\xi \right\} \begin{bmatrix} \xi_1^0 & \xi_1^2 & \xi_1^4 \\ \xi_2^0 & \xi_2^2 & \xi_2^4 \\ \xi_3^0 & \xi_3^2 & \xi_3^4 \end{bmatrix}^{-1} \qquad (A3\text{-}2)$$

The Jacobi Polynomial for $i = 2$ is

$$P_2(\xi^2) = 1 - 6\xi^2 + \frac{33}{5}\xi^4 \qquad (A3\text{-}3)$$

The collocation points ξ_j^2, which are roots of $P_j(\xi^2) = 0$, can be obtained by solving Eq. (A3-3). Thus

$\xi_1 = 0.468849$

$\xi_2 = 0.830224$

$\xi_3 = 1$ (point at the outer surface of the floc)

Therefore,

$$\bar{B} = \begin{vmatrix} 0 & 6 & 4.396388 \\ 0 & 6 & 13.785438 \\ 0 & 6 & 20 \end{vmatrix} \begin{vmatrix} 1 & 0.219819 & 0.048321 \\ 1 & 0.689272 & 0.475096 \\ 1 & 1 & 1 \end{vmatrix}^{-1} \qquad (A3\text{-}4)$$

$$\bar{w} = \{0.333333 \quad 0.2 \quad 0.142857\} \begin{vmatrix} 1 & 0.219819 & 0.048321 \\ 1 & 0.689272 & 0.475096 \\ 1 & 1 & 1 \end{vmatrix}^{-1} \qquad (A3\text{-}5)$$

Now

$$\bar{Q} = \begin{vmatrix} 1 & 0.219819 & 0.048321 \\ 1 & 0.689272 & 0.475096 \\ 1 & 1 & 1 \end{vmatrix}$$

The transpose of $\bar{Q}$, $\bar{Q}^T$ is

$$\bar{Q}^T = \begin{vmatrix} 1 & 1 & 1 \\ 0.219819 & 0.689272 & 1 \\ 0.048321 & 0.475096 & 1 \end{vmatrix}$$

Therefore the adjoint of $\bar{Q}$, $Adj\bar{Q}$, is

$$Adj\bar{Q} = \begin{vmatrix} 0.214176 & -0.171498 & 0.071129 \\ -0.524904 & 0.951679 & -0.426775 \\ 0.310728 & -0.780728 & 0.469453 \end{vmatrix}$$

The value of determinant of $\bar{Q}$ is

$$|\bar{Q}| = \begin{vmatrix} 1 & 0.219819 & 0.048321 \\ 1 & 0.689272 & 0.475096 \\ 1 & 1 & 1 \end{vmatrix} = 0.113807$$

Therefore

$$\bar{Q}^{-1} = \frac{Adj\bar{Q}}{|\bar{Q}|} = \begin{vmatrix} 1.881926 & -1.506922 & 0.624998 \\ -4.612237 & 8.362232 & -3.749995 \\ 2.730311 & -6.860116 & 4.124999 \end{vmatrix}$$

Thus

$$\bar{B} = \begin{vmatrix} 0 & 6 & 4.396388 \\ 0 & 6 & 13.785438 \\ 0 & 6 & 20 \end{vmatrix} \begin{vmatrix} 1.881926 & -1.506922 & 0.624998 \\ -4.612237 & 8.362232 & -3.749995 \\ 2.730311 & -6.860116 & 4.124999 \end{vmatrix}$$

$$= \begin{vmatrix} -15.669962 & 20.034878 & -4.364917 \\ 9.965122 & -44.330038 & 34.364917 \\ 26.932855 & -86.932855 & 60 \end{vmatrix} \qquad (A3-6)$$

$$\bar{w} = \{0.0949059 \quad 0.1908084 \quad 0.04761905\} \qquad (A3-7)$$

APPENDIX 4

PROCEDURES FOR THE MEASUREMENT OF AMMONIA BY
THE ORION SPECIFIC ION METER MODEL 407A

(i)   Required equipment

  (a) Meter: Orion Specific Ion Meter Model 407A.

  (b) Magnetic stirrer.

  (c) Beaker: 20 mℓ in volume.

(ii) Required solutions

  (a) Distilled deionized water: Water must be ammonia-free.

  (b) 10 N NaOH: To adjust solution pH to the operating range

    of the electrode. To prepare 10 N NaOH, add 40

    grams reagent-grade NaOH to 80 mℓ distilled water

    in a 100-mℓ volumetric flask, dissolved, and dilute

    to volume with distilled water.

  (c) Standard solution: To prepare a 0.1 M ammonium

    chloride standard solution, add 0.535 grams

    reagent-grade NH_4Cl to 50 mℓ distilled water in a

    100-mℓ volumetric flask, stir to dissolve, and

    dilute to volume with distilled water.

  (d) Internal solution: To fill the electrode, Orion Cat.

    No. 95-10-02.

(e) pH 4 buffer solution: For checking inner body

operation. Add 1.16 grams reagent-grade NaCl to

200 mℓ pH 4 buffer solution.

(f) pH 7 buffer solution: For checking inner body

operation. Add 1.16 grams reagent-grade NaCl to

200 mℓ pH 7 buffer solution.

(iii)   Checking inner body with the 407A Specific Ion Meter

Disassemble the ammonia probe. Rinse the inner body of

the electrode with distilled water and immerse it in the pH 4 buffer

solution so that the reference element is covered. Turn the function

switch of the meter to MV position. Stir the buffer throughout the

procedure. Record the potential reading on the blue MV scale. Rinse

the inner body with distilled water and place it in the pH 7 buffer.

Record the new reading. The difference between the readings should be

160-170 mv if the inner body sensing elements are operating correctly.

(iv)   Direct measurement using the 407A Specific Ion Meter (high

concentration)

(a) Prepare 10^{-2} and 10^{-3} M standards by serial dilution

of the 0.1 M standard.

(b) Place electrode in the 10^{-3} M standard. Add 1 mℓ

10 M NaOH to each 100 mℓ of standard. Turn function

switch to X^-. Adjust the meter needle to "1" on the red logarithmic scale with the calibration control. Use magnetic stirring throughout the procedure.

(c) Rinse electrode and place in the 10^{-2} M standard. Repeat step (b) and turn the temperature compensator knob until the meter needle reads "10" on the red logarithmic scale.

(d) Rinse electrode and place in sample. Repeat step (b). Multiply the meter reading on the red logarithmic scale by 10^{-3} M to determine sample concentration in moles per liter.

(v) Direct measurement using the 407A Specific Ion Meter (low concentration)

(a) Place electrode in a pH 4 buffer for several minutes. Use magnetic stirring throughout this procedure.

(b) Prepare 10^{-3} M and 10^{-4} M standards by serial dilution of the 0.1 M standard.

(c) Turn function switch to X^-. Follow step (b) in (iv). Wait for a stable reading and adjust the meter needle to "1" on the red logarithmic scale with the

calibration control. Rinse electrode and place
it in the more concentrated standard. Repeat the
procedure and turn the temperature compensator knob
until the meter reads "10" on the red logarithmic
scale.

(d) Rinse electrode and place in sample. Repeat the
procedure and multiply the reading by 10^{-5} M to
determine sample concentration.

APPENDIX 5

EXPERIMENTAL DATA

TABLE 1

DENSITY OF FLOC PARTICLES

Run	Dry Weight of Solids (mg)	Deposited Volume (ml)	Density ρ (mg/ml)
1	12.90	0.20	64.50
2	7.80	0.10	78.00
3	8.00	0.10	80.00
4	7.60	0.10	76.00
5	13.60	0.20	68.00
6	7.10	0.10	71.00
7	11.70	0.20	58.50
8	12.10	0.20	60.50
9	11.90	0.20	59.50
10	13.00	0.20	65.00
11	11.70	0.20	58.50
12	11.60	0.20	58.00
13	7.20	0.15	48.00
14	5.70	0.10	57.00
15	5.70	0.10	57.00
16	6.00	0.10	60.00
17	6.15	0.15	41.00
18	6.75	0.15	45.00
19	5.70	0.10	57.00
20	7.05	0.15	47.00
21	5.80	0.10	58.00
22	6.60	0.15	44.00
23	6.40	0.10	64.00
24	6.75	0.15	45.00
25	7.20	0.15	48.00
26	7.05	0.15	47.00
27	7.65	0.15	51.00
28	8.40	0.15	56.00
29	7.95	0.15	53.00
30	6.75	0.15	45.00

$\rho_{average}$ = 57.35 mg/ml   standard deviation = 10.372 mg/ml

TABLE 2

AVERAGE PARTICLE SIZE AT DIFFERENT
IMPELLER ROTATIONAL SPEEDS

RPM	Average Radius, μ *
50	52
100	46
200	36
300	26
400	22
500	18
900	18
1000	18

* Based on average value of 50 measurements

TABLE 3

DETERMINATION OF OPTIMUM OPERATING CONDITIONS
UNDER BATCH CONDITIONS

(a) Determination of Optimum Impeller Rotational Speed.   Raw Data
Operating conditions: pH = 8, Temperature = 30°C

RPM	Time(min)	Concentration of NH_4^+-N $\times$ 10^5(mol/ℓ)	MLVSS(mg/ℓ)
100	$0^{(1)}$	7.14	76
	15	6.36	68
	30	5.93	76
	45	5.64	76
	60	5.21	72
300	$0^{(1)}$	7.14	64
	15	6.50	76
	30	6.14	68
	45	5.64	72
	60	5.36	72
400	$0^{(1)}$	7.14	60
	15	6.36	56
	30	5.93	56
	45	5.00	52
	60	4.36	56
500	$0^{(1)}$	7.14	56
	15	6.43	52
	30	5.71	52
	45	5.07	48
	60	4.50	48

TABLE 3 (a) (continued)

RPM	Time(min)	Concentration of NH_4^+-N $\times 10^5$ (mol/ℓ)	MLVSS(mg/ℓ)
700	0[1]	7.14	56
	15	6.57	60
	30	5.71	68
	45	5.00	60
	60	4.43	56
900	0[1]	7.14	60
	15	6.57	60
	30	5.21	64
	45	5.00	56
	60	4.21	60

(1) Time zero starts after a 5 minute lag period.

TABLE 3 (a-1)

INITIAL AMMONIUM UPTAKE RATES AT DIFFERENT
IMPELLER ROTATIONAL SPEEDS

RPM	$k_o' \times 10^6$, (mol/mg-day)
100	5.84
300	6.36
400	11.94
500	12.39
700	12.86
900	12.57

TABLE 3 (b)

DETERMINATION OF OPTIMUM pH

Operating conditions: 900 RPM, Temperature = $30^{\circ}C$.

pH	Time(min)	Concentration of Ammonium×10^5(mol N/ℓ)	MLVSS(mg/ℓ)
6.0	0	7.14	80
	15	7.14	68
	30	7.14	84
	45	7.14	80
	60	7.14	72
6.5	0	7.14	64
	15	7.14	60
	30	7.14	60
	45	7.14	64
	60	7.14	42
7.0	0	7.14	56
	15	7.14	68
	30	7.14	64
	45	7.07	56
	60	7.00	64
7.5	0	7.14	68
	15	6.71	80
	30	6.43	76
	45	5.86	72
	60	5.43	64
8.5	0	7.14	60
	15	6.14	56
	30	5.93	64
	45	5.14	60
	60	4.50	60

TABLE 3 (b-1)

INITIAL AMMONIUM UPTAKE RATES AT DIFFERENT pH'S

pH	$k'_0 \times 10^6$, (mol/mg-day)
6.0	0
6.5	0
7.0	0.55
7.5	5.71
8.0	12.57
8.5	10.57
9.0	8.57

TABLE 3 (c)

DETERMINATION OF OPTIMUM TEMPERATURE

Operating conditions: 900 RPM, pH = 8.0

Temperature (^{o}C)	Time(min)	Ammonium $\times 10^{5}$ (mol N/ℓ)	MLVSS(mg/ℓ)
15	0	7.14	72
	15	6.86	68
	30	6.50	68
	45	6.21	72
	60	5.86	60
20	0	7.14	64
	15	6.79	60
	30	6.21	52
	45	5.71	60
	60	5.21	56
25	0	7.14	48
	15	6.57	48
	30	5.86	52
	45	5.50	52
	60	4.86	48
35	0	7.14	48
	15	6.86	52
	30	6.29	40
	45	5.71	44
	60	5.36	40

TABLE 3 (c-1)

INITIAL AMMONIUM UPTAKE RATES AT
DIFFERENT TEMPERATURES

Temperature(^{o}C)	$k'_0 \times 10^6$,(mol/mg-day)
15	4.53
20	8.87
25	11.00
30	12.57
35	12.57

TABLE 4

DETERMINATION OF EFFECT OF INITIAL AMMONIUM CONCENTRATION
ON k AND K_s UNDER BATCH CONDITIONS

$S_0 \times 10^4$ (mol N/ℓ)	Time(min)	Concentration of Ammonium $\times 10^4$ (mol N/ℓ)	MLVSS(mg/ℓ)
0.42	0	0.42	44
	15	0.30	40
	30	0.19	40
	45	0.11	32
	60	0.09	32
0.59	0	0.59	56
	15	0.45	60
	30	0.33	56
	45	0.21	52
	60	0.12	48
	75	0.05	52
0.66	0	0.66	48
	30	0.44	40
	60	0.24	48
	75	0.17	44
	90	0.12	48
0.79	0	0.79	48
	15	0.68	52
	30	0.56	56
	45	0.46	64
	60	0.40	60
	90	0.24	52
	120	0.13	52
	135	0.09	56

. TABLE 4 (continued)

$S_o \times 10^4$ (mol N/ℓ)	Time(min)	Concentration of Ammonium $\times 10^4$ (mol N/ℓ)	MLVSS(mg/ℓ)
0.96	0	0.96	40
	30	0.63	40
	60	0.40	40
	90	0.23	36
	120	0.10	40
1.07	0	1.07	52
	30	0.69	56
	60	0.46	60
	90	0.27	52
	120	0.13	60
	135	0.09	56
1.19	0	1.19	56
	30	0.77	64
	60	0.36	64
	90	0.19	64
	105	0.12	56
3.17	0	3.17	68
	60	2.29	68
	120	1.64	64
	180	1.04	68
	240	0.54	76
	270	0.39	68
	300	0.28	72
4.00	0	4.00	68
	30	3.00	80
	60	2.36	60
	90	1.50	76
	120	0.96	76
	135	0.61	68

TABLE 4 (continued)

$S_o \times 10^4$ (mol N/ℓ)	Time(min)	Concentration of Ammonium $\times 10^4$(mol N/ℓ)	MLVSS(mg/ℓ)
4.43	0	4.43	48
	60	3.21	52
	120	2.36	52
	180	1.75	60
	240	1.14	52
	300	0.79	52
	360	0.57	52
4.86	0	4.86	88
	60	2.57	92
	90	1.79	92
	120	1.21	92
	150	0.71	100
8.93	0	8.93	132
	60	6.43	132
	120	4.14	128
	180	2.07	132
	210	1.21	132
12.10	0	12.10	128
	60	7.40	132
	120	5.00	124
	150	3.40	132
	180	2.20	124
	210	1.40	128
14.60	0	14.60	152
	60	11.10	156
	120	7.40	144
	180	4.30	148
	240	2.00	140
	270	1.10	148

TABLE 5

VALUES OF k AND K_s OBTAINED UNDER DIFFERENT INITIAL
AMMONIUM CONCENTRATIONS, BATCH EXPERIMENTS

$S_o \times 10^4$, (mol N/ℓ)	$k \times 10^4$, (mol/mg-day)	$K_s \times 10^4$, (mol/ℓ)
0.421	0.552	0.259
0.586	0.303	0.134
0.657	0.341	0.239
0.786	0.686	0.495
0.964	0.516	0.807
1.070	0.683	1.074
1.190	0.675	0.839
3.710	0.726	2.700
4.000	1.056	3.331
4.430	1.114	4.957
4.860	1.378	4.894
8.930	0.527	1.200
12.100	0.924	2.894
14.600	0.754	2.946

TABLE 6

DETERMINATION OF INTRINSIC RATES IN CFSTR

$Q(\text{m}\ell/\text{min})$	Holding Time(min)	$S_i \times 10^3$ (mol N/ℓ)	$S_e \times 10^3$ (mol N/ℓ)	X_e (mg/ℓ)	$v_o \times 10^4$ (mol/mg-day)
1	300	1.06	<0.01	64	-
		2.54	0.01	56	1.08
		3.79	0.04	56	1.58
		5.43	0.14	64	1.93
		6.79	0.59	64	2.11
2	200	1.17	0.07	40	1.28
		2.71	0.52	44	2.11
		4.14	1.14	32	3.64
		5.71	1.61	32	4.96
		6.71	2.64	40	2.54
3	150	0.60	0.03	36	1.12
		1.21	0.16	32	2.26
		1.75	0.26	36	2.80
		2.61	0.69	32	3.81
		2.79	0.89	32	3.59
		3.71	1.64	24	4.57
		5.00	2.07	32	5.04
		6.71	3.29	32	5.25
4	120	0.69	0.03	28	1.81
		1.46	0.31	24	3.55
		3.17	1.03	28	5.39
		4.54	1.76	28	4.69
5	100	0.53	0.11	16	2.94
		1.14	0.31	16	4.57
		2.43	0.82	20	5.41
		3.64	1.68	16	4.44

Operating conditions (see Figure 6-1)

$Q' = 1$ mℓ/min, $X' = 120$ to 140 mg/ℓ, pH = 8.0

Temperature = $30°C$, RPM = 900

TABLE 7

VALUES OF k AND K_s UNDER DIFFERENT DETENTION TIMES

Detention Time(min)	$k \times 10^4$(mol/mg-day)	$K_s \times 10^4$(mol/ℓ)
100	5.446	0.930
120	4.931	0.595
150	4.456	0.942
200	3.322	1.162
300	2.104	0.128

TABLE 8

VALUES OF k' AND K_s' AT DIFFERENT PARTICLE SIZES

Particle Radius(μ)	RPM	$k' \times 10^4$(mol/mg-day)	$K_s' \times 10^4$(mol/ℓ)	k'/k	K_s'/K_s
52	50	1.176	3.483	0.264	3.710
46	100	2.591	3.850	0.581	4.100
36	200	3.886	5.643	0.872	6.000
26	300	5.387	4.166	1.210	4.100
22	400	3.952	1.600	0.887	1.700
18	500	4.477	0.830	1.000	0.880
18	900	4.456	0.939	1.000	1.000

TABLE 9

EVALUATION OF EXPERIMENTAL EFFECTIVENESS FACTOR n_e

RPM	$S_e \times 10^3$ (mol N/ℓ)	$v_9 \times 10^4$ (mol/mg-day)	$v_i \times 10^4$ (mol/mg-day)	n_e
50	0.25	0.47	3.24	0.144
	0.54	0.92	3.79	0.242
	1.57	0.79	4.20	0.187
	2.64	1.07	4.30	0.249
	3.36	0.71	4.33	0.165
100	0.17	0.81	2.88	0.281
	0.51	1.37	3.77	0.364
	1.43	2.00	4.18	0.478
	2.07	2.45	4.26	0.575
	2.64	3.24	4.30	0.752
200	0.19	0.77	3.00	0.257
	0.28	1.32	3.34	0.396
	1.11	2.06	4.11	0.502
	1.46	2.88	4.19	0.687
	2.43	4.12	4.29	0.961
300	0.11	0.93	2.41	0.385
	0.19	1.73	3.00	0.576
	0.64	2.94	3.89	0.756
	1.57	3.64	4.21	0.863
	2.21	4.34	4.27	1.000
400	0.06	0.85	1.66	0.531
	0.17	1.89	2.88	0.655
	1.57	3.80	4.20	0.903
	2.50	4.39	4.29	1.000
500	0.05	1.45	1.49	0.977
	0.14	2.46	2.38	1.000
	0.26	4.23	4.10	1.000
	1.18	4.41	4.25	1.000
	1.64	4.33	4.28	1.000

TABLE 10

EVALUATION OF EFFECTIVE DIFFUSIVITY D_e

Particle Radius(μ)	RPM	$S_e \times 10^3$ (mol N/ℓ)	β	ϕ^2	η_e	$D_e \times 10^7$ (cm^2/sec)
36	200	0.28	3.00	500	0.396	0.76
26	300	0.11	1.18	350	0.385	0.61
26	300	0.19	2.05	70	0.576	3.04
26	300	0.64	6.84	110	0.756	1.94
22	400	0.06	0.59	44	0.513	3.46
22	400	0.17	1.83	45	0.655	3.54